

SAGA UNIVERSITY

Applications of Cucurbiturils for Supramolecular Catalysis in Organic Chemistry



A dissertation presented for doctoral degree

Department of Science and Advanced Technology

By

Hang Cong

Supervisor: **Professor Dr. Takehiko Yamato**

September 2014

Catalogue

Abstract	I
Chapter 1 Introduction of Cucurbiturils and Hemicucurbiturils	1
1. Structures and Host-guest Properties of Cucurbiturils	2
1.1 Structures and host-guest principles of Cucurbiturils	2
1.2 Host-guest interactions of cucurbit[5]uril	4
1.3 Host-guest interactions of cucurbit[6]uril	7
1.4 Host-guest interactions of cucurbit[7]uril	12
1.5 Host-guest interactions of cucurbit[8]uril	17
1.6 Host-guest interactions of cucurbit[10 and 14]urils	19
2. Development of the supramolecular catalysis of cucurbiturils	22
2.1 Supramolecular catalysis of cucurbit[6]uril	22
2.2 Supramolecular catalysis of cucurbit[7]uril	24
2.3 Supramolecular catalysis of cucurbit[8]uril	27
3. Hemicucurbit[n]urils and their derivatives	31
3.1 Hemicucurbit[n]urils and their supramolecular properties	31
3.2 Cyclohexylhemicucurbit[6]uril and its supramolecular property	33
3.3 Bambus[6]urils and their supramolecular properties	34
4. Outline of the doctor research	36
References	37
Chapter 2 IBX Oxidation of Aromatic Alcohols in the Presence of Cucurbit[8]uril	48
1. Introduction	49
2. Results and discussion	51
2.1 Host-guest interaction between IBX, veratryl alcohol and cucurbit[8]uril	51
2.2 IBX oxidation of methoxybenzyl alcohols in the presence of cucurbit[8]uril	55

2.3 IBX oxidation of pyridinemethanol hydrochlorides in the presence of cucurbit[8]uril	58
3. Conclusion	62
4. Experimental	63
4.1 Materials and apparatus	63
4.2 Interaction of Q[8] with veratryl alcohol and IBX.....	64
2.3 Catalytic oxidation experiments.....	64
References.....	66
Chapter 3 Hemicucurbit[6]uril-catalytic IBX oxidation of hydroxybenzyl alcohols with chemo-selectivity	68
1. Introduction.....	69
2. Results and discussion	71
2.1 IBX oxidation of different hydroxybenzyl alcohols in the absence or in the presence of hemicucurbit[6]uril	71
2.2 Kinetic analysis of IBX oxidation of hydroxylbenzyl alcohols in the presence of hemicucurbit[6]uril	73
2.2 Host-guest interactions between hemicucurbit[6]uril and hydroxylbenzyl alcohols ..	77
3. Conclusions.....	83
4. Experimental	84
4.1 Materials and apparatus	84
4.2 IBX oxidation of hydroxybenzyl alcohols in the absence of HemiQ[6].....	84
4.3 host-guest interactions.....	84
References.....	86
Chapter 4 Esterification with Supramolecular Catalysis of Hemicucurbit[6]uril	88
1. Introduction.....	89
2. Results and discussion	91

2.1 Esterification of 4-methoxy-4-oxobut-2-enoic acid (MA) in the presence of hemicucurbit[6]uril.	91
2.2 Esterification of acrylic acid (AA) in the presence of hemicucurbit[6]uril.	94
2.3 Esterification of benzoic acid (BA) in the presence of hemicucurbit[6]uril.	95
2.4 Esterification of other acids in the presence of hemicucurbit[6]uril.	97
2.4 Effect of macrocycle species, amount of methanol on the esterification of acids.	99
2.5 Proposed mechanism of the esterification of acids in the presence of hemicucurbit[6]uril.	100
3. Conclusion	101
4. Experimental	102
4.1 Materials and apparatus	102
4.2 Catalytic esterification experiments	102
4.3 IR annlysis of host-guest interactions	103
References	104
Chapter 5 Aerobic Oxidation of Furans and Thiophene in the Presence of Hemicucurbit[6]uril	105
1. Introduction	106
2. Results and discussion	108
2.1 Aerobic oxidation of furan in the presence of hemicucurbit[6]uril	108
2.2 Host-guest interaction of furan with of hemicucurbit[6]uril, and protonation of hemicucurbit[6]uril.	110
2.3 Kinetics of aerobic oxidation of furan in the presence of hemicucurbit[6]uril.	113
2.4 Mechanism of aerobic oxidation of furan in the presence of hemicucurbit[6]uril...	116
2.5 Aerobic oxidation of 2-methylfuran in the presence of hemicucurbit[6]uril.	120
2.6 Aerobic oxidation of thiophene in the presence of hemicucurbit[6]uril.	121
3. Conclusion	124

4. Experimental	125
4.1 Materials and apparatus	125
4.2 Catalytic Oxidation experiments.....	125
4.3 Computational method.....	125
References.....	126
Summary	128
Acknowledgements.....	131
Publications.....	132

Abstract

Based on the formation of the ternary host-guest inclusion complex between veratryl alcohol, *o*-iodoxybenzoic acid (IBX) and cucurbit[8]uril (Q[8]), the effect of substrate substituent on the IBX oxidation of aryl alcohols to the corresponding aldehyde with supramolecular catalysis by cucurbit[8]uril (Q[8]) in aqueous solvent was investigated. Aromatic alcohols with different substituent effect on electron, 2,3,4-methoxybenzyl alcohols and 2,3,4-pyridinemethanol hydrochlorides, were subjected to the procedure for IBX oxidizing in the absence or presence of Q[8] at room temperature. The catalytic ability of Q[8] revealed that the electronic effect of the substituent on the α -carbon of the aryl alcohol was crucial factor to the Q[8]-catalytic activity, and the supramolecular catalysis of Q[8] was mechanistically suggested to contribute to the alcohols with mainly negative inductive effect of substituent.

The chemo-selective oxidation of bifunctional substrates *via* a supramolecular strategy was achieved. IBX (*o*-iodoxybenzoic acid) oxidation of hydroxybenzyl alcohols produced the corresponding aldehyde and quinones, while the presence of HemiQ[6] was able to restrain the IBX oxidation of phenolic hydroxyl groups to afford the aldehyde as the only product. The conversion and reaction rates were greatly affected by the structures of substrates, and the stereo effect and electronic effect played very important role in this selective oxidation system. Various spectroscopies, including ^1H NMR, IR, and UV-vis were employed to confirm the host-guest interactions of HemiQ[6] with hydroxybenzyl alcohols. The energy-minimized optimization suggested the host-guest interactions were stabilized by the formation of hydrogen bonding between the carbonyl groups on the macrocycle and the phenolic hydroxyl groups on substrates.

Hemicucurbit[6]uril (HemiQ[6])-induced esterification of acids with CH_3OH was investigated. Esterification of the model substrate MA (4-methoxy-4-oxobut-2-enoic acid) in the presence of different amounts of HemiQ[6]

had reaction rate constants of $k_{0.5} = 0.18 \text{ h}^{-1}$, $k_{1.0} = 0.36 \text{ h}^{-1}$ and $k_{2.0} = 0.52 \text{ h}^{-1}$. These results confirmed that the reaction rate increased with the ratio of catalyst to substrate. Ineffective catalysis of MA esterification with a stoichiometric amount of CH_3OH suggested that the essence for the HemiQ[6]-catalyzed reaction was solvolysis. Compare the kinetics of substrate MA with AA (acrylic acid) and BA (benzoic acid) shown that the catalytic activities should bear relation to the dimension of substrates. The different conversion of sorts of substrates in the presence of HemiQ[6] revealed that the supramolecular catalysis was favor in the conjugated structures. The inefficacy of HemiQ[12] demonstrated that the catalytic capability depended on the structure of the macrocyclic compound used.

The aerobic oxidation of furan in aqueous solution in the presence of HemiQ[6] was investigated, and the product furan-2,5-diol was stabilized by encapsulation of HemiQ[6], which could be transformed to the dione confirmation in acidic solution and escaped from the macrocyclic compound. The ^1H NMR titration experiments of the host-guest interaction at different pH values suggested protonation should improve the encapsulation, and therefore an unique property that HemiQ[6] can be protonated was revealed. The oxidizing kinetics suggested that the procedure was a consecutive reaction with a series of constants $k_1 = 2.9 \times 10^{-2} \text{ min}^{-1}$, $k_2 = 2.7 \times 10^{-2} \text{ min}^{-1}$, and $k_3 = 5.7 \times 10^{-3} \text{ min}^{-1}$, respectively. The kinetic investigation at $\text{pD} = 2.0$ indicated the HemiQ[6]-catalytic oxidation of furan could be accelerated by acidification of solution. As a consequence, a plausible mechanism was established on the above evidences, which was supported by the calculation results of quantum chemistry. 2-Methylfuran was employed to give the product 2-methylfuran-5-ol exhibiting a satisfied activity in this aerobic oxidation with the supramolecular catalysis of HemiQ[6], but the oxidation of thiophene was very slow in either neutral or acidic condition.

Chapter 1

Introduction of Cucurbiturils and Hemicucurbiturils

1. Structures and Host-guest Properties of Cucurbiturils

1.1 Structures and host-guest principles of Cucurbiturils

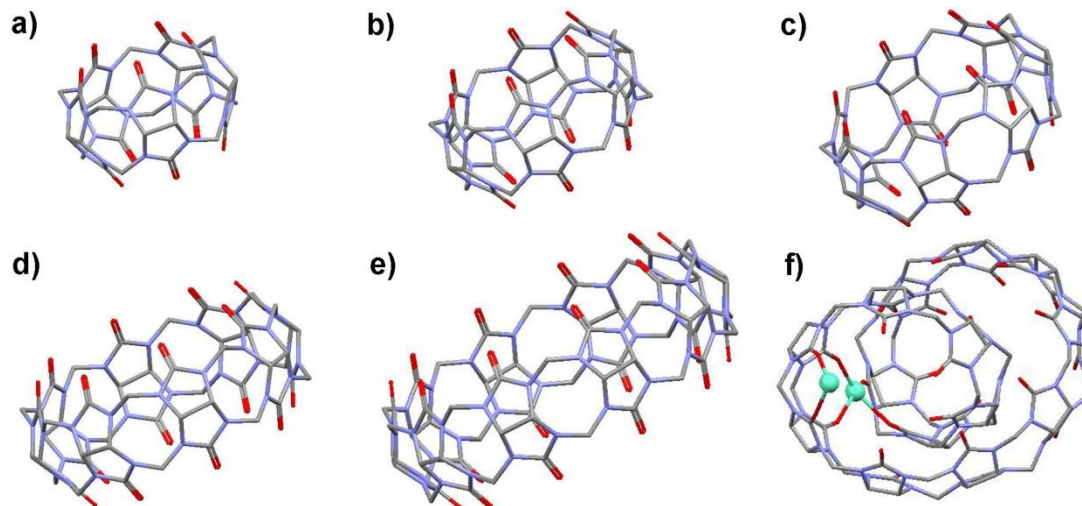
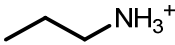
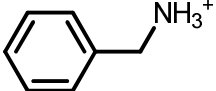
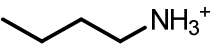
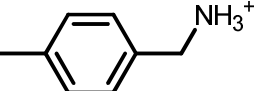
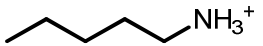
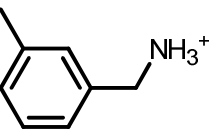
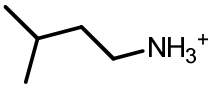
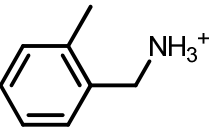
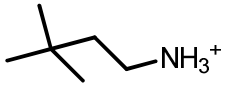
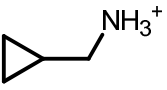
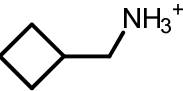

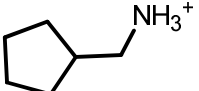
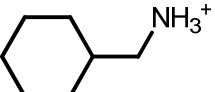


Figure 1-1 Structures of a) cucurbit[5]uril, b) cucurbit[6]uril, c) cucurbit[7]uril, d) cucurbit[8]uril, e) cucurbit[10]uril, and f) coordination compound of cucurbit[14]uril with Eu^{3+} . Color codes: carbon, gray; nitrogen, blue; oxygen, red; Eu^{3+} , light blue.

In 1905, Behrend and co-workers reported a white solid product from acidic condensation of formaldehyde, urea and glyoxal with very poor solubility, so the structure could not be able to be determined correctly due to that few analytic methods and technologies were available in the Early 20th Century, and they proposed it was a cross-linked, aminal-type polymer [1]. This reaction did not attract any attention in the next decades until 1980's, when Mock and co-workers reinvestigated it and prepared the single crystals of a coordination compound including Ca_2SO_4 and this condensation product. Consequently, an X-ray crystallographic analysis shown this product has a pumpkin shape with six glycoluril units bridged by six methene groups (Figure 1-1b), which was named 'cucurbituril' accordingly [2], and designated 'cucurbit[6]uril' now. The work by Kim's and Day's groups on the synthesis and separation of cucurbituril homologues (cucurbit[n], $n = 5, 7, 8, 10$]uril, Q[n], Figure 1-1a, 1-1c-e) in the Early 2000s have enriched this family

[3-5], and the member with the most size cavity, (cucurbit[14]uril, Q[14], Figure 1-1f), was reported by Tao's group very recently, which shown a very interesting twist and chiral structure in the coordination compound with Eu^{3+} [6].

Table 1-1 Association constants (K_a) for interactions of alkylamino with Q[6]^a

Guests	$K_a (\text{L} \cdot \text{mol}^{-1})$	Guests	$K_a (\text{L} \cdot \text{mol}^{-1})$
	1.2×10^4		2.7×10^2
	1.0×10^5		3.2×10^2
	2.4×10^4		unbound
	3.6×10^4		unbound
	1.8×10^1		$n = 2$ 1.5×10^5
	1.5×10^4		$n = 3$ 2.4×10^6
	3.7×10^5		$n = 4$ 2.8×10^6
	3.3×10^5		$n = 5$ 4.3×10^4
	unbound		$n = 6$ 9.1×10^2

^a From ref. [11]

It is now well known that cucurbituril's cavity surrounding with glycoluril units is hydrophobic, which intends to encapsulate small organic molecules depending on

the relative size of guest, and the two portals lined with carbonyl groups are hydrophilic, which bind guest with hydrogen bonding, ion-dipole interaction and so on [7-10]. The first case of investigation on host-guest interactions has been carried out in the beginning of 1980s, and cucurbit[6]uril (Q[6]) has been employed as a host to shown very high selectivity to encapsulate aliphatic ammonium ions (Table 1-1) [11]. The hydrophobic moiety of the guest can readily enter into the hollow core of Q[6], that is, hydrophobic effect of cavity of Q[6] played an important role in these encapsulations; On the other hand, the selectivity obviously depending on dimensions of the aliphatic substituent shown geometric match of substituent group for the cavity of host, namely, it is called as 'size effect'. The hydrogen bonding and ion-dipole interaction between ammonium cation of guest and carbonyl groups on Q[6] made the host-guest system more stable, and these kinds of weak interactions on the portals of cucurbiturils were defined as 'portal effect' in cucurbituril chemistry. The hydrophobic effect in the cavity could be detected easily by ^1H NMR, which usually causes an upshift of resonance signals of guest due to the shield effect, while the resonance signals of guest performs a downshift when guest stays at Q[n]'s portal for there is deshield effect by carbonyl groups of the macrocyclic compound. All of above mentioned principles are the academic fundamentals of host-guest chemistry and supramolecular functionalization of the cucurbit[n]urils.

1.2 Host-guest interactions of cucurbit[5]uril

Cucurbit[5]uril (Q[5]) has the smallest cavity in cucurbituril family, so the host-guest interactions of Q[5] has mostly been limited to stay at the portal as exclusion complexes including metal and ammonium cations guests. K^+ , Ba^{2+} , Ca^{2+} , and La^{3+} bound to carbonyl groups at the portals of Q[5], interestingly, chlorine, as the counter anions, has been included in the cavity to form the molecular capsules with barrel-shape structure [12]. And this experimental evidence suggested the electrostatic potential on inner surface of Q[5] could be positive and intend to interact with the electron-rich groups or ions. The further studies shown the selectivity of Q[5]

encapsulating NO_3^- and Cl^- depending on coordination of the host to La^{3+} . In the absence of lanthanide cation, Q[5] exhibited preference to containing nitrate anion, while in the presence of the metal cation, the host has been demonstrate to accommodate chlorine anion (Figure 1-2) [13].

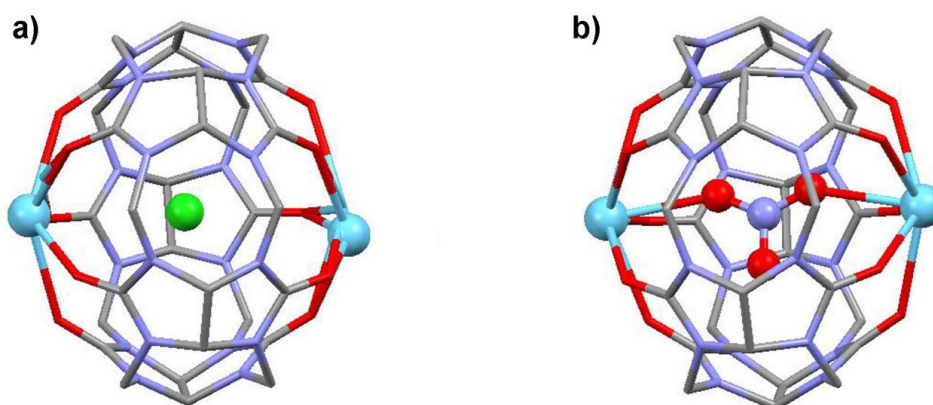


Figure 1-2 Crystallographic structure of molecular capsules of $(\text{La}^{3+})_2\text{Q}[5]$ with a) chloridion, and b) nitrate anion inside the cavity of Q[5]. Color codes: carbon, gray; nitrogen, blue; oxygen, red; La^{3+} , light blue; chloridine, green.

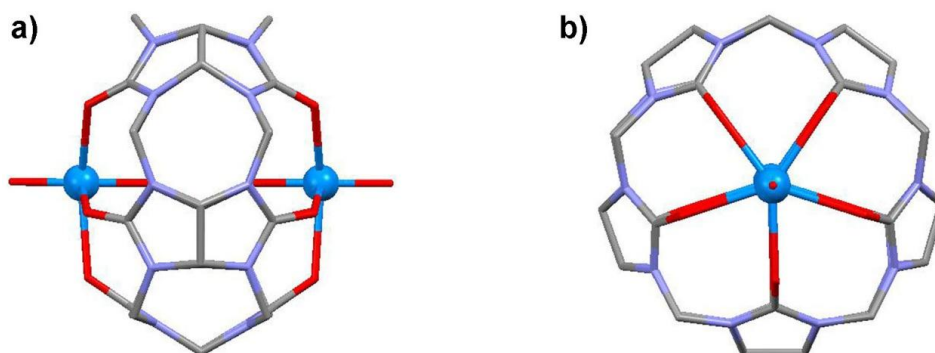


Figure 1-3 Crystallographic structure of coordination compound of UO_2 to Q[5] in a ratio of 2 : 1. a) side-view; b) top-view. Color codes: carbon, gray; nitrogen, blue; oxygen, red; uranium, light blue.

Uranyl ion (UO_2^{2+}) coordinated to five carbonyl groups at one portal of Q[5], and in the presence of alkali metal salts, K^+ or Cs^+ occupied another portal to form mixed capsules as discrete dicationic species [14]. Recently, the coordination of

uranyl ion to Q[5] has been applied for analytic purpose. The complex of uranyl ion and Q[5] oligomer has been sustained on the surface of palm shell powder to realize a selective extraction for uranium, and the key point of selectivity could be the high capability of the carbonyl groups on the portals of cucurbit[5]uril to bind uranyl cation [15]. The fluorescence of uranyl cation has been improved by the formation of exclusion complex between Q[5] and the metal ion in a ratio of 1 : 2, which formed a molecular capsule (Figure 1-3) [16].

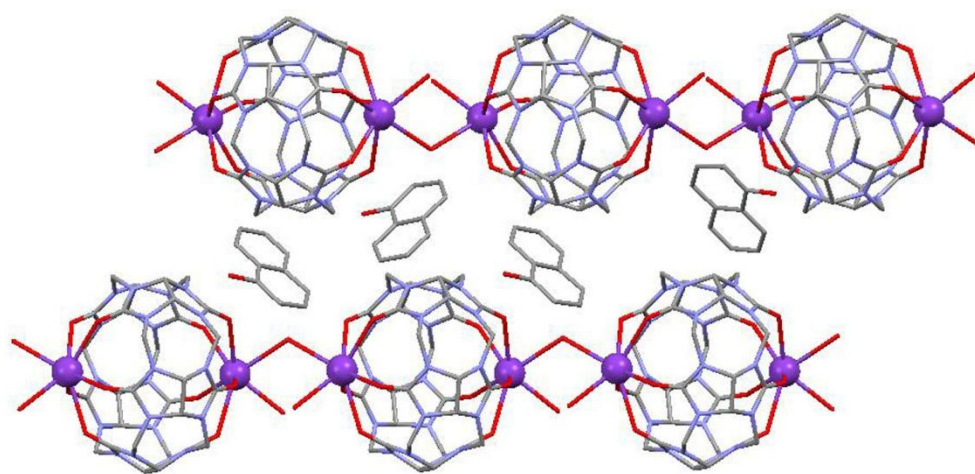
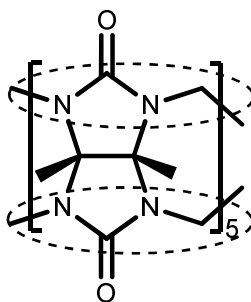


Figure 1-4 Crystallographic structure of 1D supramolecular chains making of the molecular capsules of $(K^+)_2Q[5]$ and α -naphthol. Color codes: carbon, gray; nitrogen, blue; oxygen, red; potassium, purple.

The coordination compounds of Q[5] with mono-cationic species, K^+ and Tl^+ , has the ability to induce room-temperature phosphorescence (RTP) of α -naphthol and β -naphthol (luminophores). The X-ray crystallographic structures revealed that metal cation (K^+ or Tl^+) and the macrocyclic compound formed the 1 dimension infinite supramolecular chains in a cross-linking model of $(\dots Q[5] \dots M^+ \dots Q[5] \dots M^+ \dots)$, which surrounded the luminophores to provide a microenvironment that enclosed the luminophore and the heavy atom together (Figure 1-4) [17]. The organic molecule induced supramolecular self-assemblies of Q[5] to alkali and alkaline earth metal ions play more and more important role in the Molecular and Crystal Engineering of cucurbiturils [18–20], to design and prepare novel crystal materials. The

self-assembly of Q[5] to K^+ in the presence of *p*-hydroxybenzoic acid formed 6-membered ring structures in crystal state, and this material is able to absorb some organic gas with selectivity depending on the size of substrate molecule [21].

1H NMR suggested cucurbit[5]uril exhibited the capability to include organic ammonium ions, pentan-1-aminium and 6-aminohexan-1-aminium, inside the hydrophobic cavity, while in the case that a modified cucurbit[5]uril, Decamethylcucurbit[5]uril (DMQ[5], Scheme 1-1), served as the host, both above guests just stayed at the portal of DMQ[5] as a lid [22]. In further investigations, the exclusion complex of ammonium lidded DMQ[5] has been designed as the material to act as an absorber to gas guest, such as NO_2 , O_2 , methanol and acetonitril [23].



Scheme 1-1 Structure of Decamethylcucurbit[5]uril (DMQ[5])

1.3 Host-guest interactions of cucurbit[6]uril

Cucurbit[6]uril (Q[6]) was the first discovered member of cucurbituril family as an organic ligand to Ca^{2+} in acidic condition as mentioned above [2]. The solubility of this macrocyclic compound is very poor in aqueous solution, interestingly, the presence of alkaline or alkaline earth metal cations could improve its solubility greatly, which dropped a hint of coordination of metals to Q[6] [24-27]. The evidences of X-ray crystallographic analysis supported the formation of coordination compounds. Despite of above mentioned case that two molecules Ca^{2+} lidded two portals of Q[6] to produce a molecular capsule, Cs^+ bound one portal of Q[6] to form a molecular bowl (Figure 1-5) [28]. The interesting property could provide an opportunity to

develop the novel Metal-Organic-Frameworks (MOFs) materials involving cucurbit[6]uril as building block. For the different diameter from Q[5], Q[6] coordinated to Cd^{2+} in a ratio of 1 : 2, and the single crystal structure shown the two Cd^{2+} cations occupied two portals of Q[6] separately through ion-dipole interactions, in which a two-dimensional network was observed, and the association constant of $K_a \approx 10^{10} \text{ L} \cdot \text{mol}^{-1}$ suggested there was very strong binding affinity [29]. Rubidium cation and Q[6] formed a one-dimensional coordination polymer in the solid state in which cucurbituril molecules bound Rb^+ through coordination of their carbonyl groups to the metals in a cross-linking fashion, and the supramolecular chains were organized to form a honeycomb structure with linear, hexagonal cells filling with water molecules [30]. Another alkali metal, K^+ , can also coordinate to Q[6] to produce the honeycomb structure with hexagonal cells in crystal state like that in the case of coordination of Rb^+ and cucurbit[6]uril [31]. The coordination of Q[6] to lanthanide(III) species shown different models depending on the conditions of crystallization, and the coordination ratios of 1 : 1, 1 : 2, and 2 : 3 could be found in the complexes of cucurbituril and metal ions [32].

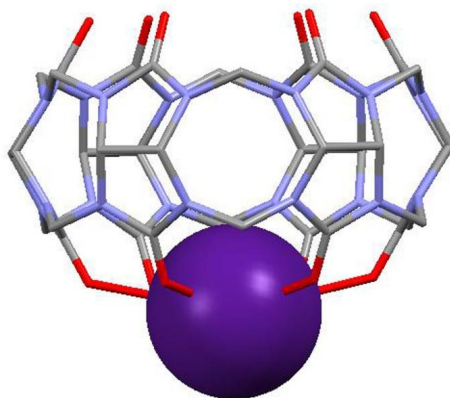


Figure 1-5 X-ray crystal structure of a molecular bowl from complex of Q[6] and Cs^+ .

Color codes: carbon, gray; nitrogen, blue; oxygen, red; cesium, purple.

In the host-guest interactions of Q[6] with alkylamino, the host shown very high selectivity depending on the structures of guest (Table 1) [11]. Based on the pioneering work of Mock's group, a great development of the host-guest chemistry

has been achieved in last three decades. The hydrophobic cavity has ability to contain neutral guest such as Xe, THF, and $\text{CF}_3\text{CO}_2\text{H}$ [33,34], and encapsulation of halogen, molecular dibromine and diiodine, within the cavity of Q[6] have been described by x-ray single crystal structures (Figure 1-6) [35].

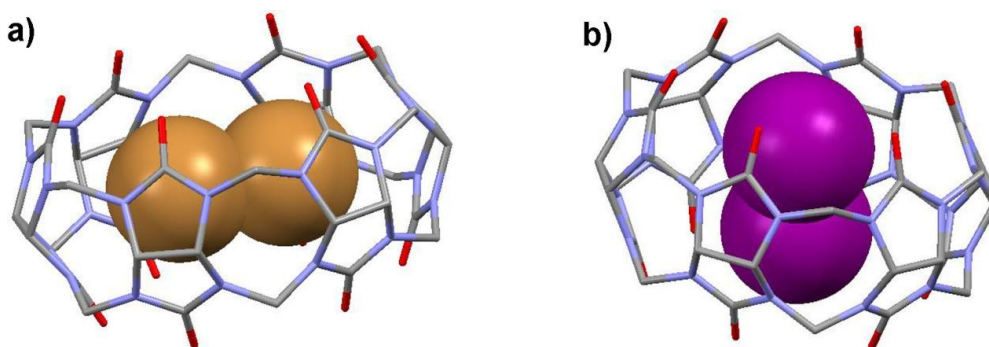
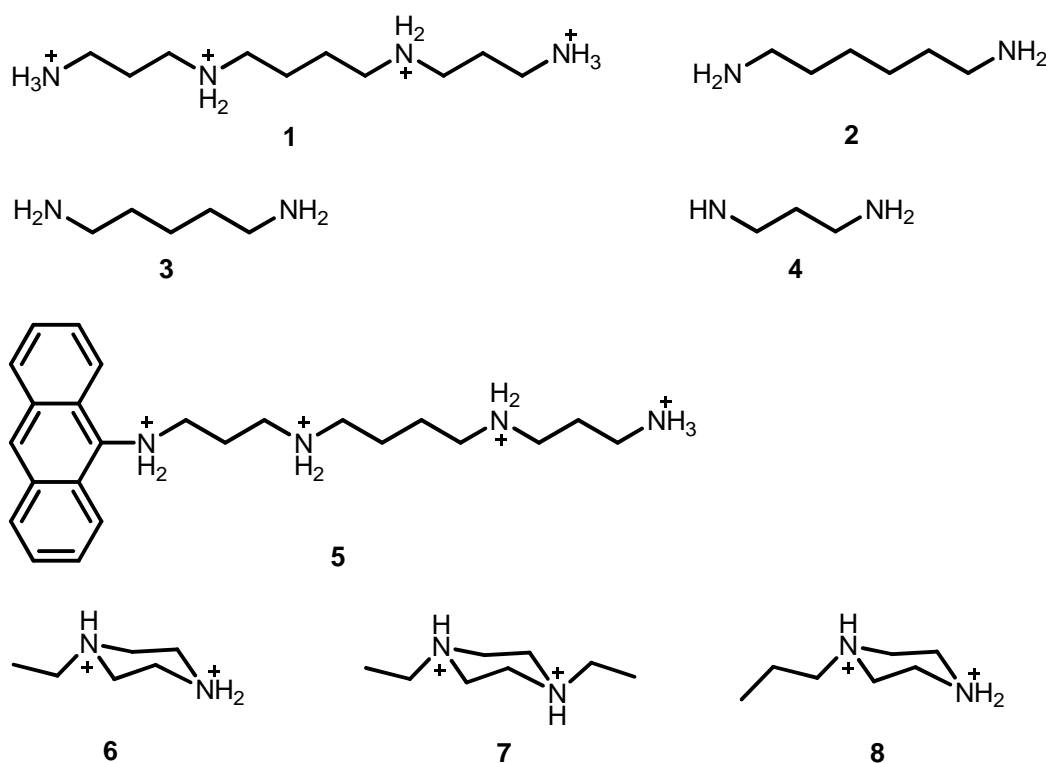


Figure 1-6 X-ray crystal structures of a) dibromine and b) diiodine within the cavity of Q[6]. Color codes: carbon, gray; nitrogen, blue; oxygen, red; bromine, brown; iodine, purple.

Cucurbituril exhibits extra high affinity to positively charged guests binding carbonyl groups on the portals through ion-dipole interactions, especially, protonated amines. This could also be the reason for the enhanced solubility of Q[6] in salt solutions. The most stable interaction has been found in the case of encapsulation of protonated spermine (Scheme 1-2, 1) by Q[6] to form a pseudorotaxane with the association constant $K_a = 3.3 \times 10^9 \text{ L} \cdot \text{mol}^{-1}$. With decrease of number of protonated amino groups and the chain length, the stabilities are decreasing gradually. The association constants of interactions of 1,6-hexane-diammonium (Scheme 1-2, 2), 1,5-pentanediammonium (Scheme 1-2, 3) and 1,4-butanediammonium (Scheme 1-2, 4) with Q[6] are 2.9×10^8 , 1.5×10^8 , and $2.0 \times 10^7 \text{ L} \cdot \text{mol}^{-1}$, respectively, while 1,3-propane-diammonium (Scheme 1-2, 5) cannot enter into the cavity of Q[6] and just stays at the portal as an exclusion complex with a very low constant of $3.3 \times 10^2 \text{ L} \cdot \text{mol}^{-1}$ for the small dimension [36]. The very strong binding of spermine with Q[6] allow the macrocyclic compound to be delivered to DNA. The acridine modified spermine has been designed to be included in the cavity of Q[6] to produce a

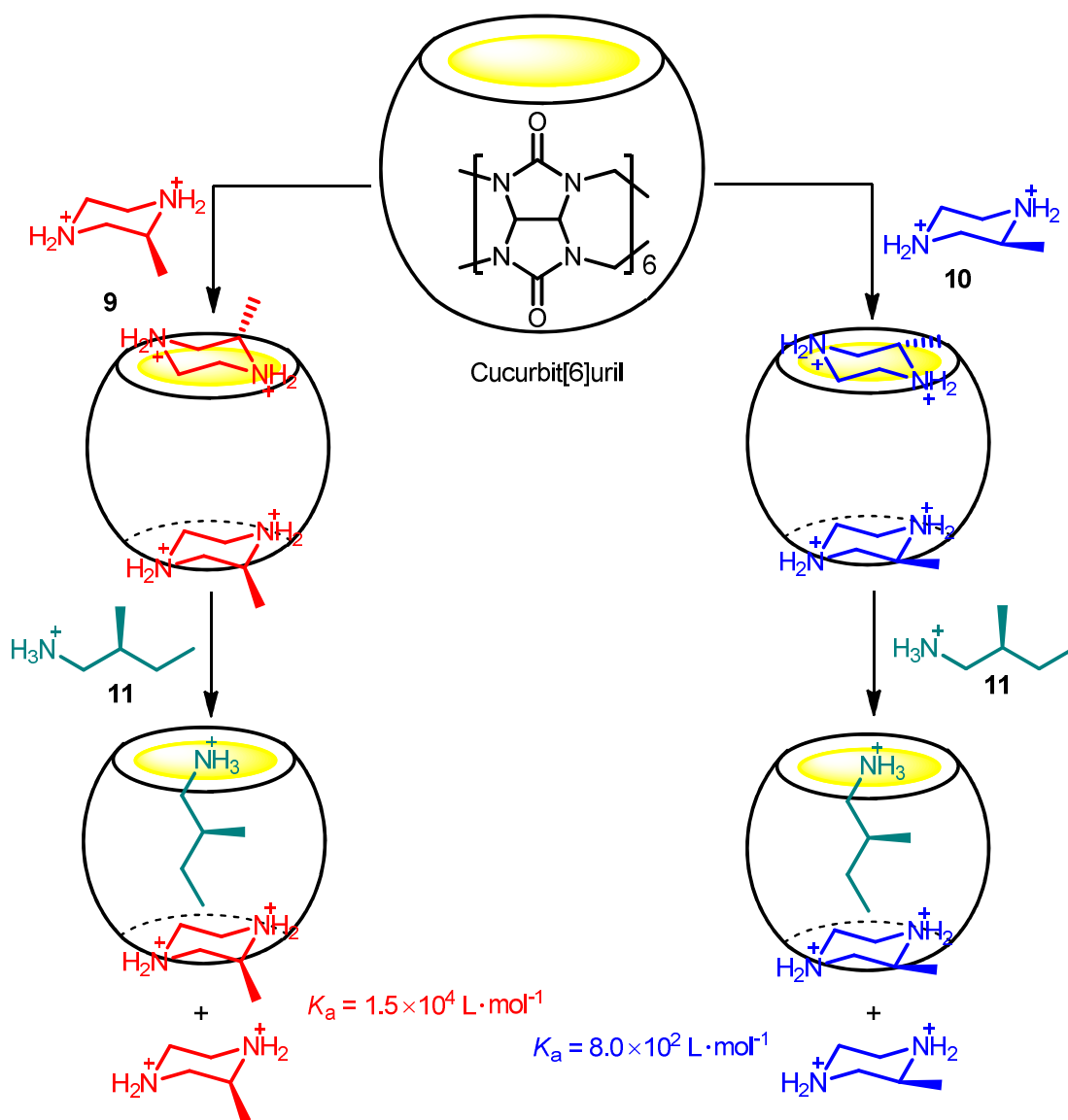
pseudorotaxane, with acridine group inserted into DNA, a ternary supramolecular system of Q[6]-guest-DNA was formed, which restrained supercoiled DNA from cleavage by the restriction enzyme BanII. [37,38]. *N*-alkyl- and *N,N'*-dialkylpiperazine dications induced the oligomeric supramolecular complex formation involving cucurbit[6]uril as the monomers by host-guest interactions. The stabilities of the interactions were dependence on the structures of substrates. The association constant of interaction between protonated *N*-ethylpiperazine (Scheme 2, 6) and Q[6] was only $2.3 \times 10^2 \text{ L} \cdot \text{mol}^{-1}$, and when one more ethyl group was induced on the piperazine body (*N,N'*-diethylpiperazin) (Scheme 1-2, 7), stability of the interaction was improved by almost 4.5 times with the constant of $1.2 \times 10^3 \text{ L} \cdot \text{mol}^{-1}$. In the case of host-guest interaction between protonated *N*-propylpiperazine (Scheme 1-2, 8) with Q[6], the constant was increased to $1.6 \times 10^4 \text{ L} \cdot \text{mol}^{-1}$ [39].



Scheme 2 Protonated amines serving as the guests of cucurbit[6].

The chiral recognition property has been realized by the formation of achiral host, cucurbit[6]uril, and chiral guest, protonated 2-methylpiperazine (Scheme 1-3). (*R*)- or

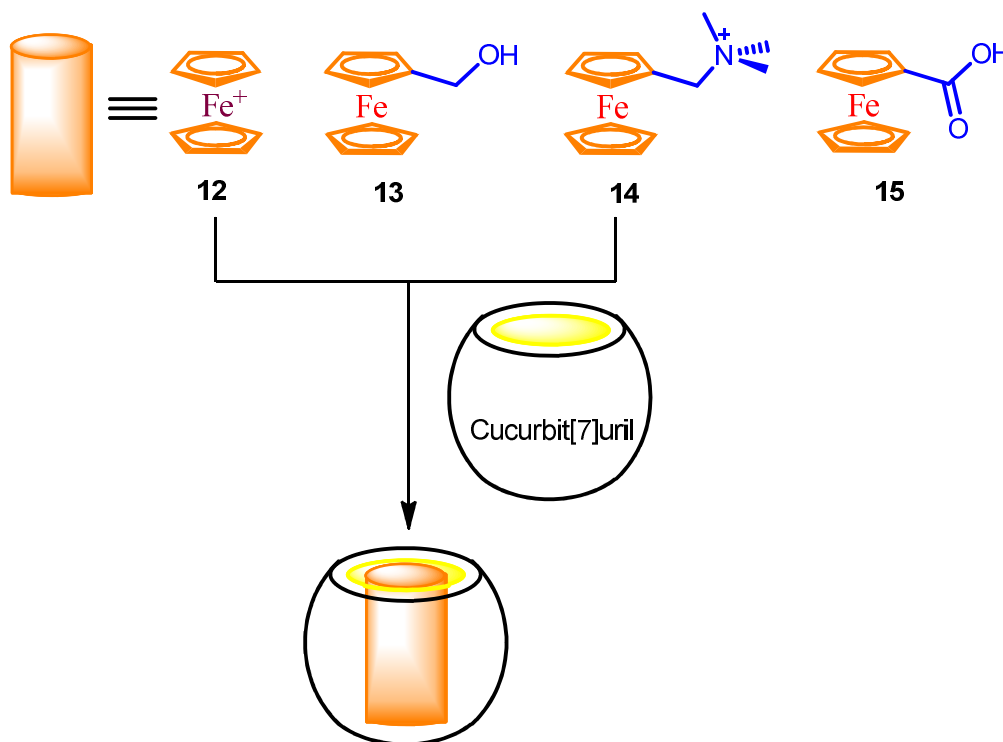
(*S*)-2-methylpiperazine (Scheme 1-3, **9** or **10**, respectively) interacted with Q[6] to produce exclusions in a ratio of 1 : 2 (host : guest). Both the interaction complexes were able to accommodate a chiral guest, (*S*)-2-methylbutylamine (Scheme 1-3, **11**) with different capabilities, and the one of guests binding in the first step have been released synchronously. When the portals was lidded by (*R*)-2-methylpiperazine, the inclusion complex of (*S*)-2-methylbutylamine in Q[6] was very stale, and the association constant is $1.5 \times 10^4 \text{ L} \cdot \text{mol}^{-1}$, which was almost twenty times of that induced by (*S*)-2-methylpiperazine, in which the constant was found as $8.0 \times 10^2 \text{ L} \cdot \text{mol}^{-1}$ [40].



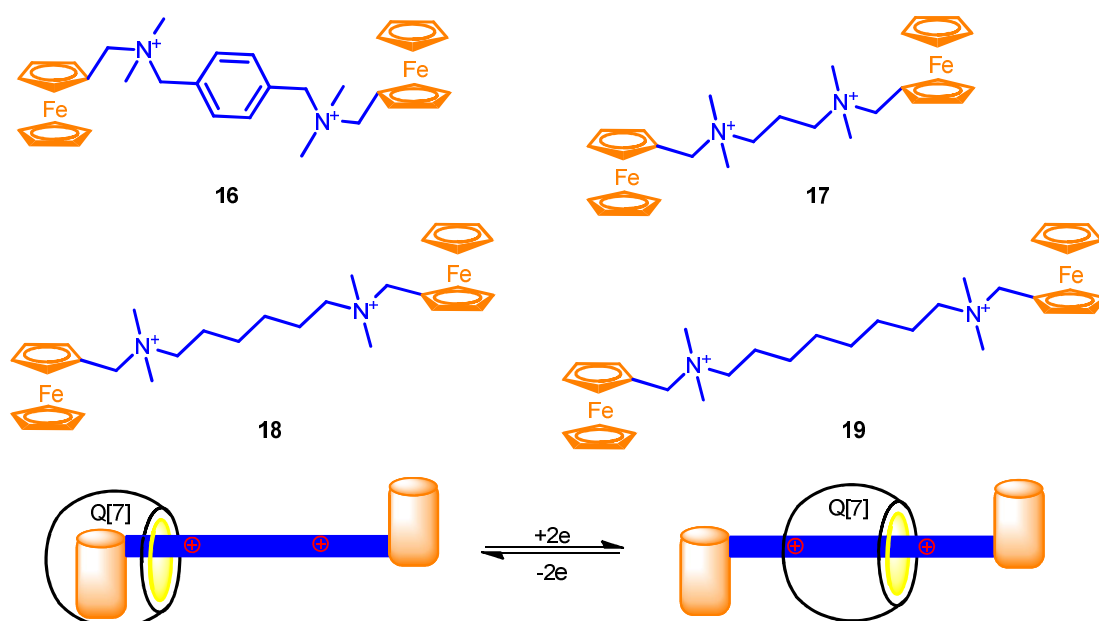
Scheme 3 Guest-induced chiral recognition of achiral host, cucurbit[6]uril.

1.4 Host-guest interactions of cucurbit[7]uril

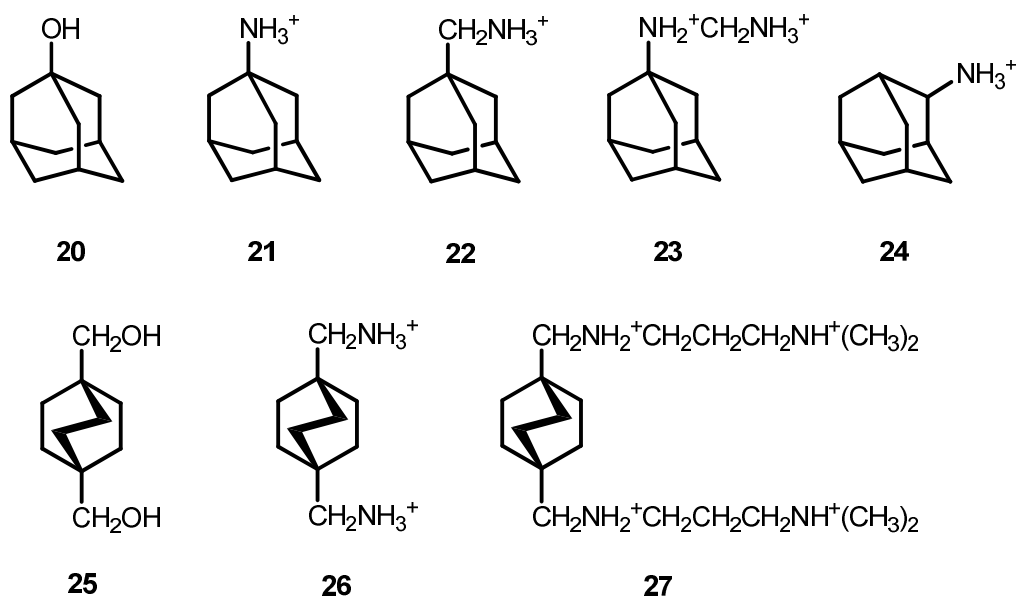
Cucurbit[7]uril (Q[7]), which has the best solubility in aqueous solution in cucurbituril family, was able to encapsulate tightly guest molecules too large to enter into the cavity of Q[6]. The monocationic ferrocenium (Scheme 1-4, **12**) could reside in the cavity of Q[7] with a association constant of $K_a > 10^6 \text{ L} \cdot \text{mol}^{-1}$, and its reduced species was also able to be encapsulated within the cavity [41]. Surprisingly, when hroxymethylferrocene (Scheme 1-4, **13**) was employed as the substrate, the neutral guest could form an inclusion complex with Q[7], and the association constant of $3.0 \times 10^9 \text{ L} \cdot \text{mol}^{-1}$ suggested the stability has been improved possibly due to inducing hroxymethyl group; The further enhanced stability has been achieved (K_a reached $3.0 \times 10^{12} \text{ L} \cdot \text{mol}^{-1}$) by modification of trimethylammoniomethyl group on ferrocene core (Scheme 1-4, **14**) to produce a positive charge; the anionic species, ferrocenecarboxylate (Scheme 1-4, **15**), could not be interact with Q[7] [42-43].



Scheme 1-4 Interaction of ferrocene substrates with Q[7]



Scheme 1-5 Electrochemical forced molecular shuttles based on the interactions of Q[7] with ferrocene derivatives.

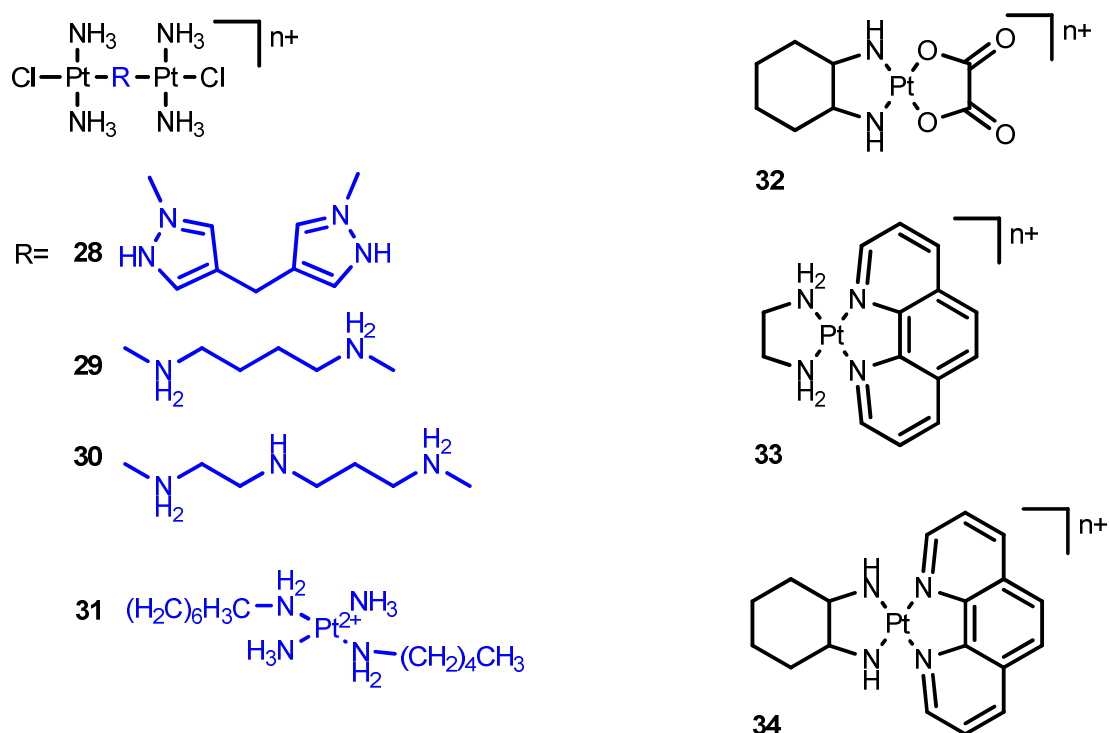


Scheme 1-6 substituted adamantanes and bicyclo[2.2.2]octanes served as Q[7]'s bicyclo[2.2.2]octanes

The response of Q[7] to positively charged ferrocene impelled the molecular shuttles drove by electrochemical redox have been designed and synthesized based on simple pseudorotaxane structures, in which the substrates included ferrocene

terminals linked by a spacer bar with positively charged quaternary ammoniums (Scheme 1-5, 16-19). Q[7] encapsulated one of ferrocene group of guest, and then the host slid to the chain spacer forced by electrochemical oxidation (Scheme 1-5) [44,45]. A very genius design to prepare a kind of Supramolecular Velcro has been realized based on the stable host-guest interaction of Q[7] and ferrocene substrate [46].

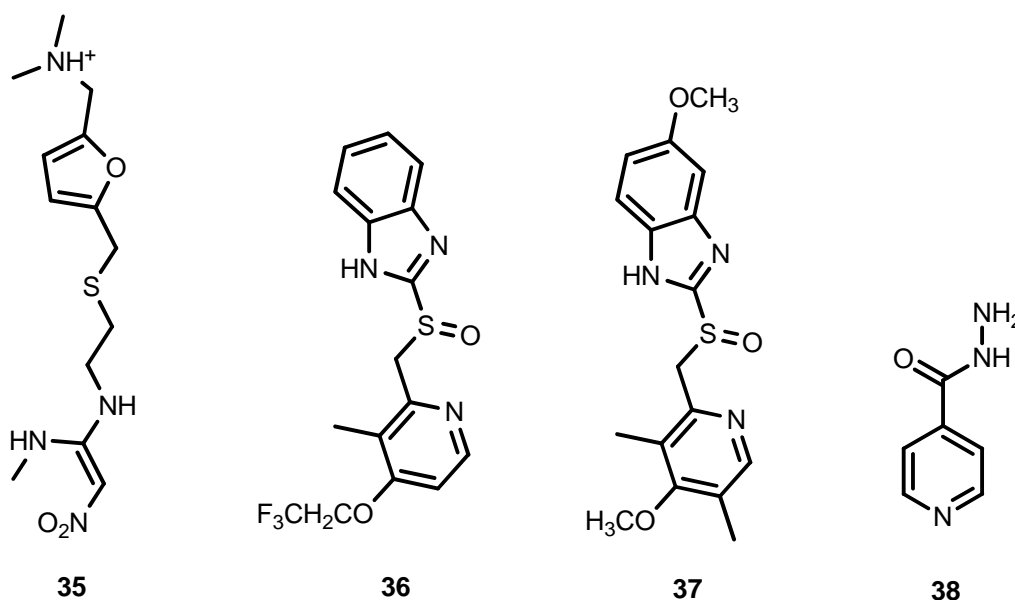
Recently, new guests, substituted adamantanes (Scheme 1-6, 20-24) and bicyclo[2.2.2]octanes (Scheme 1-6, 25-27) binding Q[7] very tightly were discovered. The most stable host-guest interactions were found in the cases of compounds 23 and 27 with association constants $> 10^{15} \text{ L} \cdot \text{mol}^{-1}$. In the other cases, the constants also reached $10^9 - 10^{14} \text{ L} \cdot \text{mol}^{-1}$. The investigation of thermodynamic data indicated entropy changes contributed to the molecular recognition more than did enthalpy changes [47,48].



Scheme 1-7 Platinum complex drugs encapsulated by Q[7]

The acceptable solubility of Q[7] in aqueous solution endow this host with the potential application for drug delivery [49-52]. The vitro studies indicated that Q[7] could be served as a stabilizing, and delivering agent for drugs with low toxicity, and

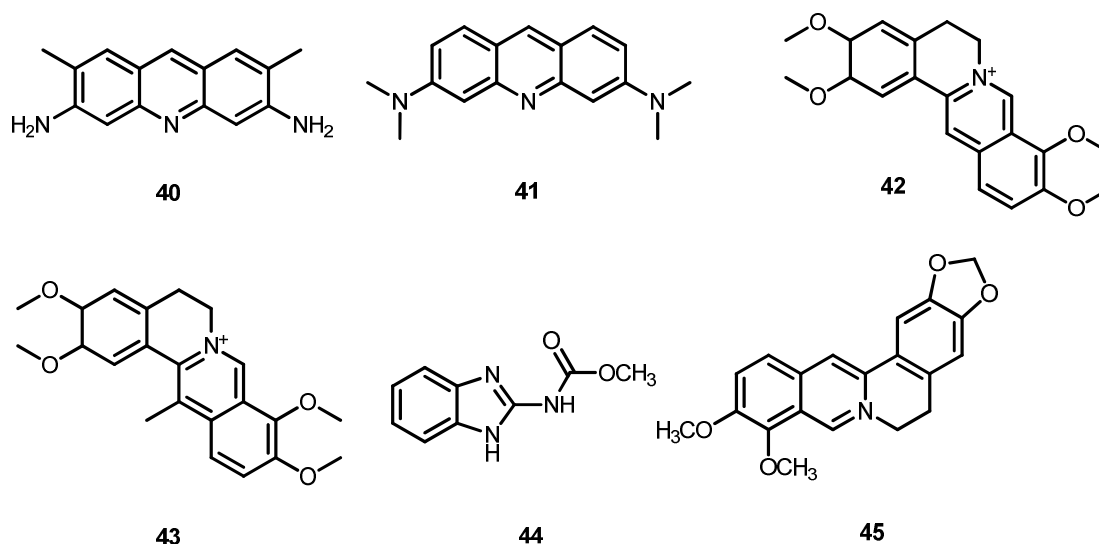
the results of investigation on cell cultures revealed an IC_{50} value of 0.53 ± 0.02 mM for CB[7], corresponding to around 620 mg of CB[7] per kg of cell material [53]. The pioneering investigation on Q[7]-encapsulated complexes with dinuclear platinum and multinuclear platinum (Scheme 1-7, 28-34), which are anti-cancer drugs commonly in clinical application, revealed that the participancy of cucurbit[7]uril were inefficient to improve the activity of this drug, but decreased the cytotoxicity greatly [55-58]. Further investigations of the screening of Q[n]-bound platinum complexes suggested that the cytotoxicity of macrocyclic compounds depends strongly on the cavity size, that is, Q[8] had the same effect as Q[7], but Q[6] increased the cytotoxicity [58].



Scheme 1-8 Organic drugs encapsulated by Q[7]

Ranitidine (Scheme 1-8, 35), Lansoprazole (Scheme 1-8, 36), and Omeprazole (Scheme 1-8, 37) are used for treatment towards gastric disease. The encapsulation of Ranitidine with in Q[7] protected this drug from thermal degradation in 2 weeks rather than a half-life of 4 days for free drugs at 50 °C and pH 1.5 [59]. The formation of host-guest interaction complexes between Q[7] and drugs, Lansoprazole or Omeprazole, improved the solubility of guest in aqueous solution and acidic solution by host-induced pK_a shift by even 4 pH units [60]. Isoniazid (Scheme 1-8, 38) is a powerful bactericidal agent to treat tuberculosis, and its encapsulation by Q[7]

resisted the acylation of this drug, which is believed to be responsible for the hepatotoxicity in treatment [61]. Further more potential applications of Q[7] for drug deliveries have been reported in last several years [62-65].



Scheme 1-9 Substrate dyes encapsulated by Q[7]

The host-guest interactions of Q[7] with luminescent molecules usually bring out the variety of photochemical and photophysical character of substrates [66-70]. The formation of interaction complex of Rhodamine B dye (Scheme 1-9, 39) with Q[7] shown a narrow-band high-efficiency dye laser [71], and the presence of Q[7] host also disrupted the aggregation of Rhodamine B dye in solid state to improve the photophysical property of dye-doped photonic materials [72]. The binding of Acridine Yellow (Scheme 1-9, 40) to Q[7] in a ratio of 1 : 2 improved fluorescence intensity by almost 10 times with longer life-time [73], and its homologue, Acridine Orange (Scheme 1-9, 41), was also able to be encapsulated within the cavity of Q[7] with enhanced fluorescence [74]. The competition of amino acids and oligopeptides to Acridine Orange in the interaction with Q[7] could impel a sensitive determining in biologic analysis [75]. The fluorescence of other dyes involving palmatine, dehydrocorydaline, carbendazim, and berberine (Scheme 1-9, 42-45) could be improved by formation of host-guest complexes [76-79]. The green emission of

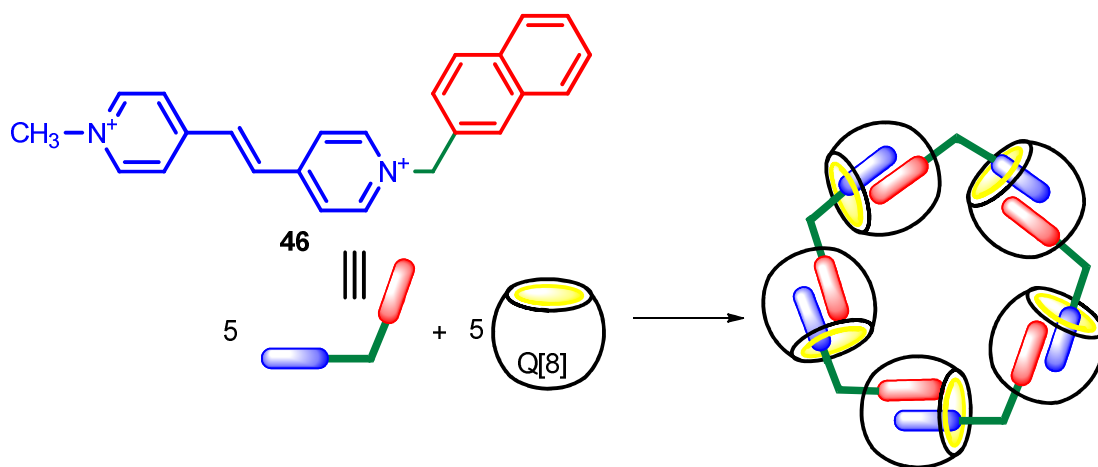
substrates shifting to blue with addition of Q[7] host has been designed as supramolecular switches [80,81], and more molecular devices based on Q[7]-induced changes of molecular luminescence have been reported recently [82-84].

1.5 Host-guest interactions of cucurbit[8]uril

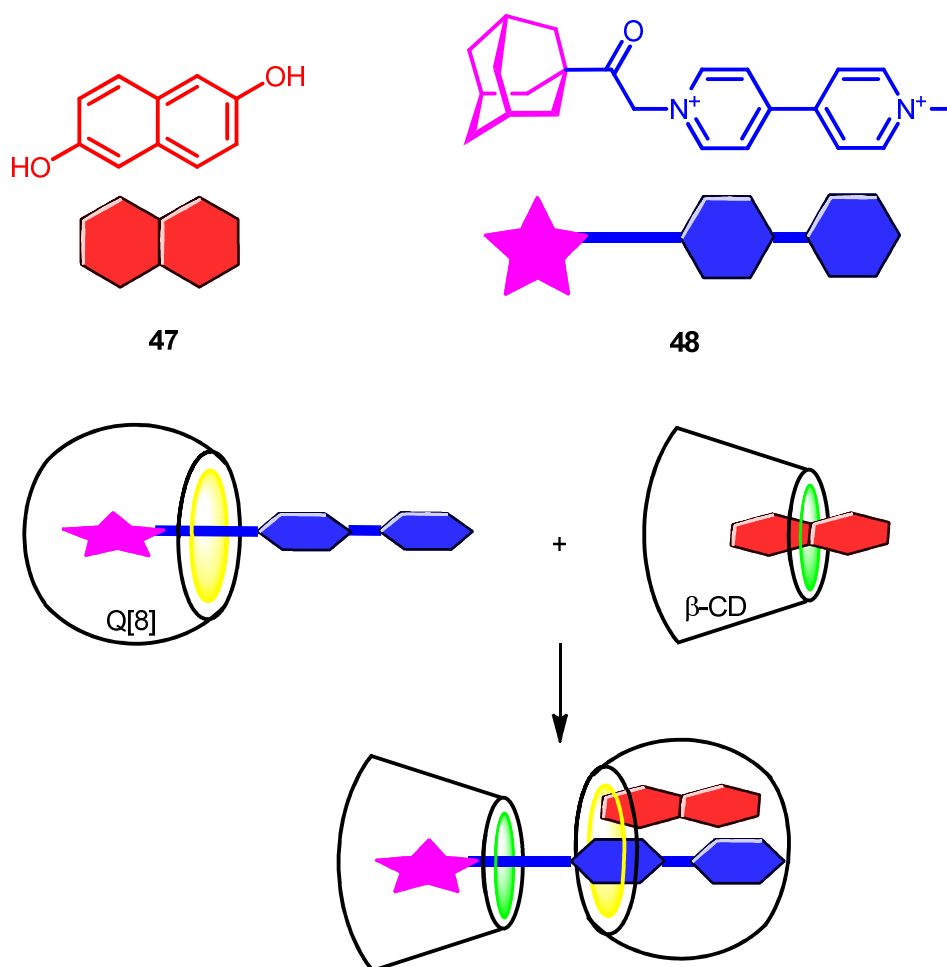
The larger cavity of cucurbit[8]uril (Q[8]) than those of above mentioned members in cucurbituril family has the capability to accommodate two guests. The electrochemical investigation shown that cation radical of methylviologen could be encapsulated within the cavity of Q[8] to form a 1 : 2 inclusion complex [85]. The seminal work on Q[8] with the mixed guests dihydroxynaphthalene and methylviologen (or its N-alkyl substitutions) in aqueous solution showed that the 1 : 1 : 1 ternary inclusion complexes of viologens, naphthalene diol and Q[8] were formed with charge-transfer interactions, in which naphthalene diol served as an electron-rich substrate to interact with electron-poor viologen [86]. The Q[8]-induced assembly of electron donors and acceptors should result from the matched electronic construction according to classic Fischer lock-and-key theory in the hydrophobic cavity. The unique properties of Q[8]-controlled stoichiometry and charge-transfer in host-guest interactions have been used extensively to design, construct and functionalize novel supramolecular building blocks, and to drive supramolecular machines and command devices confined within the Q[8] cavity.

Structural and functional supramolecular architectures and machines have been constructed inside the cavity of Q[8], according to the principles of stabilized assembly and enhanced charge-transfer of electron donors and acceptors by coupled encapsulation. The guest **46** (Scheme 1-10) including the electron donor and acceptor units bridged by a methylene vertex with an approximate angle of the equivalent pentagon, was self-assembled by encapsulation within the cavity of Q[8] to provide a cyclic pentameric supramolecular necklace [87]. On the same principle, a few redox-driven supramolecular devices and machines have been designed and

synthesized [88-91].



Scheme 1-10 Cucurbit[8]uril-induced supramolecular necklace.



Scheme 1-11 Formation of a heterowheel[3]pseudorotaxane including β -cyclodextrin and cucurbit[8]uril hosts.

A delivery of dihydroxynaphthalene (Scheme 1-11, 47) guest between the cavities of different macrocyclic compounds, β -cyclodextrin (β -CD) and cucurbit[8]uril to form a heterowheel[3]pseudorotaxane. The guest dihydroxynaphthalene could enter into the cavity of β -CD, and a viologen derivative (Scheme 1-11, 48) could be potential included by encapsulated adamantine moiety with Q[8]. The mixture of above two kinds of inclusion complexes brought on an interesting result that adamantine moiety on guest 48 has been included by β -CD, while dihydroxynaphthalene was transported into the cavity of Q[8] by the formation of ternary complex of the two guest with cucurbit[8]uril, that is, Q[8]-induced charge-transfer triggered the exchange of guests between different hosts [92]. With the charge-transfer effect, guests formed different inclusion complexes with Q[8] depending on acidity, amount of host, and structures of substrates [93-96]. Moreover, the Q[8]-induced charge transfer provide potential application for chemical and biologic analysis [97-100].

The Q[8]-induced assembly of polymers with viologen and naphthol terminal groups produced a supramolecular polymerization responding to electrochemical or optic signals [101, 102]. More supramolecular polymers have been synthesized with the formation of Charge-Transfer interaction between electron-donor and acceptor moieties in the cavity of Q[8] [103-106], recently, and the approach also has been applied for preparation and modification for nano- materials [107-110].

1.6 Host-guest interactions of cucurbit[10 and 14]urils

Cucurbit[10]uril (Q[10]) was obtained as a host of an inclusion complex in a macrocycle-in-macrocycle fashion, in which Q[5] was encapsulated in the cavity to be the largest guest of cucurbituril family so far (Figure 1-7). In the synthesis process, no Q[5]-free Q[10] has been isolated or detected, consequently, that Q[5] severed as a template has been speculated, however, the experimental evidence that the synthetic

yield of Q[10] could not be improved with addition of Q[5] disagreed this viewpoint. Both ^1H and ^{13}C NMR investigations revealed Q[5] was fast rotating in the cavity of Q[10] to produce a molecular gyroscope [111].

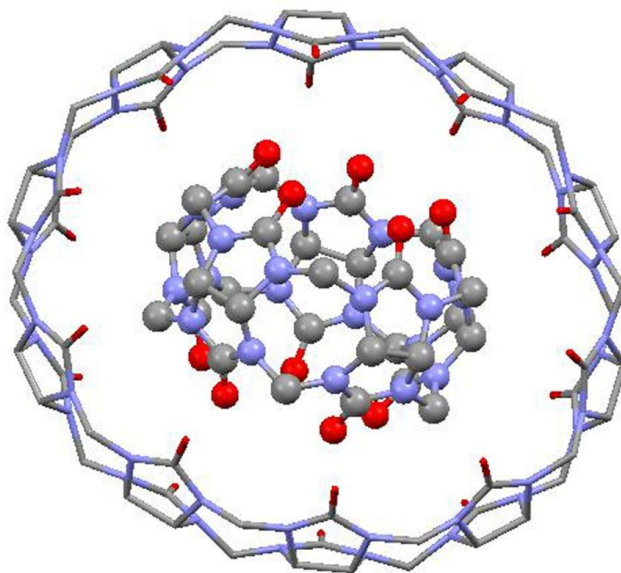


Figure 1-7 X-ray crystal structures of Q[10]-encapsulated Q[5]. Color codes: carbon, gray; nitrogen, blue; oxygen, red.

The formation of inclusion complexes of Q[10] host could be achieved by competition of Q[5] guest with other guests [112]. The cavity of cucurbit[10]uril was large enough for containing porphyrin and another guest to form ternary supramolecular assemblies [113], and the encapsulation of a Ir(III) polypyridyl complex within Q[10] enhanced the luminescence of guest [114]. The competition between guests has been developed as a effect method to isolated free Q[10] [115]. A homologue of Q[10], named nor-seco-cucurbit[10]uril (*ns*-Q[10]), has also been isolated, which was considered as the product of reorganization from Q[10] under heating condition, however, unlike Q[10], *ns*-Q[10] was obtained as a free host from isolation directly. The crystallographic structure revealed that *ns*-Q[10] included *p*-phenylenediamine in a ratio of 1 : 2, and two guests insert into the cavity of host simultaneously, to induce the macrocyclic compound to a bow tie shape (Figure 1-8). [116]. In the aspect of recognition of *ns*-Q[10] towards small organic molecules,

ns-Q[10] trended to encapsulate two similar guests which could be contained by Q[6] or Q[7] due to the comparable size of cavities, furthermore, the structure of *ns*-Q[10] is more flexible than that of other members of cucurbituril family; the investigations of a few host-guest interactions indicated the cavity could orientate unsymmetrical guests to different arrangement on dependence of structures of guests [116-118].

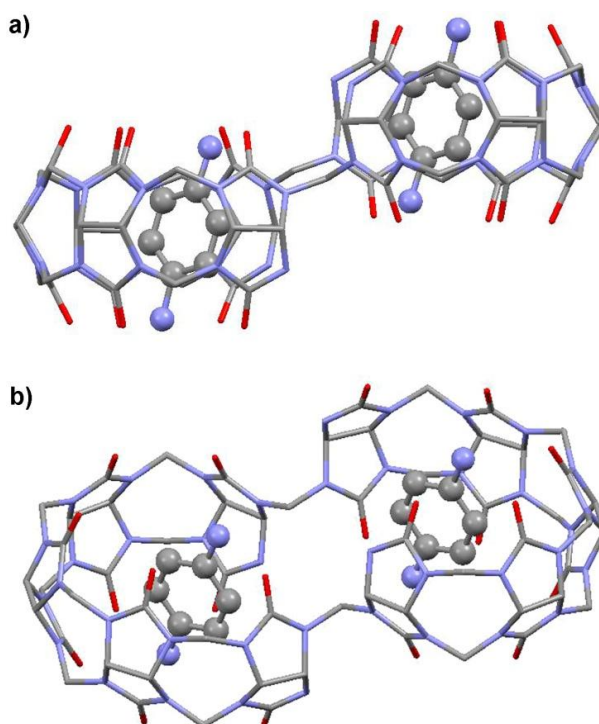
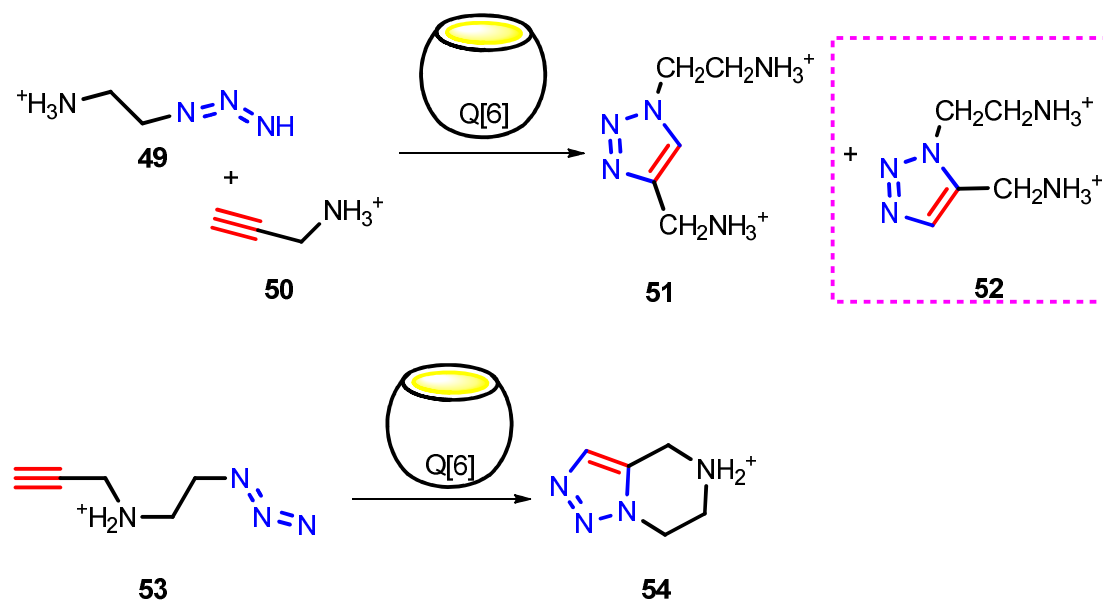


Figure 1-8 X-ray crystal structures of inclusion complex of *p*-phenylenediamine with nor-seco-cucurbit[10]uril. a) side view; b) cross-side view. Color codes: carbon, gray; nitrogen, blue; oxygen, red.

Cucurbit[14]uril (Q[14]) was reported very recently, which could be induced by coordination to Eu^{3+} to be a twist and chiral complex in crystallographic structure (Figure 1-1f) [6]. The structure of free Q[14] did not be characterized by crystallography, but ^1H and ^{13}C NMR suggested this macrocyclic compound should be symmetrical in solution for the similar assignment of resonance signals as other cucurbiturils.

2. Development of the supramolecular catalysis of cucurbiturils

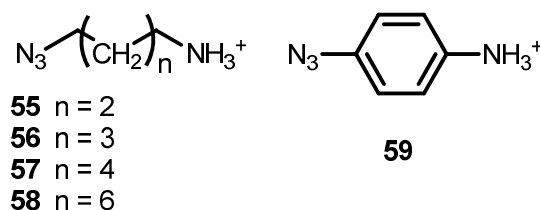
2.1 Supramolecular catalysis of cucurbit[6]uril



Scheme 1-12 Cucurbit[6]uril-catalytic 1,3-dipole cycloadditions

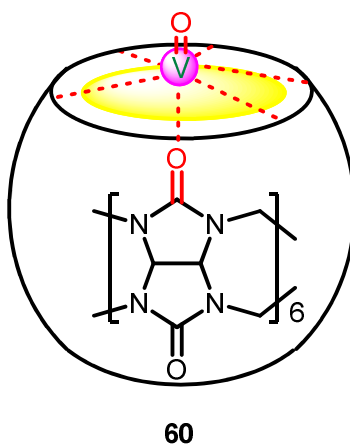
The first successful case of supramolecular catalysis of cucurbituril family was a Q[6]-improved 1,3-dipole cycloaddition of an alkyl azide (Scheme 1-12, **49**) with an alkynes (Scheme 1-12, **50**). The reaction provided both products **51** and **52** (Scheme 1-12) in the absence of macrocyclic compound; while just compound **51** was observed as the only product in the presence Q[6]. The above results indicated the cycloaddition could be controllable by Q[6] in thermodynamics. The key step in the supramolecular catalysis was release of product **51** from the cavity of macrocycle, which suggested the stereo-selectivity could be related to Q[6]-induced self-assemble of materials [119]. The host-guest interaction enhanced reactivity could be further proofed by kinetic evidence that the intramolecular cycloaddition of designed substrate **53** (Scheme 1-12) was accelerated by a factor of 10^3 with catalysis of Q[6] [120]. The Q[6]-catalytic reaction and slow release of product was used for synthesis of kinds of polyrotaxanes and supramolecular device including Q[6]-encapsulated

triazole components [121-124]. The mechanism of this supramolecular catalysis has been investigated by quantum chemistry. The 1,3-dipole cycloaddition had a thermodynamic barrier (calc. 60 kcal·mol⁻¹), which could be overcome by addition of Q[6] to conquer decrease of entropy in the cycloaddition. On the other hand, the transition state of product **52** was too large to be encapsulated within the cavity of Q[6], consequently, the regioisomer could not be produced [125].



Scheme 1-13 Substrates of Q[6]-catalytic decomposition

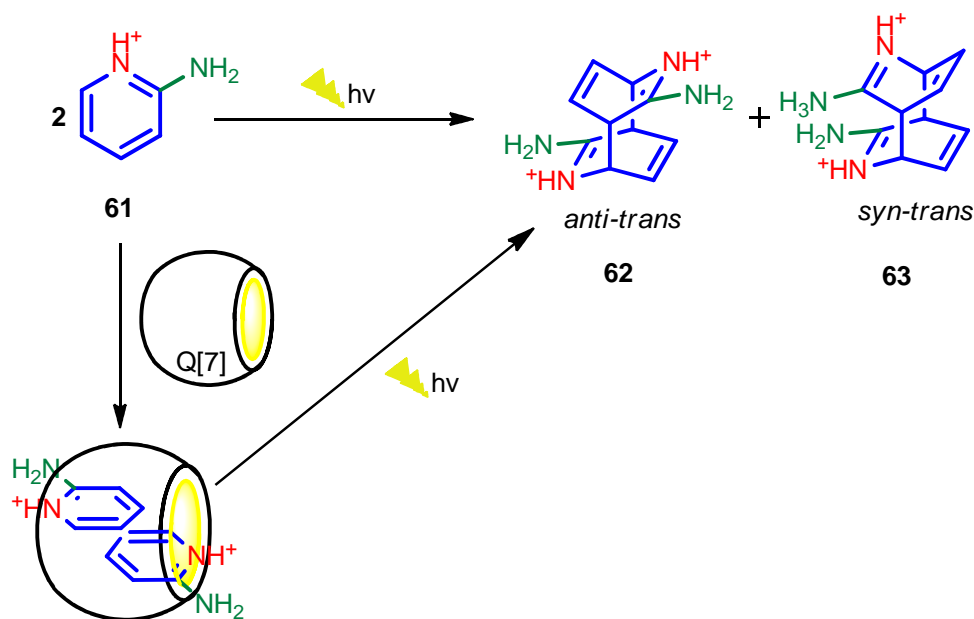
The azidoalkyl-1-amines (Scheme 1-13, **55-58**) and p-azidoaniline (Scheme 1-13, **59**) could form stable inclusion complexes with cucurbit[6]uril, and the stabilities were seriously dependence on the structures of substrates. The association constant K_a of **55** was $5.5 \times 10^3 \text{ L} \cdot \text{mol}^{-1}$, while the constants of other encapsulation complexes were decreased about 10 times. All of the substrates were stable in acidic aqueous solution, however, in the presence of Q[6] host, they were able to be decomposed with formation of inclusion complexes even in dark in few hours. The mechanism was proposed be related to host-induced $\text{p}K_a$ shifts of substrates [126].



Scheme 1-14 Formation of coordination complex of oxovanadium with Q[6].

The metal-participated supramolecular catalysis of cucurbit[6]uril has been discovered. Oxovanadium(IV) could form a complex with Q[6] at one portal of the macrocycle (Scheme 1-14, **60**). The oxovanadium-Q[6] complex catalyzed oxidation of linear alkanes in organic solution (Acetonitrile, Acetone, Dichloromethane, or benzene) as a heterogeneous catalyst. Oxovanadium(IV) was activated by coordination to carbonyl groups on cucurbit[6]uril, and substrates could be oxidized in the cavity of host, so the reactivity depended on the structures of substrates, and the catalytic oxidation was inactive in the cases of styrene, cyclohexane or *z*-cyclooctene, which were too large to be encapsulated by Q[6] [127].

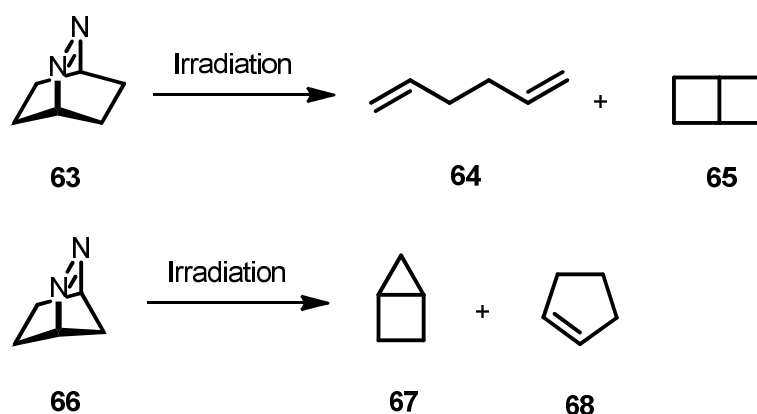
2.2 Supramolecular catalysis of cucurbit[7]uril



Scheme 1-15 Q[7]-catalytic photodimerization of 2-aminopyridine hydrochloride.

Two 2-aminopyridine hydrochloride **61** (Scheme 1-15) could be carried out a [4 + 4] photodimerization reaction to yield two isomers, *anti-trans* and *syn-trans* products (Scheme 1-15, **62** and **63**, respectively). The simultaneously encapsulated

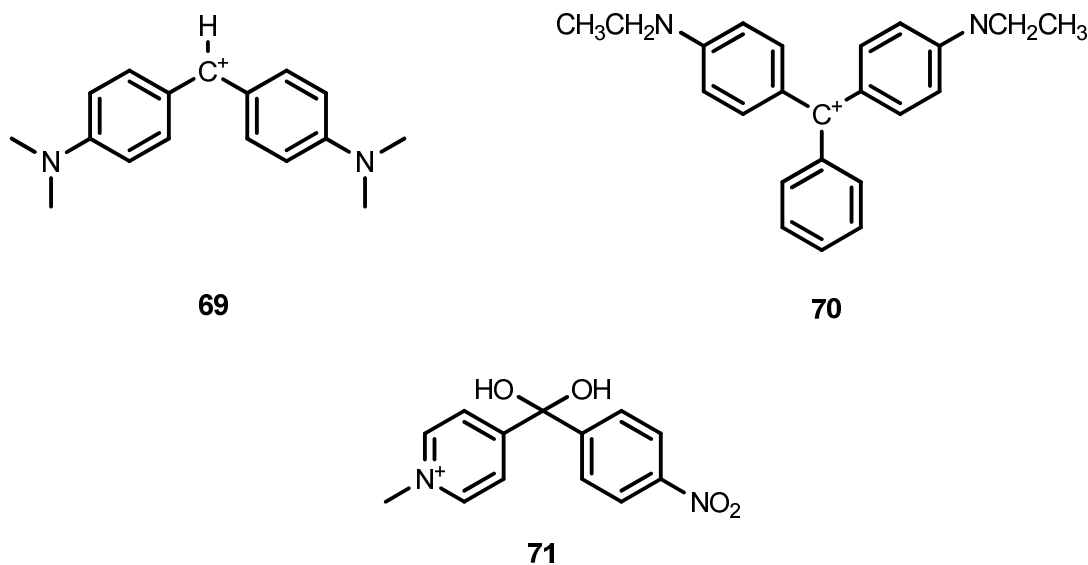
substrates by Q[7] realized a stereoselective photochemical dimerization, 4,8-diamino-3,7-diazatricyclo-[4.2.2.2^{2,5}]dodeca-3,7,9,11-tetraene (Scheme 1-15, 62). Investigation on the host-guest interaction revealed two pyridine guests enter into the cavity of Q[7] from the alternative portal and overlap each other in the *anti*-form, which could be stabilized by the ion–dipole interaction of the protonated nitrogen atoms on the guest with the carbonyl oxygen atoms distributed around the portals of Q[7]. Rotation of substrates in the cavity has been restrained, which resulted in the stereoselective photodimerization. However, kinetics of the photochemical dimerization indicated that the reaction rate could not be improved by the addition of Q[7] [128]. The chemoselective photoreactions have been achieved by the employment of complex of Q[7] with metal cations such as Ti^+ , Fe^{3+} , Co^{2+} , Ni^{2+} , Cu^{2+} , and Ag^+ . The distribution of products of irradiated compound 63 (Scheme 1-16, 63) was 65 : 35 (64 : 65, Scheme 1-16), while the addition of Q[7] tended to produce more product 64, consequentially, the distribution was improved to 87 : 13 (64 : 65). In the case of photolysis of compound 66 (Scheme 1-16), the presence of complex of Q[7] with Ag^+ afforded both products of 67 and 68 (Scheme 1-16) in a ratio of 59 : 41 (67 : 68), while product 67 was exclusively observed in the absence of the macrocycle and metal cations [129].



Scheme 1-17 Photolysis of bicyclic azoalkanes.

With ion-dipolar interactions, the positively charge chemical intermediates could be stabilized by cucurbit[7]uril. 4,4'-Bis(dimethylamino)diphenylmethane

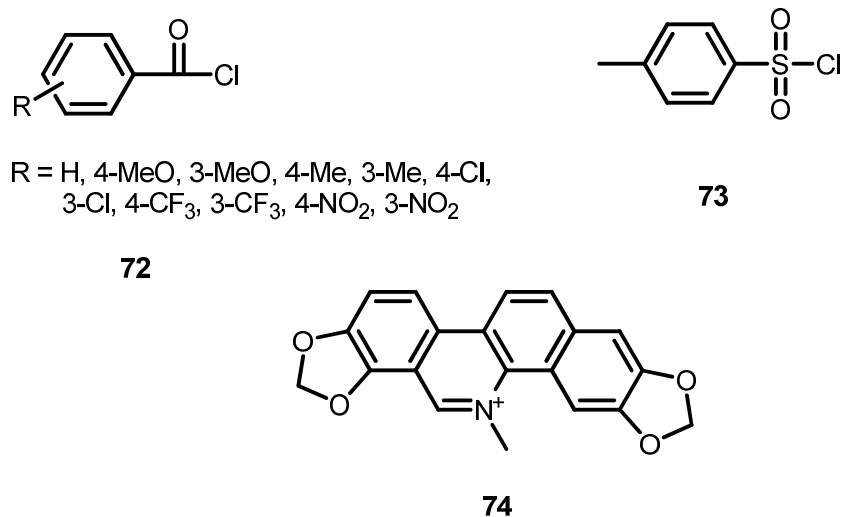
carbocation (Scheme 1-17, **69**), a classic diarylmethane carbocation, was able to be encapsulated within the cavity of Q[7] with a moderate association constant of $K_a = 2.0 \times 10^4 \text{ L} \cdot \text{mol}^{-1}$, and the content of **69** was maximized up to 90% among the three resonance forms in the presence of Q[7] [130]. The triarylmethane carbocation brilliant green **70** (Scheme 1-17) has been stabilized by encapsulation within Q[7] [131]. The transformational equilibrium of ketone to the hydrated ketal of *N*-methyl-4- (*p*-substituted benzoyl)pyridinium cation **71** (Scheme 1-17) has been evaluated in the presence of Q[7], and the ketone form with a positively charged carbon on carbonyl group could be partially included in the cavity of Q[7] [132,133]. The Q[7]-stabilized chemical intermediate has also been applied for novel route of organic synthesis. The radical cation of benzenamine encapsulated within the cavity of Q[7] has been used directly to synthesize polypseudorotaxane with the polyaniline axle threaded through cucurbit[7]uril macrocycles [134].



Scheme 1-17 Chemical intermediates stabilized by Q[7].

In the aspect of negative catalysis, the encapsulation of Q[7] has been able to restrain the substrate from chemical reaction. A comparative investigation on the solvolysis of a series of substituted benzyl chlorides (Scheme 1-18, **72**) in the presence of cucurbit[7]uril and β -cyclodextrins (β -CD) indicated that the reaction

could be catalyzed by β -CD but inhibited by Q[7] for electron withdrawing substituted substrates, while the solvolysis of electron donating substituted benzyl chlorides could be improved by Q[7] but inhibited by β -CD. The above difference has been explained by different pathway of the solvolysis going through, associative mechanism or dissociative mechanism [135]. 4-Methoxybenzenesulfonyl chloride (Scheme 1-18, 73) could also been protected from hydrolysis by the encapsulation in the cavity of Q[7] [136]. Sanguinarine (Scheme 1-18, 74), a biologically active natural benzophenanthridine alkaloid, interacted Q[7] with a slow shift between 1 : 1 and 1 : 2 (G : H) interaction models, which resulted in an inhibition from nucleophilic attack and photooxidation of substrate [137].

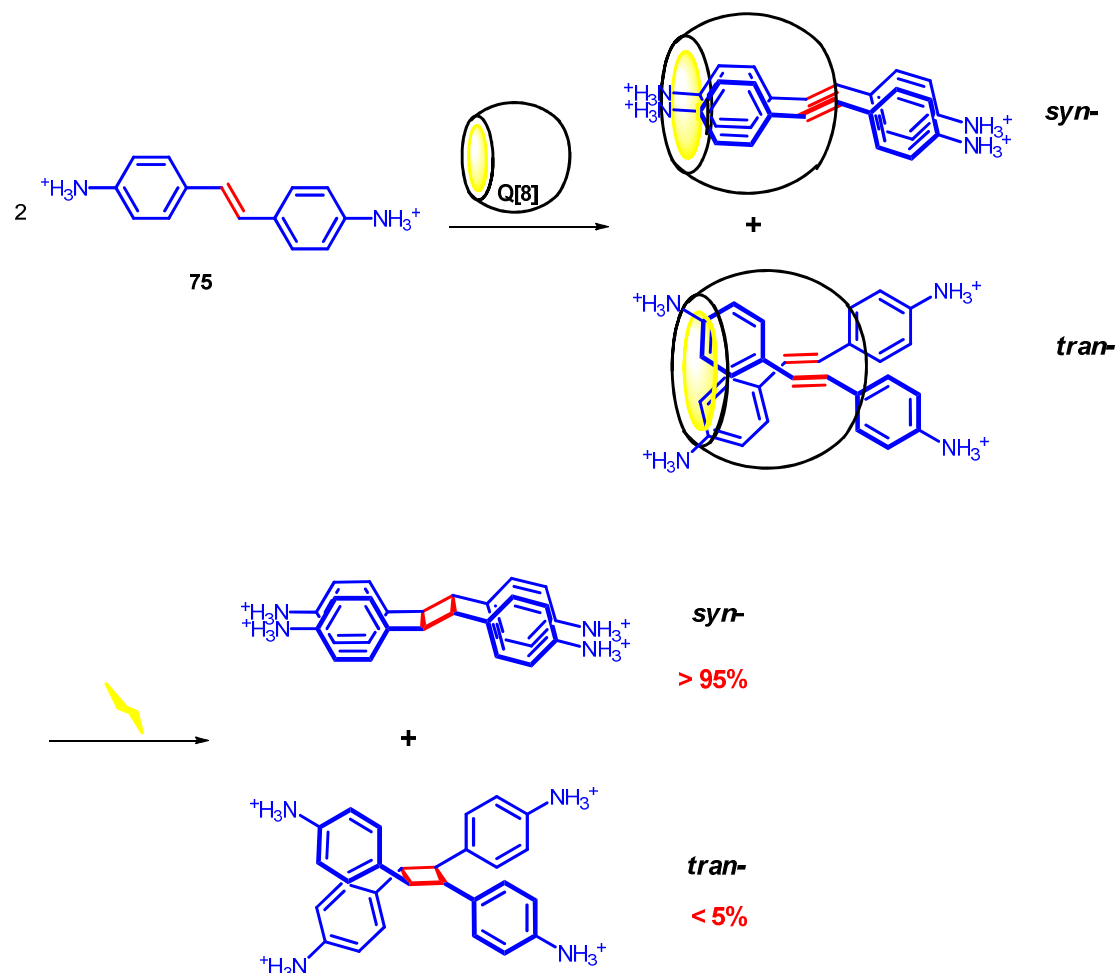


Scheme 1-18 Substrates inhibited from chemical reactions by Q[7].

2.3 Supramolecular catalysis of cucurbit[8]uril

As mentioned above, the cavity of cucurbit[8]uril is enough large to contain two small organic guest, and the unique property makes this macrocycle proper for a micro-cell to catalyze reactions. The first case of Q[8]-catalytic photodimerization was discovered in 2001, in which (*E*)-diaminostilbene dihydrochloride (Scheme 1-19, 75) carried out a [2 + 2] photoreaction in the presence of Q[8], and the reaction rate and stereoselectivity was improved obviously, that is, with the supramolecular

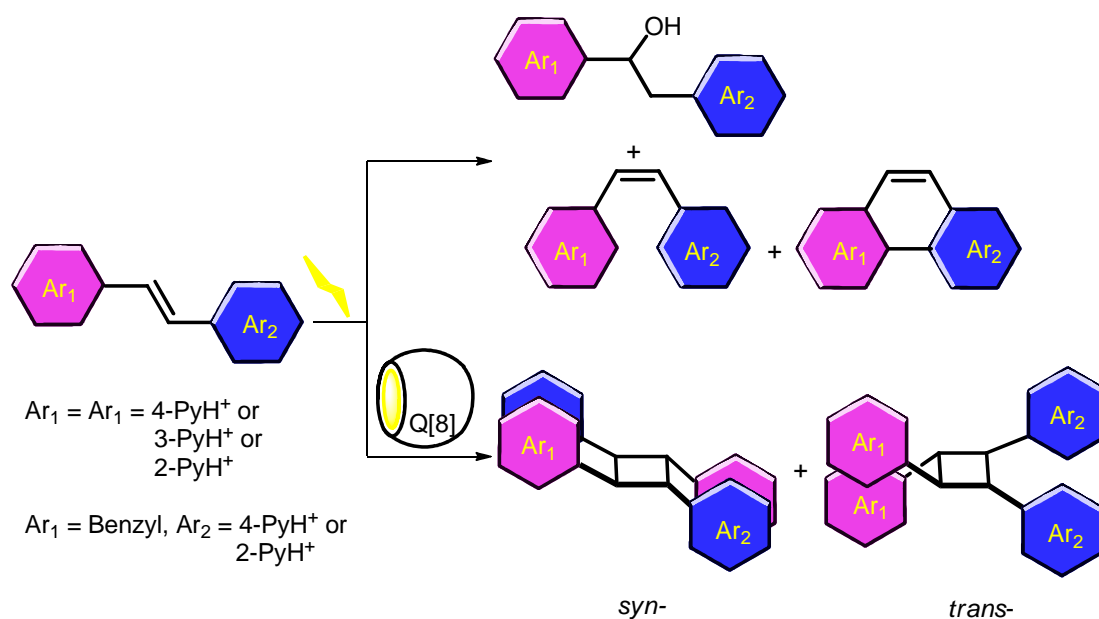
catalysis, the ratio of *syn*- to *trans*- products was 95 : 1, while the stereoselective ratio was 80 : 20 in the presence of γ -CD. The formation of ternary complex was confirmed with an association constant of $3.8 \times 10^4 \text{ L}^2 \cdot \text{mol}^{-2}$, and orientation to *syn*-conformation of two guest was favorite in the cavity of Q[8] [138].



Scheme 1-19 Photodimerization of (*E*)-diaminostilbene dihydrochloride in the presence of cucurbit[8]uril.

The further investigations on the photodimerization of 1,2-bis(n-pyridyl)ethylenes and stilbazoles revealed that only addition of water, isomerization and intramolecular photoreaction of substrates were observed in the absence of Q[8]; while the photodimerization with addition of Q[8] afforded *syn*-products mainly with very high yield from 81-91% (Scheme 1-20). The controllability of stereo conformation of products was considered as the result of host-induced

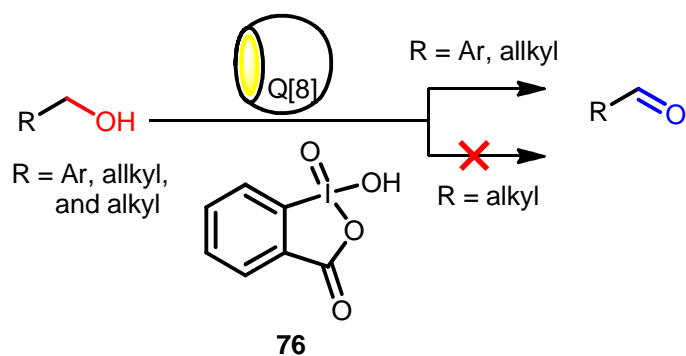
parallel arrangement of two guest molecules in the cavity of Q[8], which was proofed by crystallographic evidence of formation of ternary host-guest inclusion complex [139-143]. More cases have been discovered that cinnamic acids [144,145], 2-naphthoates or 2-naphthalenecarbonitrile [146-148], coumarins [149-152], and anthracene [153-156], could also be employed as the substrates of Q[8]-induced photodimerization, and the macrocycle always plays an important role to realize high stereoselectivity.



Scheme 1-20 Q[8]-induced photodimerization 1,2-bis(n-pyridyl)ethylenes and stilbazoles.

Cucurbit[8]uril has also been applied to enhance IBX (*o*-Iodoxybenzoic acid, Scheme 1-21, 76) oxidation of alcohols, and the product yields of aldehydes was obviously improved with addition of Q[8]. With veratryl alcohol employed as model substrate, the screening of reaction conditions indicated the supramolecular catalysis was in favor high temperature (95 °C), and just 10% mol macrocycle was enough for the improvement of oxidation. Other macrocyclic compounds involving cucurbit[6,7]urils and α,β,γ -cyclodextrin, were investigated as the catalysts, and the results illustrated Q[6,7] and α,β -cyclodextrin, whose cavities were smaller than that of Q[8], were inactive, while γ -cyclodextrin with similar cavity size to Q[8] offered about 15% improvement of the oxidation, which was just half of catalytic activity of

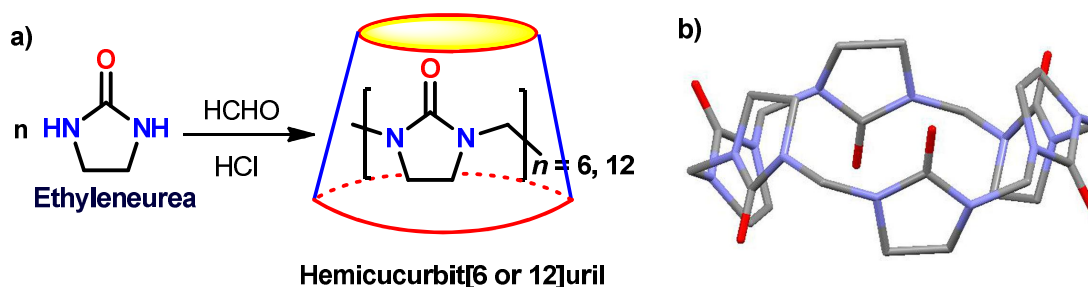
Q[8] [157]. The supramolecular catalysis was seriously depending on the structures of substrates, and oxidation of aryl and allyl alcohols were able to be enhanced by addition of Q[8], while IBX oxidation alkyl occurred hardly either in the absence or in the presence of Q[8] (Scheme 1-21). The selectivity implied the intermediate in this IBX oxidation could be stabilized by Q[8] [158].



Scheme 1-21 Q[8]-catalytic oxidation of alcohols by IBX.

3. Hemicucurbit[n]urils and their derivatives

3.1 Hemicucurbit[n]urils and their supramolecular properties



Scheme 1-22 a) Synthesis of hemicucurbit[6 or 12]uril; b) 1,3,5-alternate conformation of HemiQ[6] in crystal. Color codes: carbon, gray; nitrogen, blue; oxygen, red.

Hemicucurbit[n]urils (HemiQ[n], n = 6 or 12, [Scheme 1-22a](#)) have been found in 2004, which were synthesized by a cyclic oligomerization from ethyleneurea and formaldehyde to produce the macrocyclic compounds like cutting off a half along the equator of cucurbituril molecules. Unlike synthesis of cucurbit[n]uril, in which the mixture of kinds of Q[n] was produced, the formation of HemiQ[n] with different dimension was simply controllable with very high yields (usually more than 90%) by reaction acidity and temperature, that is, HemiQ[6] could be afforded in 4M HCl aqueous solution, at room temperature, while the cyclic reaction offered HemiQ[12] in a heating 1M HCl aqueous solution (55 °C) ([Scheme 1-22a](#)) [\[159\]](#). Since there is only one methylene chain bridged ethyleneurea units, the structures of HemiQs were flexible in solution with free rotation of ethyleneurea moieties, it intended to adopt a 1,3,5-alternate confirmation in crystalline state ([Scheme 1-22b](#)). On the other hand, HemiQs could dissolve into organic solvents, such as chloroform, methanol, and DMSO, while only Q[5 and 7] can dissolve into water and the solubility of Q[6 and 8] in aqueous solution is very poor without protonation or aid of guest. The unique

property offers a new opportunity to develop supramolecular chemistry of cucurbituril family in nonaqueous media.

Table 1-2 Solubility of HemiQ[6] with or without addition of metal cations, and the association constants (K_a) for coordination to metals^a

Salt	Solubility of HemiQ[6] (mol·L ⁻¹)	log K_a
—	$(3.8 \pm 0.2) \times 10^{-4}$	—
Co(NO ₃) ₂	$(5.5 \pm 0.2) \times 10^{-4}$	1.18 ± 0.02
Co(ClO ₄) ₂	$(5.4 \pm 0.3) \times 10^{-4}$	1.18 ± 0.02
Ni(NO ₃) ₂	$(6.2 \pm 0.2) \times 10^{-4}$	1.34 ± 0.04
Ni(ClO ₄) ₂	$(5.8 \pm 0.3) \times 10^{-4}$	1.34 ± 0.04
Cu(NO ₃) ₂	$(3.8 \pm 0.1) \times 10^{-4}$	—
AgNO ₃	$(4.5 \pm 0.2) \times 10^{-4}$	—
Cd(NO ₃) ₂	$(4.0 \pm 0.3) \times 10^{-4}$	—
TiNO ₃	$(4.0 \pm 0.2) \times 10^{-4}$	—
Pb(NO ₃) ₂	$(4.6 \pm 0.1) \times 10^{-4}$	—
CeCl ₃	$(3.8 \pm 0.3) \times 10^{-4}$	—
TmCl ₃	$(3.7 \pm 0.2) \times 10^{-4}$	—
LuCl ₃	$(3.8 \pm 0.2) \times 10^{-4}$	—
UO ₂ (NO ₃) ₂	$(9.2 \pm 0.3) \times 10^{-4}$	1.78 ± 0.03
UO ₂ Cl ₂	$(9.1 \pm 0.2) \times 10^{-4}$	1.78 ± 0.03

^a From ref. [160].

HemiQ[6] could also coordinate to some metal cations, and the results of dissolvability tests of this macrocycle in water in the presence of kinds of metals shown that the solubility could be improved by addition of only Co²⁺、Ni²⁺ and UO²⁺ with little increase of association constants (Table 1-2), and the interactions were obviously independent of the species of anions. The association constants of smaller than 100 indicated that the coordination of HemiQ[6] to metal cation should be very

weak, and the selectivity was different from that of Q[6] [160]. Comparatively, the affinities of HemiQ[6] with anions were stronger than that with above metals from the measured association constants in Table 1-3, and the independence of the interactions on species of cations was also observed [161].

Table 1-3 association constants (K_a) for interactions of HemiQ[6] with anions^a

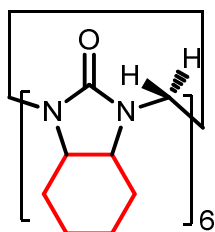
Salts	$\log K_a$
NaSCN	2.21 ± 0.002
KSCN	2.17 ± 0.002
NH ₄ SCN	2.15 ± 0.002
NaI	2.02 ± 0.001
KI	1.96 ± 0.001
RbI	2.00 ± 0.001
CsI	2.00 ± 0.001

^a From ref. [161].

3.2 Cyclohexylhemicucurbit[6]uril and its supramolecular property

Cyclohexylhemicucurbit[6]uril (CycHemiQ[6], Scheme 1-23), a derivative of HemiQ[6] with cyclohexyl group on each ethyleneurea unit, was oligomerized with *cis*-octahydro-2*H*-benzimidazol-2-one and formaldehyde, which also adopted 1,3,5-alternate confirmation in crystalline state, and crystallization from different solvent, CH₂Cl₂, CHCl₃, and CCl₄, exhibited different interaction models of CycHemiQ[6] with solvent molecules [162]. The chiral cyclohexyl moiety granted the host recognition towards chiral guests, and for carboxylic acid guests, the selectivity of CycHemiQ[6] was dependent on the structures of substrates. Acetic acid was too small to form a tight interaction complex, so the association constant was 10 times smaller than the constant of interaction between monoethyl fumarate and CycHemiQ[6]. α -Substituted guests were unfavorable to bind this macrocycle by

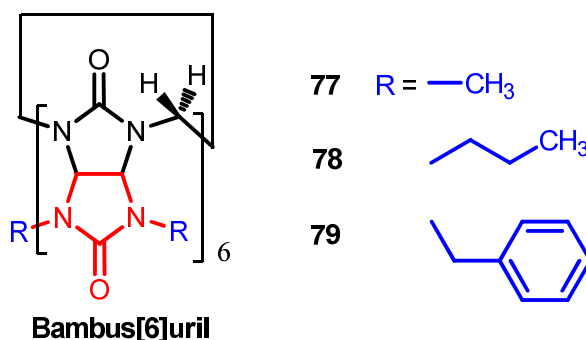
steric effect. The host-guest interaction of thioic acid guest was obviously weaker than carboxyl acids possibly due to the hydrogen binding between sulfhydryl group and carbonyl groups on CycHemiQ[6] was weak [163].



Cyclohexylhemicucurbit[6]uril

Scheme 1-23 Structure of cyclohexylhemicucurbit[6]uril (CycHemiQ[6]).

3.3 Bambus[6]urils and their supramolecular properties



Bambus[6]uril

Scheme 1-24 Structures of Bambus[6]urils (BU[6]s).

Bambus[6]uril (BU[6]) was firstly found as a methyl substituted macrocycle (Scheme 1-23) [164], which had the structure features of both cucurbituril and hemicucurbituril, namely, the structure of BU[6] included the glycolurils bridged with only one methylene chain, and the flexible structure resulted in a 1,3,5- alternate confirmation in crystalline state like the cases of above hemicucurbiturils. *n*-Propyl and benzyl group substituted species of BU[6]s (Scheme 1-23) has been reported recently [165], which bore similar structure character and supramolecular properties

of affinity for anions. In the case of methyl group substituted BU[6], the association constants of host-guest interactions between kinds of anions and this macrocycle shown selectivity of the host for the dimension of guest (Table 1-4), and the affinity was also independent on the species of cations [166].

Table 1-4 association constants (K_a) for interactions of BU[6] with anions^a

Anions	K_a (L · mol ⁻¹)
Cl ⁻	780
Br ⁻	4.8×10 ⁴
BF ₄ ⁻	2.1×10 ⁴
NO ₃ ⁻	1.6×10 ⁴
CN ⁻	5.9×10 ³
I ⁻	8.9×10 ⁵

^a From ref. [166].

4. Outline of the doctor research

Based on the above literature review, this doctor research was beginning with the further investigation on IBX oxidation of aromatic alcohols in the presence of cucurbit[8]uril, in which the host-guest interaction between veratryl alcohol, IBX and Q[8] was studied to propose a mechanism of the supramolecular catalysis, and substituent effect was investigated by employ a few aryl alcohols in this Q[8]-catalytic oxidation. Hemicucurbit[6]uril was also applied for the chemical control of IBX oxidation of hydroxyl benzylalcohols to realized a chemo-selective oxidation. More supramolecular catalysis of HemiQ[6] were developed including esterification and aerobic oxidation in the presence of the macrocycle.

References

- [1] Behrend, R.; Meyer, E.; Rusche, F. *Justus Liebigs Ann. Chem.* **1905**, 339, 1–37.
- [2] Freeman, W. A.; Mock, W. L.; Shih, N. Y. *J. Am. Chem. Soc.* **1981**, 103, 7367–7368.
- [3] Kim, J.; Jung, I. –S.; Kim, S. –Y.; Lee, E.; Kang, J. –K.; Sakamoto, S.; Yamaguchi, K.; Kim, K. *J. Am. Chem. Soc.* **2000**, 122, 540–541.
- [4] Day, A.; Arnold, A. P.; Blanch, R. J.; Snushall, B. *J. Org. Chem.* **2001**, 66, 8094–8100.
- [5] Day, A. I.; Blanch, R. J.; Arnold, A. P.; Lorenzo, S.; Lewis, G. R.; Dance, I. *Angew. Chem. Int. Ed.* **2002**, 41, 275–277.
- [6] Cheng, X. –J.; Liang, L. –L.; Chen, K.; Ji, N. –N.; Xiao, X.; Zhang, J. –X.; Zhang, Y. –Q.; Xue, S. –F.; Zhu, Q. –J.; Ni, X. –L.; Tao, Z. *Angew. Chem. Int. Ed.* **2013**, 52, 7252–7255.
- [7] Kim, K.; Selvapalam, N.; Oh, D. H. *J Incl. Phenom. Macro.* **2004**, 50, 31–36.
- [8] Mukhopadhyay, P.; Wu, A.; Isaacs, L. *J. Org. Chem.* **2004**, 69, 6157–6164.
- [9] Lagona, J.; Mukhopadhyay, P.; Chakrabarti, S.; Isaacs, L. *Angew. Chem. Int. Ed.* **2005**, 44, 4844–4870.
- [10] Isaacs, L. *Chem. Commun.* **2009**, 619–629.
- [11] Mock, W. L.; Shih, N. –Y. *J. Org. Chem.* **1986**, 51, 4440–4446.
- [12] Liu, J. –X.; Long, L. –S.; Huang, R. –B.; Zheng, L. –S. *Crystal Growth & Design* **2006**, 6, 2611–2614.
- [13] Liu, J. –X.; Long, L. –S.; Huang, R. –B.; Zheng, L. –S. *Inorg. Chem.* **2007**, 46, 10168–10173.
- [14] Thuéry, P. *Crystal Growth & Design* **2009**, 9, 1208–1215.
- [15] Kushwaha, S.; Sudhakar, P. P. *Analyst* **2012**, 137, 3242–3245.
- [16] Kushwaha, S.; Rao, S. A.; Sudhakar, P. P. *Inorg. Chem.* **2012**, 51, 267–273.
- [17] Gao, Z. –W.; Feng, X.; Mu, L.; Ni, X. –L.; Liang, L. –L.; Xue, S. –F.; Tao, Z.; Zeng, X.; Chapman, B. E.; Kuchel, P. W.; Lindoy, L. F.; Wei, G. *Dalton Trans.* **2013**, 42, 2608–2615.

- [18] Chen, K.; Feng, X.; Liang, L. -L.; Zhang, Y. -Q.; Zhu, Q. -J.; Xue, S. -F.; Tao, Z. *Crystal Growth & Design* **2011**, *11*, 5712–5722.
- [19] Chen, K.; Hu, Y. -F.; Xiao, X.; Xue, S. -F.; Tao, Z.; Zhang, Y. -Q.; Zhu, Q. -J.; Liu, J. -X. *RSC Adv.* **2012**, *2*, 3217–3220.
- [20] Chen, K.; Liang, L. -L.; Liu, H. -J.; Zhang, Y. -Q.; Xue, S. -F.; Tao, Z.; Xiao, X.; Zhu, Q. -J.; Lindoy, L. F.; Wei, G. *CrystEngComm.* **2012**, *14*, 7994–7999.
- [21] Feng, X.; Chen, K.; Zhang, Y. -Q.; Xue, S. -F.; Zhu, Q. -J.; Tao, Z.; Day, A. I. *CrystEngComm.* **2011**, *13*, 5049–5051.
- [22] Jansen, K.; Buschmann, H. -J.; Wego, A.; Döpp, D.; Mayer, C.; Drexler, H. -J.; Holdt, H. -J.; Scheollmeyer, E. *J Incl. Phenom. Macro.* **2001**, *39*, 357–363.
- [23] Kellersberger, K. A.; Anderson, J. D.; Ward, S. M.; Krakowiak, K. E.; Dearden, D. V. *J. Am. Chem. Soc.* **2001**, *123*, 11316–11317.
- [24] Buschmann, H. -J.; Cleve, E.; Schollmeyer, E. *Inorg. Chim. Acta* **1992**, *193*, 93–97.
- [25] Hoffmann, R.; Knoche, W.; Fenn, C.; Buschmann, H. -J. *J. Chem. Soc., Faraday Trans.* **1994**, *90*, 1507–1511.
- [26] Jeon, Y. -M.; Kim, J.; Whang, D.; Kim, K. *J. Am. Chem. Soc.* **1996**, *118*, 9790–9791.
- [27] Karcher, S.; Kornmüller, A.; Jekel, M. *Acta hydrochim. hydrobiol.* **1999**, *27*, 38–42.
- [28] Whang, D.; Heo, J.; Park, J. H.; Kim, K. *Angew. Chem. Int. Ed.* **1998**, *37*, 78–80.
- [29] Feng, X.; Lu, X. -J.; Xue, S. -F.; Zhang, Y. -Q.; Tao, Z.; Zhu, Q. -J. *Inorg. Chem. Commun.* **2009**, *12*, 849–852.
- [30] Heo, J.; Kim, S. Y.; Whang, D.; Kim, K. *Angew. Chem. Int. Ed.* **1999**, *38*, 641–643.
- [31] Heo, J.; Kim, J.; Whang, D.; Kim, K. *Inorg. Chem. Acta.* **2000**, *279*, 307–312.
- [32] Samsonenko, D. G.; Lipkowski, J.; Gerasko, O. A.; Virovets, A. V.; Sokolov, M. N.; Fedin, V. P.; Platas, J. G.; Hernandez–Molina, R.; Mederos, A. *Eur. J. Inorg. Chem.* **2002**, 2380–2388.
- [33] Haouaj, M. E.; Ko, Y. H.; Luhmer, M.; Kim, K.; Bartik, K. *J. Chem. Soc. Perkin*

Trans. **2001**, 2, 2104–2107.

[34] Haouaj, M. E.; Luhmer, M.; Ko, Y. H.; Kim, K.; Bartik, K. *J. Chem. Soc. Perkin Trans.* **2001**, 2, 804–807.

[35] El-Sheshtawy, H. S.; Bassil, B. S.; Assaf, K. I.; Kortz, U.; Nau, W. M. *J. Am. Chem. Soc.* **2012**, 134, 19935–19941.

[36] Rekharsky, M. V.; Ko, Y. H.; Selvapalam, N.; Kim, K.; Inoue, Y. *Supramol. Chem.* **2007**, 19, 39–46.

[37] Isobe, H.; Tomita, N.; Lee, J. W.; Kim, H. -J.; Kim, K.; Nakamura, E. *Angew. Chem. Int. Ed.* **2000**, 39, 4257–4260.

[38] Lim, Y. -B.; Kim, T.; Lee, J. W.; Kim, S. -M.; Kim, H. -J.; Kim, K.; Park, J. -S. *Bioconj. Chem.* **2002**, 13, 1181–1185.

[39] Rekharsky, M. V.; Yamamura, H.; Mori, T.; Sato, A.; Shiro, M.; Lindeman, S. V.; Rathore, R.; Shiba, K.; Ko, Y. H.; Selvapalam, N.; Kim, K.; Inoue, Y. *Chem.–Eur. J.* **2009**, 15, 1957–1965.

[40] Rekharsky, M. V.; Yamamura, H.; Inoue, C.; Kawai, M.; Osaka, I.; Arakawa, R.; Shiba, K.; Sato, A.; Ko, Y. H.; Selvapalam, N.; Kim, K.; Inoue, Y. *J. Am. Chem. Soc.* **2006**, 128, 14871–14880.

[41] Ong, W.; Kaifer, A. E. *Organometallics*, **2003**, 22, 4181–4183.

[42] Jeon, W. S.; Moon, K.; Park, S. H.; Chun, H.; Ko, Y. H.; Lee, J. Y.; Lee, E. S.; Samal, S.; Selvapalam, N.; Rekharsky, M. V.; Sindelar, V.; Sobransingh, D.; Inoue, Y.; Kaifer, A. E.; Kim, K. *J. Am. Chem. Soc.* **2005**, 127, 12984–12989.

[43] Rekharsky, M. V.; Mori, T.; Yang, C.; Ko, Y. H.; Selvapalam, N.; Kim, H.; Sobransingh, D.; Kaifer, A. E.; Liu, S.; Isaacs, L.; Chen, W.; Moghaddam, S.; Gilson, M. K.; Kim, K.; Inoue, Y. *PNAS.* **2007**, 104, 20737–20742.

[44] Sobransingh, D.; Kaifer, A. E. *Org. Lett.* **2006**, 8, 3247–3250.

[45] Sindelar, V.; Silvi, S.; Parker, S. E.; Sobransingh, D.; Kaifer, A. E. *Adv. Funct. Materi.* **2007**, 17, 694–701.

[46] Ahn, Y.; Jang, Y.; Selvapalam, N.; Yun, G.; Kim, K. *Angew. Chem. Int. Ed.* **2013**, 52, 3140–3144.

[47] Moghaddam, S.; Yang, C.; Rekharsky, M.; Ko, Y. H.; Kim, K.; Inoue, Y.; Gilson,

- M. K. *J. Am. Chem. Soc.* **2011**, *133*, 3570–3581.
- [48] Liu, S. M.; Ruspice, C.; Mukhopadhyay, P.; Chakrabarti, S.; Zavalij, P. Y.; Isaacs, L. *J. Am. Chem. Soc.* **2011**, *127*, 15959–15967.
- [49] Nau, W. M. *Nat. Chem.* **2010**, *2*, 248–250.
- [50] Walker, S.; Oun, R.; McInnes, F. J.; Wheate, N. J. *Isr J. Chem.* **2011**, *51*, 616–624.
- [51] Ghosh, I.; Nau, W. M. *Adv. Drug Deliver. Rev.* **2012**, *64*, 764–783.
- [52] Day, A. I.; Collins, J. G. *Supramolecular Chemistry: From Molecules to Nanomaterials* Ed. Gale, P. A.; Steed, J. W. **2012**, *3*, 983–1000.
- [53] Uzunova, V. D.; Cullinane, C.; Brix, K.; Nau, W. M.; Day, A. I. *Org. Biomol. Chem.* **2010**, *8*, 2037–2042.
- [54] Hettiarachchi, G.; Nguyen, D.; Wu, J.; Lucas, D.; Ma, D.; Isaacs, L.; Briken, V. *PLoS One* **2010**, *5*, 1–10.
- [55] Wheate, N. J.; Day, A. I.; Blanch, R. J.; Arnold, A. P.; Cullinane, C.; Collins, J. G. *Chem. Commun.* **2004**, 1424–1425.
- [56] Jeon, Y. J.; Kim, S. Y.; Ko, Y. H.; Sakamoto, S.; Yamaguchi, K.; Kim, K. *Org. Biomol. Chem.* **2005**, *3*, 2122–2125.
- [57] Bali, M. S.; Buck, D. P.; Coe, A. J.; Day, A. I.; Collins, J. G. *Dalton Trans.* **2006**, 5337–5344.
- [58] Kemp, S.; Wheate, N. J.; Wang, S.; Collins, J. G.; Ralph, S. F.; Day, A. I.; Higgins, V. J.; Aldrich-Wright, J. R. *J. Biol. Inorg. Chem.* **2007**, *12*, 969–979.
- [59] Wang, R.; Macartney, D. H. *Org. Biomol. Chem.* **2008**, *6*, 1955–1960.
- [60] Saleh, N.; Koner, A. L.; Nau, W. M. *Angew. Chem. Int. Ed.* **2008**, *47*, 5398–5401.
- [61] Cong, H.; Li, C. –R.; Xue, S. –F.; Tao, Z.; Zhu Q. –J.; Wei, G. *Org. Biomol. Chem.* **2011**, *9*, 1041–1046.
- [62] Park, K. M.; Lee, D. –W.; Sarkar, B.; Jung, H.; Kim, J.; Ko, Y. H.; Lee, K. E.; Jeon, H.; Kim, K. *Small* **2010**, *6*, 1430–1441.
- [63] Saleh, N.; Meetani, M. A.; Al-Kaabi, L.; Ghosh, I.; Nau, W. M. *Supramol. Chem.* **2011**, *23*, 654–661.
- [64] Ma, D.; Hettiarachchi, G.; Nguyen, D.; Zhang, B.; Wittenberg, J. B.; Zavalij, P.

- Y.; Briken, V.; Isaacs, L. *Nat. Chem.* **2012**, *4*, 503–510.
- [65] Ma, W. –J.; Chen, J. –M.; Jiang, L.; Yao, J.; Lu, T. –B. *Mol. Pharm.* **2013**, *10*, 4698–4705.
- [66] Zhang, Y. –M.; Chen, Y.; Zhuang, R. –J.; Liu, Y. *Supramol. Chem.* **2011**, *23*, 372–378.
- [67] Fathalla, M.; Strutt, N. L.; Barnes, J. C.; Stern, C. L.; Ke, C.; Stoddart, J. F. *Eur. J. Org. Chem.* **2014**, 2873–2877.
- [68] Miskolczy, Z.; Harangozo, J. G.; Biczok, L.; Wintgens, V.; Lorthioir, C.; Amiel, C. *Photochem. Photobiol. Sci.* **2014**, *13*, 499–508.
- [69] Ghale, G.; Lanctot, A. G.; Kreissl, H. T.; Jacob, M. H.; Weingart, H.; Winterhalter, M.; Nau, W. M. *Angew. Chem. Int. Ed.* **2014**, *53*, 2762–2765.
- [70] Gavvala, K.; Sengupta, A.; Koninti, R. K.; Hazra, P. *ChemPhysChem* **2013**, *14*, 3375–3383.
- [71] Mohanty, J.; Jagtap, K.; Ray, A. K.; Nau, W. M.; Pal, H. *ChemPhysChem* **2010**, *11*, 3333–3338.
- [72] Halterman, R. L.; Moore, J. L.; Yip W. T. *J. Fluoresc.* **2011**, *21*, 1467–1478.
- [73] Chakraborty, B.; Basu, S. *Chem. Phys. Lett.* **2011**, *507*, 74–79.
- [74] Shaikh, M.; Mohanty, J.; Singh, P. K.; Nau, W. M.; Pal, H. *Photochem. Photobiol. Sci.* **2008**, *7*, 408–414.
- [75] Ghale, G.; Ramalingam, V.; Urbach, A. R.; Nau, W. M. *J. Am. Chem. Soc.* **2011**, *133*, 7528–7535.
- [76] Li, C.; Li, J.; Jia, X. *Org. Biomol. Chem.* **2009**, *7*, 2699–2703.
- [77] Pozo, M. del; Hernández, L.; Quintana, C. *Talanta* **2010**, *81*, 1542–1546.
- [78] Dong, N.; Cheng, L. –N.; Wang, X. –L.; Li, Q.; Dai, C. –Y.; Tao, Z. *Talanta*, **2011**, *84*, 684–689.
- [79] Miskolczy, Z.; Biczok, L. *J. Phys. Chem. B* **2014**, *118*, 2499–2505.
- [80] Wang, R.; Yuan, L.; Macartney, D. H.; *Chem. Commun.* **2005**, 5867–5869.
- [81] Freitag, M.; Gundlach, L.; Piotrowiak, P.; Galoppini, E. *J. Am. Chem. Soc.* **2012**, *134*, 3358–3366.
- [82] Pischel, U.; Uzunova, V. D.; Remón, P.; Nau, W. M. *Chem. Commun.* **2010**, 46,

2635–2637.

- [83] Masson, E.; Shaker, Y. M.; Masson, J. -P.; Kordesch, M. E.; Yuwono, C. *Org. Lett.* **2011**, *13*, 3872–3875.
- [84] Saleh, N.; Al-Soud, Y. A.; Al-Kaabi, L.; Ghosh, I.; Nau, W. M. *Tetrahedron Lett.* **2011**, *52*, 5249–5254.
- [85] Jeon, W. S.; Kim, H. -J.; Lee, C.; Kim, K. *Chem. Commun.* **2002**, 1828–1829.
- [86] Jeon, Y. J.; Bharadwaj, P. K.; Choi, S. W.; Lee, J. W.; Kim, K. *Angew. Chem. Int. Ed.* **2002**, *41*, 4474–4476.
- [87] Ko, Y. H.; Kim, K.; Kang, J. -K.; Chun, H.; Lee, J. W.; Sakamoto, S.; Yamaguchi, K.; Fettinger, J. C.; Kim, K. *J. Am. Chem. Soc.* **2004**, *126*, 1932–1933.
- [88] Zou, D.; Andersson, S.; Zhang, R.; Sun, S.; Aakermark, B.; Sun, L. A. *J. Org. Chem.* **2008**, *73*, 3775–3783.
- [89] Lee, J. W.; Hwang, I.; Jeon, W. S.; Ko, Y. H.; Sakamoto, S.; Yamaguchi, K.; Kim, K. *Chem. Asian J.* **2008**, *3*, 1277–1283.
- [90] Trabolsi, A.; Hmadeh, M.; Khashab, N. M.; Friedman, D. C.; Belowich, M. E.; Humbert, N.; Elhabiri, M.; Khatib, H. A.; Albrecht-Gary, A. -M.; Fraser Stoddart, J. *New J. Chem.* **2009**, *33*, 254 – 263.
- [91] Roldan, M. L.; Sanchez-Cortes, S.; Garcia-Ramos, J. V.; Domingo, C. *Phys. Chem. Chem. Phys.* **2012**, *14*, 4935–4941.
- [92] Ding, Z. -J.; Zhang, H. -Y.; Wang, L. -H.; Ding, F.; Liu, Y. *Org. Lett.* **2011**, *13*, 856 – 859.
- [93] Zhang, Z. -J.; Zhang, Y. -M.; Liu, Y. *J. Org. Chem.* **2011**, *76*, 4682–4685.
- [94] Ramalingam, V.; Urbach, A. R. *Org. Lett.* **2011**, *13*, 4898–4901.
- [95] Jiao, D.; Biedermann, F.; Scherman, O. A. *Org. Lett.* **2011**, *13*, 3044–3047.
- [96] Zhang, Z. -J.; Zhang, H. -Y.; Chen, L.; Liu, Y. *J. Org. Chem.* **2011**, *76*, 8270–8276.
- [97] Sindelar, V.; Cejas, M. A.; Raymo, F. M.; Chen, W.; Parker, S. E.; Kaifer, A. E. *Chem. Eur. J.* **2005**, *11*, 7054–7059.
- [98] Rauwald, U.; Barrio, J. del; Loh, X. J.; Scherman, O. A. *Chem. Commun.* **2011**, *47*, 6000–6002.
- [99] Zhang, T.; Sun, S.; Liu, F.; Pang, Y.; Fan, J.; Peng, X. *Phys. Chem. Chem. Phys.*

2011, *13*, 9789–9795.

[100] Biedermann, F.; Nau, W. M. *Angew. Chem. Int. Ed.* **2014**, *53*, 5694–5699.

[101] Rauwald, U.; Scherman, O. A. *Angew. Chem. Int. Ed.* **2008**, *47*, 3950–3953.

[102] Deroo, S.; Rauwald, U.; Robinson, C. V.; Scherman, O. A. *Chem. Commun.* **2009**, 644–646.

[103] Appel, E. A.; Biedermann, F.; Rauwald, U.; Jones, S. T.; Zayed, J. M.; Scherman, O. A. *J. Am. Chem. Soc.* **2010**, *132*, 14251–14260.

[104] Biedermann, F.; Rauwald, U.; Zayed, J. M.; Scherman, O. A. *Chem. Sci.* **2011**, *2*, 279–286.

[105] Geng, J.; Biedermann, F.; Zayed, J. M.; Tian, F.; Scherman, O. A. *Macromolecules.* **2011**, *44*, 4276–4281.

[106] Uhlenheuer, D. A.; Young, J. F.; Nguyen, H. D.; Scheepstra, M.; Brunsveld, L. *Chem. Commun.* **2011**, *47*, 6798–6800.

[107] Tian, F.; Cheng N.; Nouvel, N.; Geng, J.; Scherman, O. A. *Langmuir* **2010**, *26*, 5323–5328.

[108] Tian, F.; Cziferszky, M.; Jiao, D.; Wahlström, K.; Geng, J.; Scherman, O. A. *Langmuir* **2011**, *27*, 1387–1390.

[109] Coulston, R. J.; Jones, S. T.; Lee, T. –C.; Appel E. A.; Scherman, O. A. *Chem. Commun.* **2011**, *47*, 164–166.

[110] Li, D. –D.; Ren, K. –F.; Chang, H.; Wang, H. –B.; Wang, J. –L.; Chen, C. –J.; Ji, J. *Langmuir* **2013**, *29*, 14101–14107.

[111] Day, A. I.; Blanch, R. J.; Arnold, A. P.; Lorenzo, S.; Lewis, G. R.; Dance, I. *Angew. Chem. Int. Ed.* **2002**, *41*, 275–277.

[112] Liu, S.; Zavalij, P. Y.; Isaacs, L. *J. Am. Chem. Soc.* **2005**, *127*, 16798–16799

[113] Liu, S.; Shukla, A. D.; Gadde, S.; Wagner, B. D.; Kaifer, A. E.; Isaacs, L. *Angew. Chem. Int. Ed.* **2008**, *47*, 2657–2660.

[114] Liu, J. –X.; Lin, R. –L.; Long, L. –S.; Huang, R. –B.; Zheng, L. –S. *Inorg. Chem. Commun.* **2008**, *11*, 1085–1087.

[115] Pisani, M. J.; Zhao, Y.; Wallace, L.; Woodward, C. E.; Keene, F. R.; Day, A. I.; Collins, J. G. *Dalton Trans.* **2010**, *39*, 2078–2086.

- [116] Huang, W. -H.; Liu, S.; Zavalij, P. Y.; Isaacs, L. *J. Am. Chem. Soc.* **2006**, *128*, 14744–14745.
- [117] Nally, R.; Isaacs, L. *Tetrahedron* **2009**, *65*, 7249–7258.
- [118] Wittenberg, J. B.; Costales, M. G.; Zavalij, P. Y.; Isaacs, L. *Chem. Commun.* **2011**, *47*, 9420–9422.
- [119] Mock, W. L.; Shih, N. -Y. *J. Org. Chem.* **1983**, *48*, 3619–3620.
- [120] Mock, W. L.; Irra, T. A.; Wepsiec, J. P.; Adhya, M. *J. Org. Chem.* **1989**, *54*, 5302–5308.
- [121] Tuncel, D.; Steinke, J. H. G. *Chem. Commun.* **1999**, 1509–1510.
- [122] Krasia, T. C.; Steinke, J. H. G. *Chem. Commun.* **2002**, 22–23.
- [123] Tuncel, D.; Steinke, J. H. G. *Chem. Commun.* **2002**, 496–497.
- [124] Tuncel, D.; Steinke, J. H. G. *Macromolecules* **2004**, *37*, 288–302.
- [125] Carlqvist, P.; Maseras, F. *Chem. Commun.* **2007**, 748–750.
- [126] Wieland, M.; Mieusset, J. -L.; Brinker, U. H. *Tetrahedron Lett.* **2012**, *53*, 4351–4353.
- [127] Lima, S. M. de; Gómez, J. A.; Barros, V. P.; Vertuan, G. de S.; Assis, M. das D.; Graeff, C. F. de O.; Demets, G. J. -F. *Polyhedron* **2010**, *29*, 3008–3013.
- [128] Wang, R.; Yuan, L.; Macartney, D. H. *J. Org. Chem.* **2006**, *71*, 1237–1239.
- [129] Koner, A. L.; Márquez, C.; Dickman, M. H.; Nau, W. M. *Angew. Chem. Int. Ed.* **2011**, *50*, 545–548.
- [130] Wang, R.; Macartney, D. H. *Tetrahedron Lett.* **2008**, *49*, 311–314.
- [131] Bhasikuttan, A. C.; Mohanty, J.; Nau, W. M.; Pal, H. *Angew. Chem. Int. Ed.* **2007**, *46*, 4120–4122.
- [132] Rawashdeh, A. M. M.; Thangavel, A.; Sotiriou-Leventis, C.; Leventis, N. *Org. Lett.* **2008**, *10*, 1131–1134.
- [133] Thangavel, A.; Elder, I. A.; Sotiriou-Leventis, C.; Dawes, R.; Leventis, N. *J. Org. Chem.* **2013**, *78*, 8297–8304.
- [134] Liu, Y.; Shi, J.; Chen, Y.; Ke, C. -F. *Angew. Chem. Int. Ed.* **2008**, *47*, 7293–7296.
- [135] Basilio, N.; García-Río, L.; Moreira, J. A.; Pessêgo, M. *J. Org. Chem.* **2010**, *75*, 848–855.

- [136] Pessêgo, M. J.; Basilio, N.; Moreira, J. A.; García-Río, L. *ChemPhysChem* **2011**, *12*, 1342–1350.
- [137] Miskolczy, Z.; Megyesi, M.; Tárkányi, G.; Mizsei, R.; Biczók, L. *Org. Biomol. Chem.* **2011**, *9*, 1061–1070.
- [138] Jon, S. Y.; Ko, Y. H.; Park, S. H.; Kim, H. -J.; Kim, K. *Chem. Commun.* **2001**, 1938–1939.
- [139] Pattabiraman, M.; Natarajan, A.; Kaliappan, R.; Magueb, J. T.; Ramamurthy, V. *Chem. Commun.* **2005**, 4542–4544.
- [140] Kaliappan, R.; Maddipatla, M. V. S. N.; Kaanumalle, L. S.; Ramamurthy, V. *Photochem. Photobiol. Sci.* **2007**, *6*, 737–740.
- [141] Maddipatla, M. V. S. N.; Kaanumalle, L. S.; Natarajan, A. *Langmuir* **2007**, *23*, 7545–7554.
- [142] Gromov, S. P.; Vedernikov, A. I.; Kuz'mina, L. G.; Kondratuk, D. V.; Sazonov, S. K.; Strelenko, Y. A.; Alfimov, M. V.; Howard, J. A. K. *Eur. J. Org. Chem.* **2010**, 2587–2599.
- [143] Nakamura, A.; Irie, H.; Hara, S.; Sugawara, M.; Yamada, S. *Photochem. Photobiol. Sci.* **2011**, *10*, 1496–1500.
- [144] Pattabiraman, M.; Natarajan, A.; Kaanumalle, L. S.; Ramamurthy, V. *Org. Lett.* **2005**, *7*, 529–532.
- [145] Pattabiraman, M.; Kaanumalle, L. S.; Natarajan, A.; Ramamurthy, V. *Langmuir* **2006**, *22*, 7605–7609.
- [146] Wu, X. -L.; Luo, L.; Lei, L.; Liao, G. -H.; Wu, L. -Z.; Tung, C. -H. *J. Org. Chem.* **2008**, *73*, 491–494.
- [147] Lei, L.; Luo, L.; Wu, X. -L.; Liao, G. -H.; Wu, L. -Z.; Tung, C. -H. *Tetrahedron Lett.* **2008**, *49*, 1502–1505.
- [148] Chen, B.; Cheng, S. -F.; Liao, G. -H.; Li, X. -W.; Zhang, L. -P.; Tung C. -H.; Wu, L. -Z. *Photochem. Photobiol. Sci.* **2011**, *10*, 1441–1444.
- [149] Barooah, N.; Pemberton, B. C.; Sivaguru, J. *Org. Lett.* **2008**, *10*, 3339–3342.
- [150] Barooah, N.; Pemberton, B. C.; Johnson A. C.; Sivaguru, J. *Photochem. Photobiol. Sci.* **2008**, *7*, 1473–1479.

- [151] Pemberton, B. C.; Kumarasamy, E.; Jockusch, S.; Srivastava, D. K.; Sivaguru, J. *Can. J. Chem.* **2011**, *89*, 310–316.
- [152] Pemberton, B. C.; Singh, R. K.; Johnson A. C.; Jockusch, S.; Silva, J. P. D.; Ugrinov, A.; Turro, N. J.; Srivastava, D. K.; Sivaguru, J. *Chem. Commun.* **2011**, *47*, 6323–6325.
- [153] Yang, C.; Mori, T.; Origane, Y.; Ko, Y. H.; Selvapalam, N.; Kim, K.; Inoue, Y. *J. Am. Chem. Soc.* **2008**, *130*, 8574–8575.
- [154] Yang, C.; Ke, C.; Liang, W.; Fukuhara, G.; Mori, T.; Liu, Y.; Inoue, Y. *J. Am. Chem. Soc.* **2011**, *133*, 13786–13789.
- [155] Fukuhara, G.; Okazaki, T.; Lessi, M.; Nishijima, M.; Yang, C.; Mori, T.; Mele, A.; Bellina, F.; Chiappe, C.; Inoue, Y. *Org. Biomol. Chem.* **2011**, *9*, 7105–7112.
- [156] Yang, C.; Ke, C.; Liang, W.; Fukuhara, G.; Mori, T.; Liu, Y.; Inoue, Y. *J. Am. Chem. Soc.* **2011**, *133*, 13786–13789.
- [157] Cong, H.; Zhao, F. –F.; Zhang, J. –X.; Zeng, X.; Tao, Z.; Xue, S. –F.; Zhu, Q. –J. *Catal. Commun.* **2009**, *11*, 167–170.
- [158] Wang, Y. –H.; Cong, H.; Zhao, F. –F.; Xue, S. –F.; Tao, Z.; Zhu, Q. –J.; Wei, G. *Catal. Commun.* **2011**, *12*, 1127–1130.
- [159] Miyahara, Y.; Goto, K.; Oka, M.; Inazu, T. *Angew. Chem. Int. Ed.* **2004**, *43*, 5019–5022.
- [160] Buschmann, H. –J.; Zielesny, A.; Schollmeyer, E. *J Incl. Phenom. Macro.* **2006**, *50*, 181–185.
- [161] Buschmann, H.–J.; Cleve, E.; Schollmeyer, E. *Inorg. Chem. Commun.* **2005**, *8*, 125–127.
- [162] Li, Y.; Li, L.; Zhu, Y.; Meng, Xi.; Wu, A. *Crystal Growth & Design* **2009**, *9*, 4255–4257.
- [163] Aav, R.; Shmatova, E.; Reile, I.; Borissova, M.; Topić, F.; Rissanen, K. *Org. Lett.* **2013**, *15*, 3786–3789.
- [164] Svec, J.; Necas, M.; Sindelar, V. *Angew. Chem. Int. Ed.* **2010**, *49*, 2378–2381.
- [165] Havel, V.; Svec, J.; Wimmerova, M.; Dusek, M.; Pojarova, M.; Sindelar, V. *Org. Lett.* **2011**, *13*, 4000–4003.

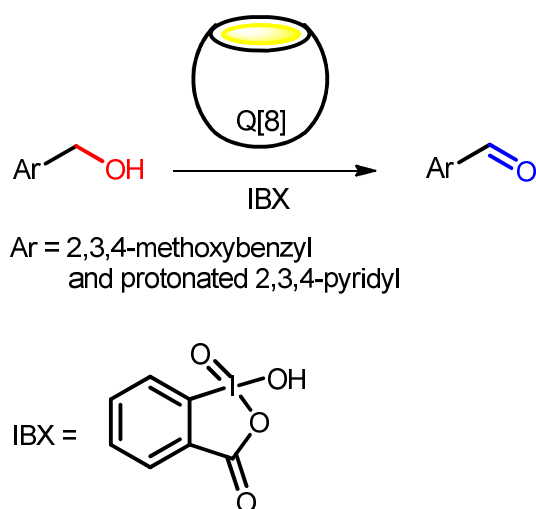
- [166] Svec, J.; Dusek, M.; Fejfarova, K.; Stacko, P.; Klán, P.; Kaifer, A. E.; Li, W.; Hudeckova, E.; Sindelar, V. *Chem. Eur. J.* **2011**, *17*, 5605–5612.

Chapter 2

IBX Oxidation of Aromatic Alcohols in the Presence of Cucurbit[8]uril

1. Introduction

The procedure for transformation of alcohols into the corresponding aldehydes is an important issue for fundamental organic synthesis [1-3], in which traditional inorganic reagents are considered hazardous and toxic, and all of these aerobic oxidations depend on the design of coordination compounds to activate the dioxygen molecule to induce the formation of singlet oxygen [4], while the organic oxidants can efficiently and smoothly perform the oxidative process in a direct way [5,6]. Recently, a few significant organic syntheses that have employed *o*-iodoxybenzoic acid (IBX, Scheme 2-1) revealed the advantages and importance of this oxidizing agent [7-9], which could be easily obtained as a precursor of Dess-Martin Periodinane (DMP) [10], and is a safe alternative to its oxidation product, with the same efficiency.



Scheme 2-1 IBX oxidation of aromatic alcohols in the presence of Q[8]

Since the presence of water can restrain the oxidation, hydrophobic solvents, such as ethyl acetate and 1,2-dichloroethane, were considered during optimization of the solvent medium in the IBX oxidation [11,12]. To explore a novel oxidative procedure by using IBX in an eco-friendly process, a supramolecular catalysis, with cucurbit[8]uril for the oxidation of alcohols was recently designed and executed, and exhibited a very satisfying conversion rate [22, 23]. To provide an elementary

understanding of the mechanism of supramolecular catalysis of macrocyclic compounds, based on the investigation of the ternary host-guest interaction between veratryl alcohol, IBX and Q[8], two series of aromatic alcohol substrates, 2,3,4-methoxybenzyl alcohol and 2,3,4-pyridinemethanol hydrochloride, have been used to reveal the substituent and electronic effect on this supramolecular catalysis ([Scheme 2-1](#)).

2. Results and discussion

2.1 Host-guest interaction between IBX, veratryl alcohol and cucurbit[8]uril

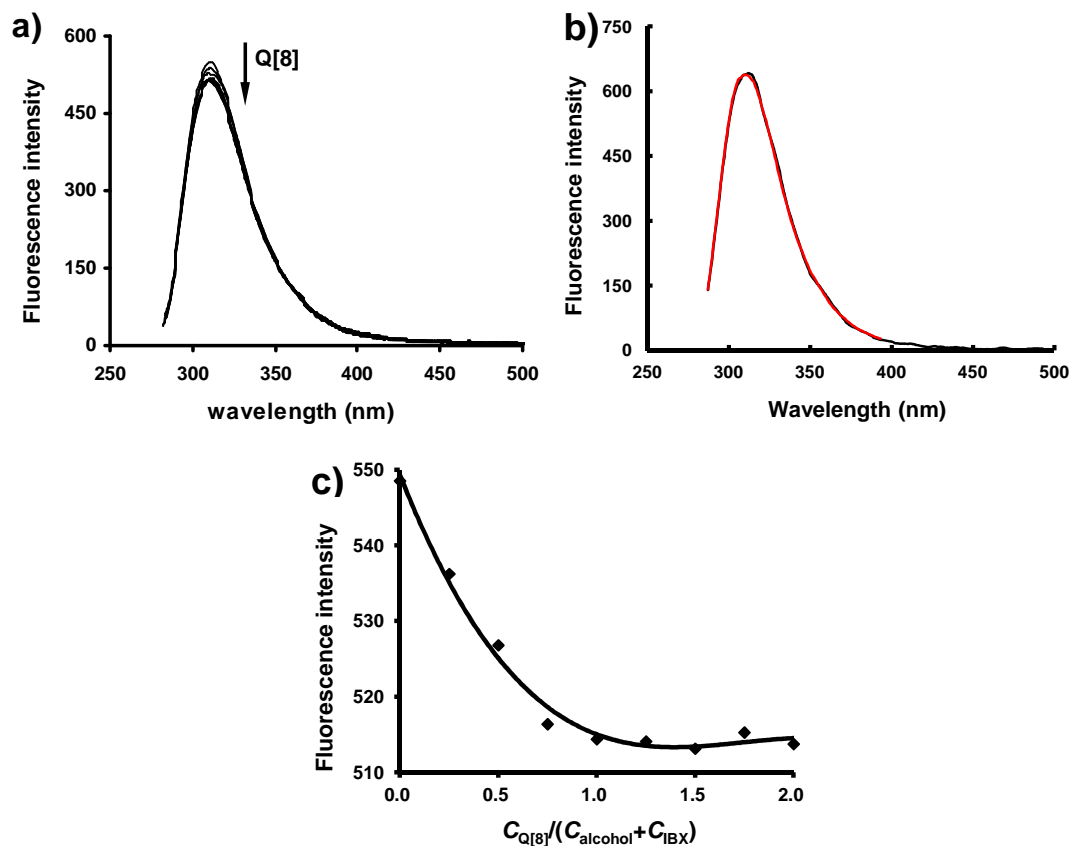


Figure 2-1 a) Fluorescence emission spectra of mixed aqueous solution of veratryl alcohol and IBX (4.00×10^{-5} mol/L) in a ratio of 1:1, and titration with increasing Q[8] (from 0 to 8×10^{-6} mol \cdot L $^{-1}$ along the arrow direction); b) Fluorescence spectra of veratryl alcohol in the absence (black) and presence of Q[8] (1 : 1, red); c)

Corresponding molar ratio plots of the fluorescence emission at 310 nm show the formation of the ternary host-guest inclusion complex in a ratio of 1:1:1, which yields an association constant $K_a = (1.6 \pm 0.4) \times 10^6$ L \cdot mol $^{-1}$.

The supramolecular catalysis of Q[8] on the IBX oxidation of veratryl alcohol has been confirmed in previous work [13], so this substrate was employed as a model to achieve the foundational understanding of the ternary host-guest interaction between Q[8] and veratryl alcohol, IBX. ^1H NMR spectroscopy is always a very

important tool to understand the association site between host and guest in supramolecular chemistry [15], but which was unavailable to investigate the formation of the inclusion complex due to the poor solubility of Q[8] in aqueous solution. The fluorescence spectrophotometric analysis was employed to study the inclusion complex of Q[8] with the alcohol substrate and IBX (Figure 2-1a). The independent experimentations indicated that fluorescence emission of veratryl alcohol can't respond to the addition of Q[8] (Figure 2-1b), and IBX was not able to be excited at 276 nm, but the fluorescence intensity of the combined solution of the alcohol and IBX in a ratio of 1 : 1 was decreasing with the increasing concentration of Q[8]. The above changes illuminated that the formation of the ternary inclusion complex in a ratio of 1 : 1 : 1 with a moderate association constant of $(1.6 \pm 0.8) \times 10^6 \text{ L}^2 \cdot \text{mol}^{-2}$ (Figure 2-1c).

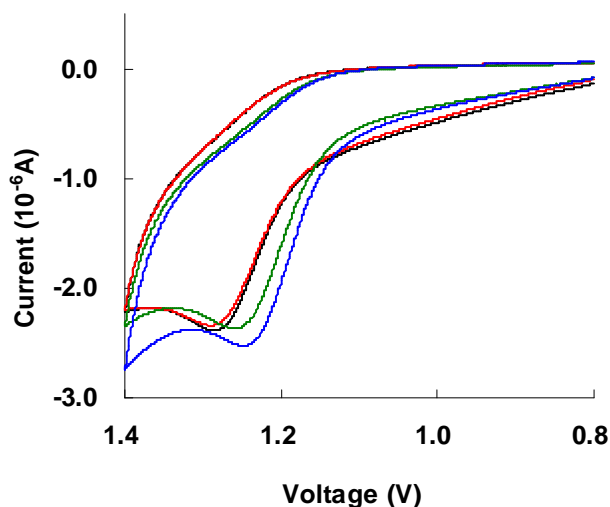


Figure 2-2 Cyclic voltammetric response of veratryl alcohol ($8.00 \times 10^{-5} \text{ mol/L}$, black), mixed aqueous solution of veratryl alcohol and IBX ($8.00 \times 10^{-5} \text{ mol/L}$, 1 : 1, red), veratryl alcohol and Q[8] ($8.00 \times 10^{-5} \text{ mol/L}$, 1:1, green) and the ternary mixture of veratryl alcohol, IBX and Q[8] ($8.00 \times 10^{-5} \text{ mol/L}$, 1 : 1 : 1, Blue).

The above host-guest interaction was also supported by Cyclic Voltammetry (CV) analysis (Figure 2-2). There was no observation of CV response to IBX, and the electrochemical activity of veratryl alcohol corresponded to an irreversible oxidation

process with the peak potential (E_p) at about 1.30 V (Figure 2-2, black), which was almost similar to that of the mixture of IBX and veratryl alcohol substrate (Figure 2-2, red), while the peak potential shifted slightly to 1.27 V with addition of Q[8] (Figure 2-2, green). In the presence of both 1 equiv mol Q[8] and IBX, the E_p shifted slightly more negative to about 1.25 V with a little increasing current (Figure 2-2, blue), that is, the encapsulation of both veratryl alcohol and IBX by Q[8] caused the bigger diffusion coefficient of the inclusion complex than the free veratryl alcohol guest and more reductive of the alcohol substrate.

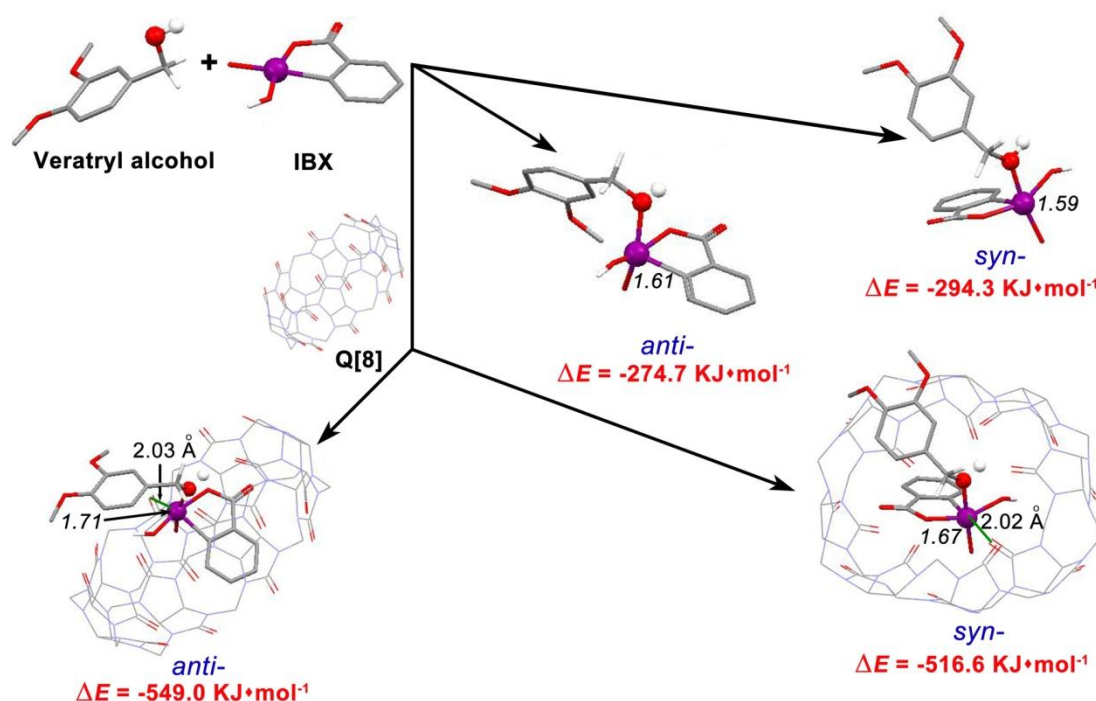
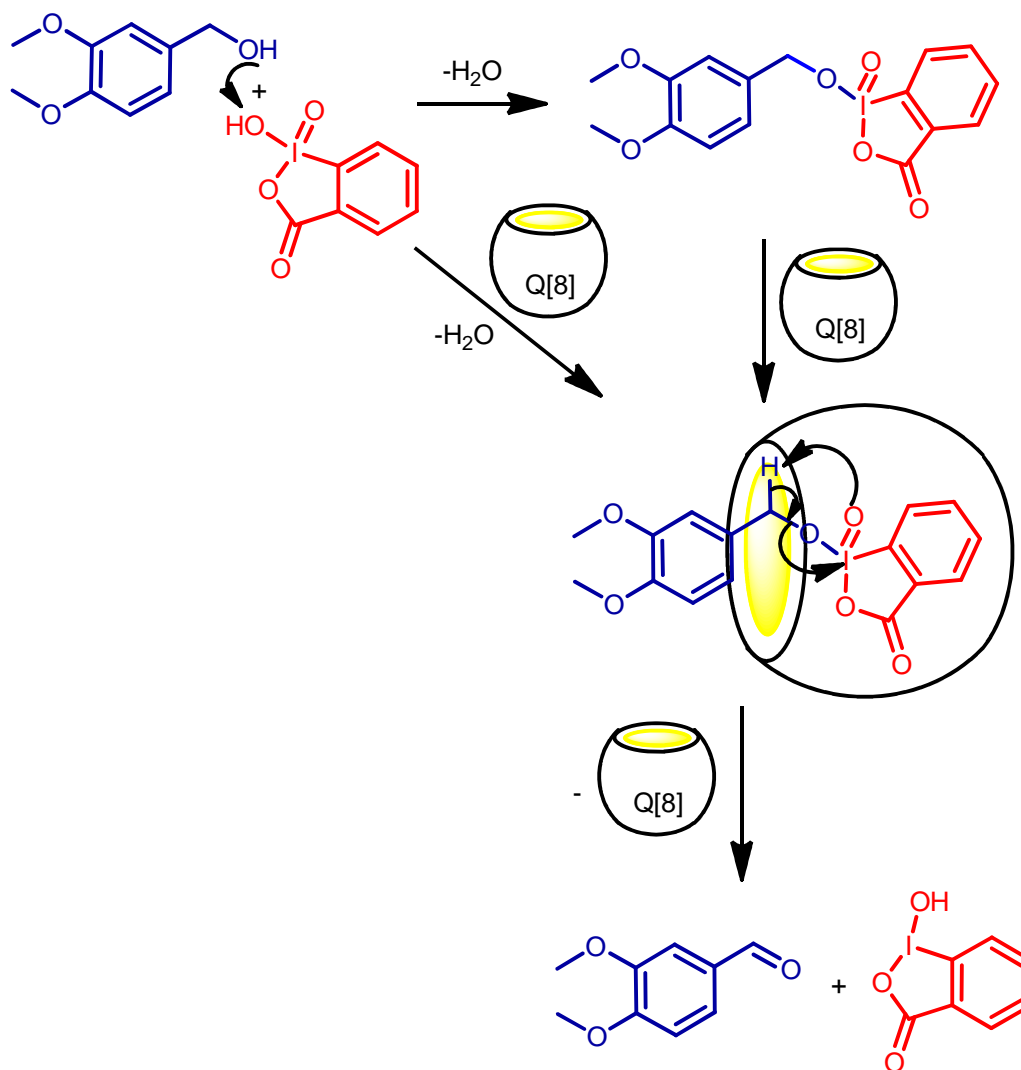


Figure 2-3 Calculation results of designed pathways to form the iodoester intermediate, the different conformations of both *syn*- and *anti*- have been optimized to give the corresponding formation energies (ΔE) of the intermediates in the absence and presence of Q[8]. The italic figures represent the net charges on the hypervalent iodine. Color codes: carbon, gray; nitrogen, blue; oxygen, red; hydrogen, white.

Based on the above investigation of the ternary host-guest interaction, quantum chemistry has been employed to understand what the static structures of the encapsulation looked like and how it was thermodynamic stable in microcosmics. The

optimized structures (Figure 2-3) indicated the intermediate formation of the iodoesters involving *syn*- and *anti*- conformations [16], which was stabilized by the encapsulation of Q[8] with the dipole-dipole interaction between the hypervalent iodine of IBX and the carboxylic group on cucurbituril with about 2 Å distances in either *syn*- or *anti*- conformations.



Scheme 2-2 Possible mechanism of the Q[8]-catalytic oxidation.

On the viewpoint of kinetics, the obvious decrease of formation energies (ΔE) of the iodoester intermediates confirmed the activity of Q[8] as a supramolecular catalyst. The formation energies (ΔE) of the iodoester intermediates were $-294.3 \text{ KJ}\cdot\text{mol}^{-1}$ for *syn*- conformation and $-274.7 \text{ KJ}\cdot\text{mol}^{-1}$ for *anti*- conformation, respectively, while

with the addition of Q[8], which were corresponding -516.6 and $-549.0 \text{ KJ}\cdot\text{mol}^{-1}$. That the formation of intermediates were more easily in the cavity of macrocycle could be the drive force to improve the oxidation.

The more positive charges on the periodine demonstrated the more oxidative of IBX in the presence of Q[8], and the electron transfer (ET) from alcohol to iodoxy group should be effected by the formation of the ternary host-guest inclusion complex, so the electronic effect of the substituent of alcohol could played a crucial role in the supramolecular catalysis of macrocycle. On the other hand, the formation of the iodoester should be orientated within the cavity of cucurbit[8]uril. In consequence, the supramolecular catalysis could provide a possible mechanism (Scheme 2-2) involving the orientation to form the iodoester and enhanced ET by the simultaneous accommodation of both alcohol and IBX in the cavity of Q[8].

2.2 IBX oxidation of methoxybenzyl alcohols in the presence of cucurbit[8]uril

A few aromatic alcohols were employed to figure out the electronic effect on the supramolecular catalysis of Q[8], according to the above proposed mechanism of the Q[8]-improved attack of alcohol to IBX to form the iodoester intermediate. The conversions of 2,3,4-methoxybenzyl alcohols into the corresponding aldehydes at different time from 12 to 60 hours, either in the absence or in the presence of the macrocyclic compound Q[8], were collected in Figure 2-4. One can see that 2-methoxybenzyl alcohol (Figure 2-4a) had the highest reaction activity in the absence of catalysis by Q[8]. The rapid achievement of about 50% conversion of the 2-methoxybenzyl alcohol implied that the oxidation with IBX could be the fast chemical equilibrium. When 10% mol Q[8] was added into the reaction system [13], the conversion was not obviously improved, showing that the supramolecular catalysis was ineffective for the oxidation of 2-methoxybenzyl alcohol.

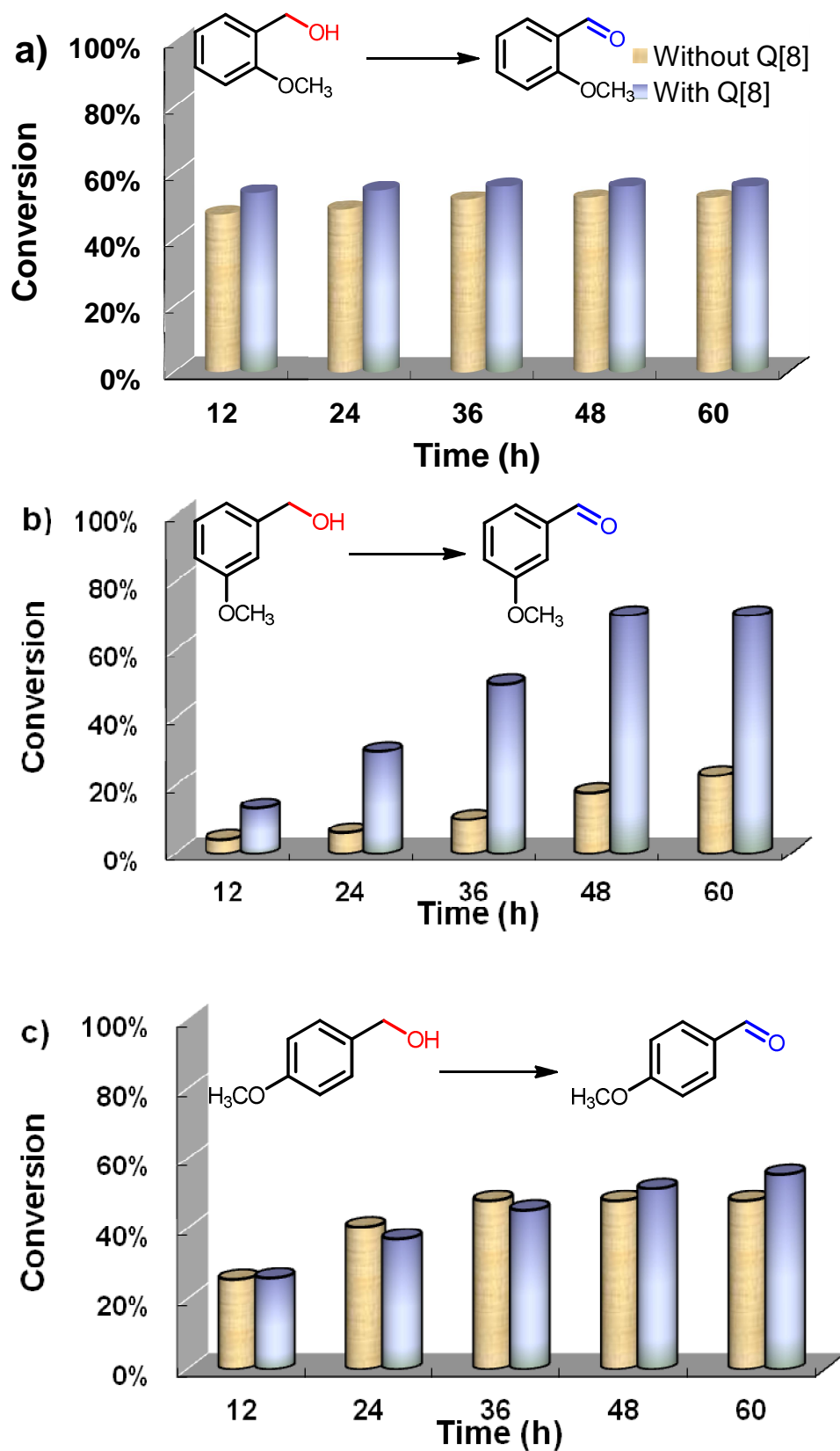
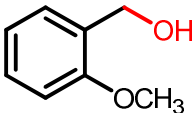
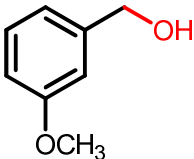
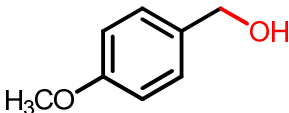


Figure 2-4 IBX oxidation of methoxybenzyl alcohols with supramolecular catalysis of cucurbit[8]uril.

The similar result was found in the case of oxidation of 4-methoxybenzyl alcohol (Figure 2-4c), although the reaction activity was slightly lower than 2-substitution. The conversion was increasing along with reaction time before the achievement of equilibrium in 36 hours and can ultimately attain a level of about 50%. The addition of Q[8] was not able to catalyze the IBX oxidation efficiently, and just very little improvement of conversion was observed.

For the substrate 3-methoxybenzyl alcohol (Figure 2-4b), the conversion was extraordinarily low in the absence of Q[8], and there was only 23% conversion even after 60 hours. However, in the presence of Q[8], the transformation of 3-methoxybenzyl alcohol oxidized by IBX exhibited a significant catalytic effect *via* a supramolecular strategy to surprisingly improve 50% conversion.

Table 2-1. Rate constants for the IBX oxidation of methoxybenzyl alcohols in the absence and presence of Q[8]

Substrates	Rate constants (s ⁻¹)		(k _{cat} /k _{uncat})
	Without Q[8], k _{uncat}	With Q[8], k _{cat}	
	5.6 × 10 ⁻⁵	7.6 × 10 ⁻⁵	1.4
	1.7 × 10 ⁻⁶	1.0 × 10 ⁻⁵	6.0
	1.4 × 10 ⁻⁵	1.4 × 10 ⁻⁵	1.0

On the kinetic aspect, the above relationship of conversions *vs.* time could be described with the First-order equation (2-1) [17]:

$$C_t = C_0 \times [1 - \exp(-k \times t)] \quad (2-1)$$

where C_t was the conversion of alcohol at t time, C_0 was the initial conversion of substrate, and k was the corresponding rate constant. With the non-linear curve-fitting, the calculated rate constants in the above oxidation system were collected in Table 2-1. One can see that the slowest reaction rate was observed in the IBX oxidation of 3-methoxybenzyl alcohol in the absence of Q[8], which was obviously accelerated by the addition of Q[8] with the largest acceleration factor ($k_{\text{cat}}/k_{\text{uncat}}$) of 6.0, while the rate constants of the other two substrates with supramolecular catalysis of Q[8] were similar to those in the absence of Q[8].

The above evidence suggested that the oxidation of alcohols with IBX should be very much dependent on the structures and electronic effect of the substrates. The methoxy group on the aromatic ring caused a generally positive conjugated (+C) effect and negative inductive (−I) effect simultaneously. In the cases of 2- and 4-methoxybenzyl alcohols, the conjugated effect was more important, but the inductive effect in 2-methoxybenzyl alcohol was stronger than the 3-substituent due to the weaker covalent bonds between the methoxy group and the α -C. Comparatively, the least oxidized activity of 3-methoxybenzyl alcohol in the absence of Q[8] could be considered as deriving only from the −I effect. It seemed that the substituent with positive conjugated effect was favorite on IBX oxidation without addition of Q[8], but the supramolecular catalysis of Q[8] took priority over the oxidizing alcohol substrate with negative inductive effect.

2.3 IBX oxidation of pyridinemethanol hydrochlorides in the presence of cucurbit[8]uril

To prove the above hypothetical mechanism, the second series of aromatic alcohols, 2,3,4-pyridinemethanol hydrochlorides, which embodied the −C effect and

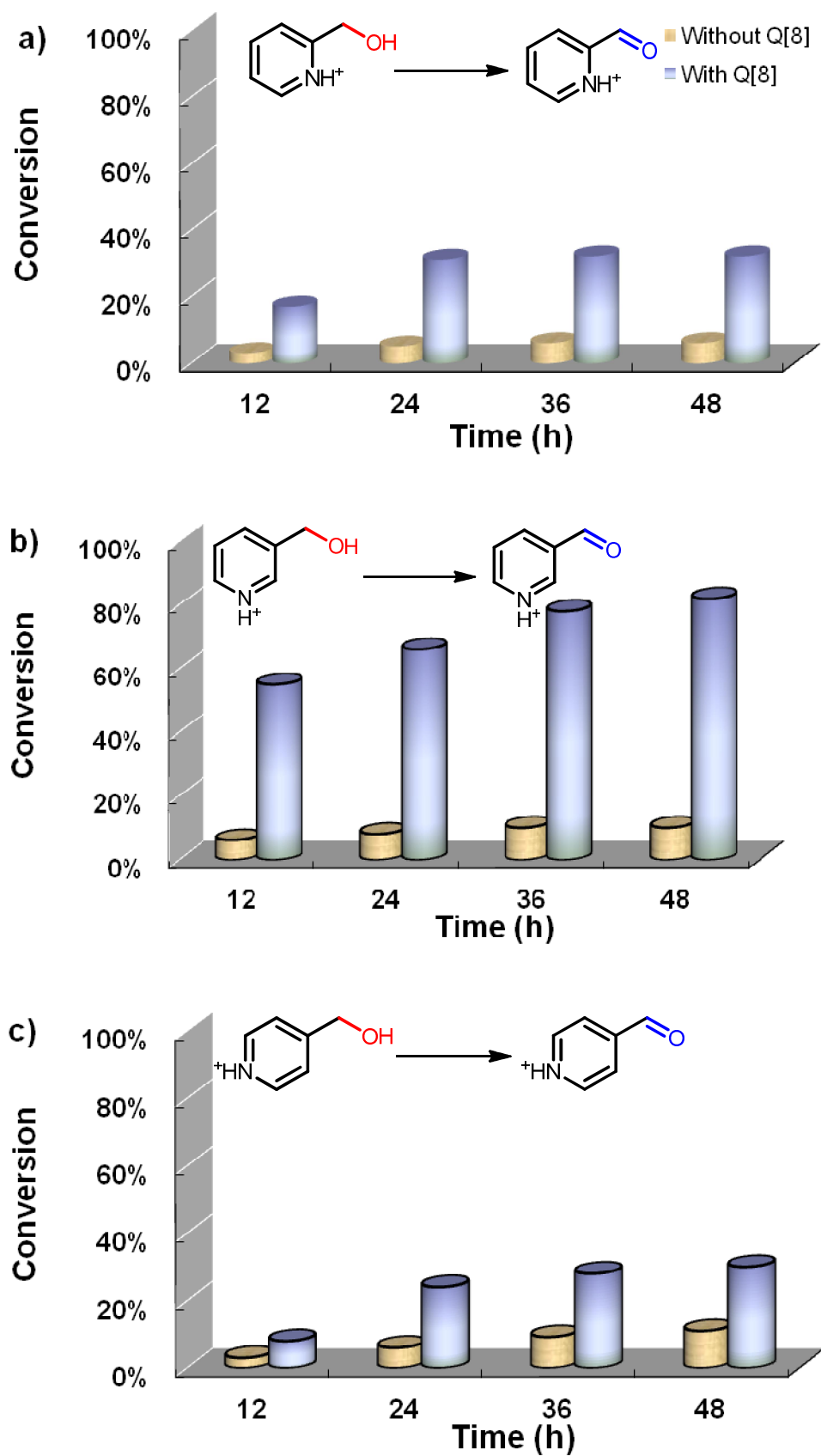
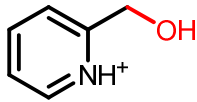
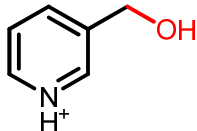
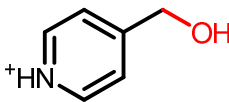


Figure 2-5 IBX oxidation of pyridinemethanol hydrochlorides with supramolecular catalysis of cucurbit[8]uril.

stronger $-I$ effect than the corresponding methoxybenzyl alcohols by reason of the protonated nitrogen atom in pyridine group, were employed to investigate the Q[8]-catalytic activity. The results were shown in Figure 2-5. As expected, all of the substrates produced very low activity for IBX oxidation without the addition of Q[8], while the supramolecular catalysis of Q[8] was on the whole efficient and the dependence of the catalytic activity on the structures of the substrates could still be observed as with the isomers of methoxybenzyl alcohols. The Q[8]-improved conversion of the oxidized 2, 4-pyridinemethanol hydrochlorides was only 20% while the conversion was significantly increased from 10% to about 80% in the presence of Q[8] for 3-pyridinemethanol hydrochloride.

Table 2 Rate constants for the IBX oxidation of pyridinemethanol hydrochlorides in the absence and presence of Q[8]

Substrates	Rate constants (s^{-1})		(k_{cat}/k_{uncat})
	Without Q[8], k_{uncat}	With Q[8], k_{cat}	
	1.3×10^{-6}	2.3×10^{-5}	17.7
	7.5×10^{-7}	2.3×10^{-5}	30.7
	1.5×10^{-6}	2.7×10^{-5}	18.0

The rate constants of IBX oxidation of pyridinemethanol hydrochlorides in the absence and presence of Q[8]-catalytic curve-fitted with equation (2-1) were exhibited in the Table 2-2. It was very obvious that the activity of Q[8] as a supramolecular catalysis on the pyridyl alcohol hydrochloride system was more effective than that on

the methoxybenzyl alcohol system.

For the oxidation reaction of 2,3,4-pyridinemethanol hydrochlorides without Q[8] catalysis, the rate constants were smaller than those in the cases of 2,3,4-methoxybenzyl alcohols, but the rate constants were improved to about $2.5 \times 10^{-5} \text{ s}^{-1}$ with the addition of macrocyclic compound Q[8]. The most acceleration with a factor of 30.7 could be found in the Q[8]-catalytic oxidation of 3-pyridinemethanol hydrochlorides, and even the other acceleration factors of about 18.0 were more than those in the methoxybenzyl alcohol system.

The relative reaction activity for different substrate structures, which was in fact an electronic effect, suggested that the transformation of aromatic alcohols into the corresponding aldehydes with IBX oxidant was mechanistically linked to an electron transfer pathway involving an electron-rich α -carbon due to a hydride transfer of the alcohols (Scheme 2-2). The stabilization by the positive conjugating effect of substituent, should promote the ET procedure from the electron-rich α -carbon to the electron-poor hypervalent iodine of IBX, resulting in the observation that the 2- and 4-methoxybenzyl alcohols could give about 50% conversion of IBX oxidizing without catalysis by Q[8]. In contrast, the $-C$ effect impeded reaction activity due to the decreased electron density on the α -carbon, exemplified by the protonated pyridyl alcohols, but the presence of Q[8] could provide some improvement of the conversion. On the other hand, the $-I$ effect of the 3-methoxybenzyl and 3-protonated pyridyl groups was preferable to the supramolecular catalysis of Q[8] on the IBX oxidation.

3. Conclusion

To explain the supramolecular catalysis of cucurbit[8]uril on the IBX oxidation of veratryl alcohol, the host-guest interaction was investigated by fluorescence spectrometry, electrochemical analysis, and the results suggested the formation of a ternary complex between IBX, veratryl alcohol and Q[8] in a molar ratio of 1 : 1 : 1. Quantum chemistry revealed the formation of the intermediate of IBX oxidizing veratryl alcohol, the iodoester, was more easy in the cavity of Q[8]. An investigation of the Q[8]-catalytic transformation of two series of aromatic alcohol substrates, 2,3,4-methoxybenzyl alcohol and 2,3,4-pyridinemethanol hydrochloride, into corresponding aldehydes in aqueous solvent revealed that the electronic property of the substituent had a significant effect on the supramolecular catalysis by Q[8] of the IBX oxidation of aromatic alcohols. The relationship between the substituent structure and the conversion of aromatic alcohol suggested that an electron-rich α -carbon was mechanistically connected to the procedure for IBX oxidation and the stabilized α -carbon with its positively conjugated electron-rich substituent could be easily oxidized in the absence of Q[8]. The presence of Q[8] provided a novel and intriguing concept for the oxidation of aromatic alcohols with IBX, that is, the oxidation of alcohols with negative inductive effect substituent can be enhanced by the supramolecular catalysis of cucurbit[8]uril.

4. Experimental

4.1 Materials and apparatus

Q[8] was prepared and purified according to the methods reported in literature [18]. Veratryl alcohol, 2,3,4-methoxybenzyl alcohol, 2,3,4-pyridinemethanol and their corresponding aldehydes were purchased from Alfa Aesar (Tianjin) Chemical Co., Ltd. and used without further purification. IBX was prepared with 2-iodobenzoic acid and ozone [35]. ^1H NMR (d_6 -DMSO, δ): 7.96 (d, $J = 7.6$ Hz, 1H), 7.68 (d, $J = 7.6$ Hz, 1H), 7.46 (t, $J = 7.6$ Hz, 1H), 7.22 (t, $J = 7.6$ Hz, 1H). Mp: 230-233 °C with explosive decomposition.

Fluorescence emission spectra have been recorded on a Varian RF-540 fluorescence spectrophotometer at 25 °C.

Cyclic voltammetry has been performed on BASi-Epsilon E2-440 (USA) electrochemical workstation with a conventional three-electrode system comprising a platinum electrode as the auxiliary electrode, a Ag/AgCl (soaked in 3M NaCl) electrode as the reference, and the glass carbon electrode (GCE, geometrical surface area = 0.07 cm²) as the working electrode. The GCE was polished to a mirror finish using 1.0, 0.3, and 0.05 μm alumina slurries and rinsed with ultrapure water before every CV testing.

High Performance Liquid Chromatography (HPLC) was performed using a Shimadzu LC-20A with a PhotoDiode Array Detector detector (PDA). The alcohols and corresponding aldehydes were successfully separated by a Sipore ODS-3 chromatographic column (150 mm \times 0.21 mm \times 5 μm) for methoxybenzyl alcohols and a Sipore SCX chromatographic column (150 mm \times 0.21 mm \times 5 μm) for pyridyl alcohol hydrochlorides. Oxidation results were calculated from the integrated peak areas and expressed in terms of the percentages of the aldehyde formed. ^1H NMR spectra were recorded at 20 °C on a VARIAN INOVA-400 spectrometer in D₂O.

4.2 Interaction of Q[8] with veratryl alcohol and IBX

The associate constant has been measured with fluorescence spectra. The aqueous solutions of both veratryl alcohol and IBX with a fixed concentrations of $4.00 \times 10^{-5} \text{ mol}\cdot\text{L}^{-1}$ in the presence of increasing concentrations of Q[8] were prepared. The emission spectra at 310nm with excitation at 276 nm have been used to curve fit. In the electrochemical analysis, the concentration of IBX and Veratryl alcohol in the aqueous was kept a constant of $8 \times 10^{-5} \text{ mol}\cdot\text{L}^{-1}$, and the experiments were conducted in $4 \times 10^{-3} \text{ mol}\cdot\text{L}^{-1}$ KCl solution prepared with ultrapure water. Scan rate is $0.5 \text{ V}\cdot\text{min}^{-1}$.

The quantum chemistry has been processed on the Mopac 2009 software package [19]. The initial geometries of all structures were constructed with the aid of Hyperchem Release 7.52 package [20]. The semi-empirical method of PM6 was used for full geometry optimization [21].

2.3 Catalytic oxidation experiments

A measure of alcohol (0.2 mmol), methoxybenzyl alcohol and pyridyl alcohol, was added to the suspended solution of 0.2 mmol IBX and Q[8] in 25 mL distilled water. The reaction was carried out at 25 °C. The product was separated from the mixture by filtration under vacuum and the filtrate was directly used for the HPLC analysis. To detect the oxidation of alcohols with ^1H NMR, 5 mg Q[8] was added to the previously prepared suspended solution of 5 μL alcohol and 10 mg IBX in D_2O . The solutions (Q[8], alcohols and IBX in an approximate 0.1 : 1 : 1 molar ratio) have been stirred for at least 48 hours in a thermostatic bath at 25 °C, and the purified liquids were measured directly after centrifugal separation. The products were identified by ^1H NMR comparing their retention time in HPLC with the aldehydes obtained commercially.

2-Methoxybenzyl aldehyde. ^1H NMR (400M Hz, D_2O) δ 10.01 (s, 1H), 7.63 (d, $J = 8.0 \text{ Hz}$, 1H), 7.55 (t, $J = 7.6 \text{ Hz}$, 1H), 7.04 (d, $J = 8.0 \text{ Hz}$, 1H), 6.98 (t, $J = 7.6 \text{ Hz}$, 1H), 3.78 (s, 3H).

3-Methoxybenzyl aldehyde. ^1H NMR (400M Hz, D_2O) δ 9.71 (s, 1H), 7.39 (m, 2H), 7.31 (s, 1H), 7.16 (d, $J = 8.0$ Hz, 1H), 3.71 (s, 3H).

4-Methoxybenzyl aldehyde. ^1H NMR (400M Hz, D_2O) δ 9.60 (s, 1H), 7.77 (d, $J = 8.4$ Hz, 2H), 6.99 (d, $J = 8.4$ Hz, 2H), 3.76 (s, 3H).

2-Pyridinecarbaldehyde hydrochloride. ^1H NMR (400M Hz, D_2O) δ 8.58 (d, $J = 5.6$ Hz, 1H), 8.50 (t, $J = 8.0$ Hz, 1H), 8.03 (d, $J = 8.0$ Hz, 1H), 7.89 (t, $J = 8.0$ Hz, 1H), 6.15 (s, 1H).

3-Pyridinecarbaldehyde hydrochloride. ^1H NMR (400M Hz, D_2O) δ 8.72 (s, 1H), 8.60 (d, $J = 5.6$ Hz, 1H), 8.55 (d, $J = 8.4$ Hz, 1H), 7.94 (d-d, $J = 8.0$ Hz, 1H), 6.07 (s, 1H).

4-Pyridinecarbaldehyde hydrochloride. ^1H NMR (400M Hz, D_2O) δ 8.69 (d, $J = 6.8$ Hz, 1H), 8.04 (d, $J = 6.4$ Hz, 1H), 6.09 (s, 1H).

References

1. Pande, S.; Saha, A.; Jana, S.; Sarkar, S.; Basu, M.; Pradhan, M.; Sinha, A. K.; Saha, S.; Pal, A.; Pal, T. *Org. Lett.* **2008**, *10*, 5179–5181.
2. Patel, S.; Mishra, B. K. *J. Org. Chem.* **2006**, *71*, 6759–6766.
3. Mueller, J. A.; Cowell, A.; Chandler, B. D.; Sigman, M. S. *J. Am. Chem. Soc.* **2005**, *127*, 14817–14824.
4. Bueno, A. C.; Gonçalves, J. A.; Gusevskaya, E. V. *Appl. Catal. A: Gen.* **2007**, *329*, 1–6.
5. Lahtinen, P.; Ahmada, J. U.; Lankinen, E.; Pihko, P.; Leskelä, M.; Repo, T. *J. Mol. Catal. A: Chem.* **2007**, *275*, 228–232.
6. More, J. D.; Finney, N. S. *Org. Lett.* **2002**, *4*, 3001–3003.
7. Lykakis, I. N.; Zaravinos, I. –P.; Raptis, C.; Stratakis, M. *J. Org. Chem.* **2009**, *74*, 6339–6342.
8. Xu, D.; Penning, T. M.; Blair, I. A.; Harvey, R. G. *J. Org. Chem.* **2009**, *74*, 597–604.
9. Bernini, R.; Mincione, E.; Barontini, M.; Crisante, F. *J. Agric. Food Chem.* **2008**, *56*, 8897–8904.
10. Dess, D. B.; Martin, J. C. *J. Org. Chem.* **1983**, *48*, 4156–4158.
11. More, J. D.; Finney, N. S. *Org. Lett.* **2002**, *4*, 3001–3003.
12. Ozanne, A.; Pouységu, L.; Depernet, D.; François, B.; Quideau, S. *Org. Lett.* **2003**, *5*, 2903–2906.
13. Cong, H.; Zhao, F. –F.; Zhang, J. –X.; Zeng, X.; Tao, Z.; Xue, S. –F.; Zhu Q. –J., *Catal. Commun.* **2009**, *11*, 167–170.
14. Wang, Y. –H.; Cong, H.; Zhao, F. –F.; Xue, S. –F.; Tao, Z.; Wei, G. *Catal. Commun.* **2011**, *12*, 1127–1130.
15. Cong, H.; Li, C. –R.; Xue, S. –F.; Tao, Z.; Zhu, Q. –J.; Wei, G. *Org. Biomol. Chem.* **2011**, *9*, 1041–1046.
16. Su, J. T.; Goddard, W. A. *J. Am. Chem. Soc.* **2005**, *127*, 14146–14147.
17. Zhen, D.; Cong, H.; Tao, Z.; Xue, S. –F.; Zhu, Q. –J. *Chin. J. Inorg. Chem.* **2008**,

24, 1684–1689.

18. Zhang, G. –L.; Xu, Z. –Q.; Xue, S. –F.; Zhu, Q. –J.; Tao, Z. *Chin. J. Inorg. Chem.* **2003**, *19*, 655–659.

19. Stewart, J. J. P. *Mopac2009 (Version 11.052W)*, Stewart Computational Chemistry.

20. *Hyperchem Release 7.52 for Windows Molecular Modeling System*, Hypercube, Inc.

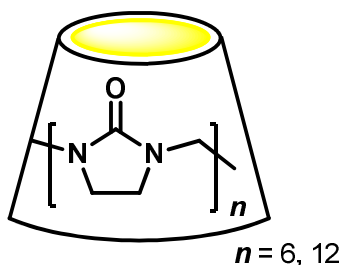
21. Stewart, J. J. P. *J. Mol. Mod.* **2007**, *13*, 1173–1213.

Chapter 3

Hemicucurbit[6]uril-catalytic IBX oxidation of hydroxybenzyl alcohols with chemo-selectivity

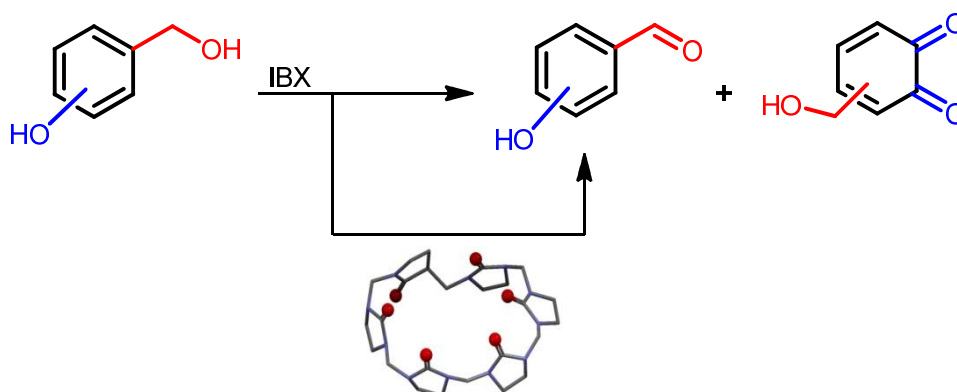
1. Introduction

The successful applications of cucurbiturils for the organic synthesis [1,2] promote us to develop new supramolecular catalysis of cucurbituril members, however, the virtual lack of solubility of cucurbiturils in common organic solvents [3] restricts the further exploration of their applications in organic chemistry. The appearance of hemicucurbiturils (HemiQ[n, n = 6 or 12], Scheme 3-1) involving two members, HemiQ[6] and HemiQ[12], provides a new platform for the exploitation of the supramolecular properties of the cucurbituril family [4].



Scheme 3-1 Structure of Hemicucurbit[6 and 12]uril

The oxidation of hydroxyl groups frequently employed chromium- and rutheniumbased reagents, Fremy's salt $[(\text{KSO}_3)_2\text{NO}]$ and TEMPO-mediated oxidants [5-10]. Organic oxidants of a series of hypervalent iodine compounds have been developed since the beginning of 1990s due to the interest in their effective oxidizing properties. The Dess–Martin reagent is an important member of the hypervalent oxidants [11], and *o*-iodoxybenzoic acid (IBX) was found as a precursor, which has received a lot of attention as a result of its ability to oxidize hydroxyl groups in an extraordinarily efficient and selective manner [12]. Actually, IBX had not been considered as a useful reagent in organic synthesis because of its poor solubility in common organic solvents. However, it has been found that IBX can dissolve in DMSO to oxidize alcohols with very satisfying conversions [13].



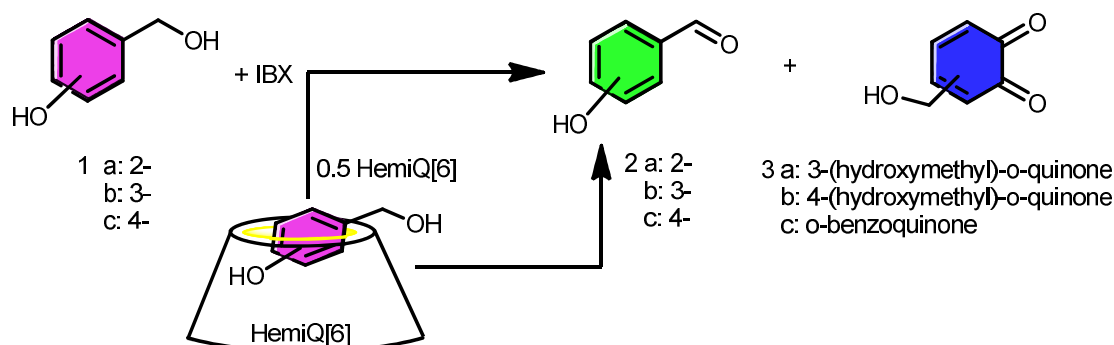
Scheme 3-2 Chemo-selective oxidation of hydroxybenzyl alcohols with IBX in the presence of Hemicucurbit[6]uril

In the last twenty years, IBX chemistry has experienced significant development in order to prove the oxidation activity of hydroxyl and amino groups [14-16]. The importance of this reagent lied in the advantage of regio-selective oxidation, for example, the oxidation of phenol with IBX provides *o*-quinone as the only product [15,17], but there were two products (*o*- and *p*-quinones) formed with the use of Fremy's salt [9]. Recently, the IBX oxidation of alcohols in aqueous solution with the supramolecular catalysis of cucurbit[8]uril was reported by our group [18-20]. Here, the chemo-selective IBX oxidation of hydroxybenzyl alcohols, a serial of substrates with bifunctional groups, in the presence of HemiQ[6] was described (Scheme 3-2).

2. Results and discussion

2.1 IBX oxidation of different hydroxybenzyl alcohols in the absence or in the presence of hemicucurbit[6]uril

For hydroxybenzyl alcohols, there are two kinds of hydroxyl groups on every substrate, phenolic hydroxyl group and alcoholic hydroxyl group, both of which can be oxidized by IBX to provide different products, aldehyde from oxidation of alcoholic hydroxyl group and quinones from phenolic hydroxyl group, and the yield distribution of the products were changed with the addition of hemicucurbit[6]uril (Scheme 3-3). The products formed by the IBX oxidation of different hydroxybenzyl alcohols in the absence or in the presence of different amounts of macrocycle were collected in Table 3-1.



Scheme 3-2 IBX oxidation of hydroxybenzyl alcohols in the absence and presence of HemiQ[6].

Pioneering work found that the IBX oxidation of phenols always produced *o*-quinones [15,17], where two *o*-quinones, 3-(hydroxymethyl)-*o*-quinone and *o*-benzoquinone, were found to form from the oxidation of phenolic group on 2-hydroxybenzyl alcohol, with yields of 25.8% and 24.7%, respectively, and the product 2-hydroxybenzaldehyde was also detected with 30.7% yield. For the purpose of the regio-selective oxidation of a bifunctional substrate *via* a supramolecular

strategy, HemiQ[6] was introduced into this system. The yields of the aldehyde product and quinones decreased with increasing amounts of HemiQ[6], namely, the yields of the quinones decreased by half in the presence of 25 mol% HemiQ[6], and the oxidation of the phenolic hydroxyl group was resisted completely in the presence of HemiQ[6] to afford 2-hydroxybenzaldehyde as the only product, with a slightly decreasing yield when using a HemiQ[6] : 2-hydroxybenzyl alcohol ratio of 0.5 : 1, and an increase in the amount of IBX to two times that of the substrate improved the yields of quinones, but the yield of the aldehyde remained almost constant (entry 1, Table 1).

Table 3-1 Product distribution of IBX oxidation of hydroxybenzyl alcohols in 1 hour in the presence or in the absence of HemiQ[6].^a

Entry	substrate	amount of HemiQ[6] (% mol.)	ratio of IBX to substrate	products			
				2	3a	3b	3c
1	1a	0	1 : 1	31	26	-	25
		25	1 : 1	28	14		13
		50	1 : 1	25	-	-	-
		50	2 : 1	21	19	-	36
		0	1 : 1	40	13	23	-
2	1b	25	1 : 1	43	3	10	
		50	1 : 1	55	-	-	-
		50	2 : 1	52	16	21	-
		0	1 : 1	63	-	14	-
		25	1 : 1	56		10	
3	1c	50	1 : 1	51	-	-	-
		50	2 : 1	87	-	13	-

^a The yield of each product was directly confirmed by ¹H NMR spectral data.

In the case of the *m*-hydroxybenzyl alcohol substrate, there was also two active sites on the benzene ring for the oxidation of the phenolic hydroxyl group, producing

12.6% 3-(hydroxymethyl)-*o*-quinone and 23.4% 4-(hydroxymethyl)-*o*-quinone, which revealed a steric hindrance effect, that the oxidation at the 4-position was more easy than at the 3-position, and brought about the double yield of 3-(hydroxymethyl)-*o*-quinone. In the mean time, 39.5% of 3-hydroxybenzaldehyde was found as the product of the oxidation of benzyl alcohol. With the increasing addition of HemiQ[6], the oxidation of the phenolic hydroxyl group was cut down and finally resisted with a 0.5 : 1 ratio of HemiQ[6] to the substrate, while the yield of the aldehyde product was increased from 39.5% to 55.3%. Using double the amount of IBX improves the conversion of 3-hydroxybenzyl alcohol to 88.9%; however, further increasing the amount of oxidant did not achieve more aldehyde product, instead the yields of the *o*-quinones were increased (entry 2, Table 1).

The results of the IBX oxidation of 4-hydroxybenzyl alcohol in the absence of HemiQ[6] were simpler than the above cases, and afforded only two products, *p*-hydroxybenzaldehyde and 4-(hydroxymethyl)-*o*-quinone, were obtained with yields of 62.7% and 14.4%, respectively. The presence of HemiQ[6] caused the phenolic hydroxyl groups to become chemically inert, that is, the corresponding quinone vanished and only 4-hydroxybenzaldehyde was observed with 50 mol% HemiQ[6], moreover, the yield of the aldehyde product was improved by 36% in company with 13.1% *o*-quinone by the addition of more than 1 equiv. IBX (entry 3, Table 1), which revealed that the ternary complex of the substrate, IBX and HemiQ[6], and additionally the reaction rate of the IBX oxidation would be slower than the dynamic interaction of 4-hydroxybenzyl alcohol with HemiQ[6].

2.2 Kinetic analysis of IBX oxidation of hydroxylbenzyl alcohols in the presence of hemicucurbit[6]uril

The IBX oxidation of 2-hydroxybenzyl alcohol was carried out with 50 mol% HemiQ[6], and the ¹H NMR spectra traces suggested that only the corresponding aldehyde product was formed (Figure 3-1a). Comparing this result with that of the

reaction without the protection, the oxidation conversion of 2-hydroxybenzyl alcohol in the presence of HemiQ[6] was less, which provided only 25.3% aldehyde in 1.0 hour, and the conversion was improved by 30.5% over the next 2.0 hours. The kinetic plots of the oxidation of 2-hydroxybenzyl alcohol in the presence of 50 mol% HemiQ[6] was displayed in Figure 3-1b, which could be described by the following first-order formula (3-1):

$$C_t = C_0 \times [1 - \exp(-k \times t)] \quad (3-1)$$

where C_0 was the initial hydroxybenzyl alcohol concentration (%) and C_t was the concentration (%) at time t , k was the corresponding reaction rate constant, which was found as $k = 2.2 \text{ h}^{-1}$ in this case.

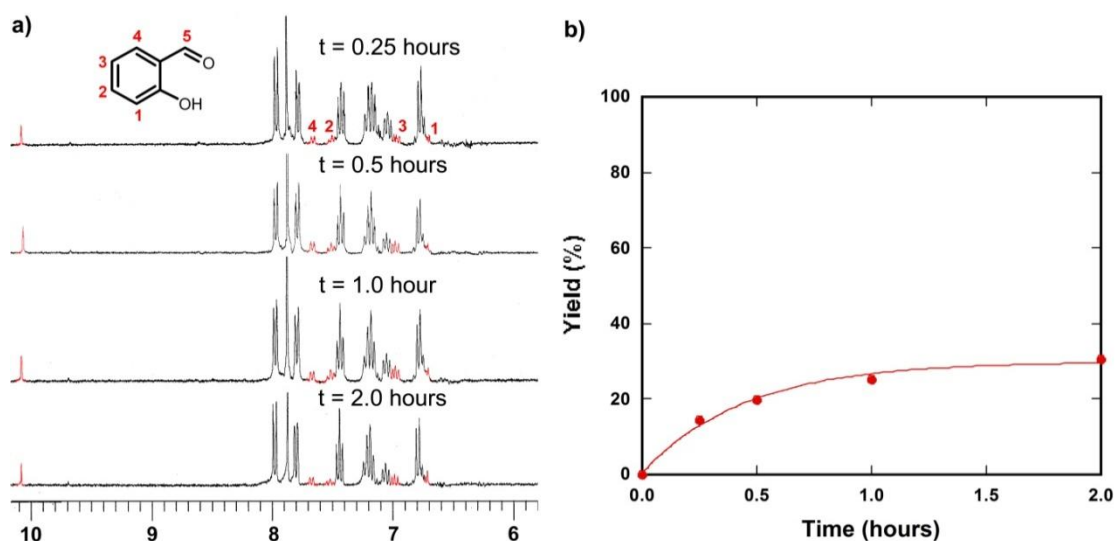


Figure 3-1 a) ¹H NMR spectra of IBX oxidation of 2-hydroxybenzyl alcohol in the presence of HemiQ[6]; b) kinetic plots of IBX oxidation of 2-hydroxybenzyl alcohol to afford 2-hydroxybenzaldehyde in the presence of HemiQ[6]

In the presence of 50 mol% HemiQ[6], the alcoholic hydroxyl group of the 3-hydroxybenzyl alcohol was oxidized by IBX to produce 3-hydroxybenzaldehyde, while the phenolic hydroxyl group was resisted to oxidation, so no quinone product

was found, as observed from the ^1H NMR spectra (Figure 3-2a). On the other hand, the reaction achieves 55.3% conversion in 1.0 hour, which was more than double the conversion of *o*-hydroxybenzyl alcohol, and the non-linear fitting of the kinetic plots with formula 3-1 gave a corresponding rate constant of $k = 4.1 \text{ h}^{-1}$ (Figure 3-2b), which was almost twice that in the case of IBX oxidation of *o*-hydroxybenzyl alcohol with protection of HemiQ[6]. Accordingly, both the above thermodynamic and kinetic evidence suggested that the IBX oxidation of 3-hydroxybenzyl alcohol in the presence of HemiQ[6] was more effective than for 2-hydroxybenzyl alcohol.

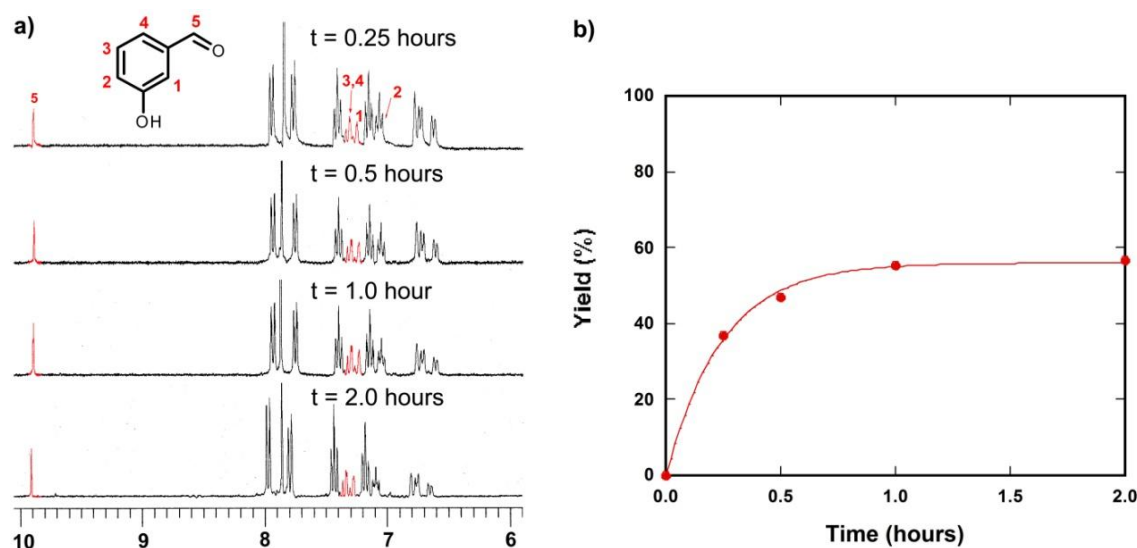


Figure 3-2 a) ^1H NMR spectra of IBX oxidation of 3-hydroxybenzyl alcohol in the presence of HemiQ[6]; b) Kinetic plots of IBX oxidation of 3-hydroxybenzyl alcohol to afford 3-hydroxybenzaldehyde in the presence of HemiQ[6].

As in the above cases, the phenolic hydroxyl group on 4-hydroxybenzyl alcohol could be protected against IBX oxidation by the addition of 50 mol% HemiQ[6], and 4-hydroxybenzaldehyde was found as the only product. The ^1H NMR spectrum (Figure 3-3a) suggested that the IBX oxidation of this substrate was also more effective than that of 2-hydroxybenzyl alcohol. A conversion of 58.6% was achieved after 2.0 hours, and a further 7.4% conversion was achieved after 3.0 hours. The degree of conversion of 4-hydroxybenzyl alcohol at different time could be

non-linearly fitted to give a kinetic constant of $k = 1.1 \text{ h}^{-1}$ with formula 3-1 (Figure 3-2b), which was surprisingly just half of the constant in 2-hydroxybenzyl alcohol system, so the oxidation of 4-hydroxybenzyl alcohol was the slowest of the studied cases.

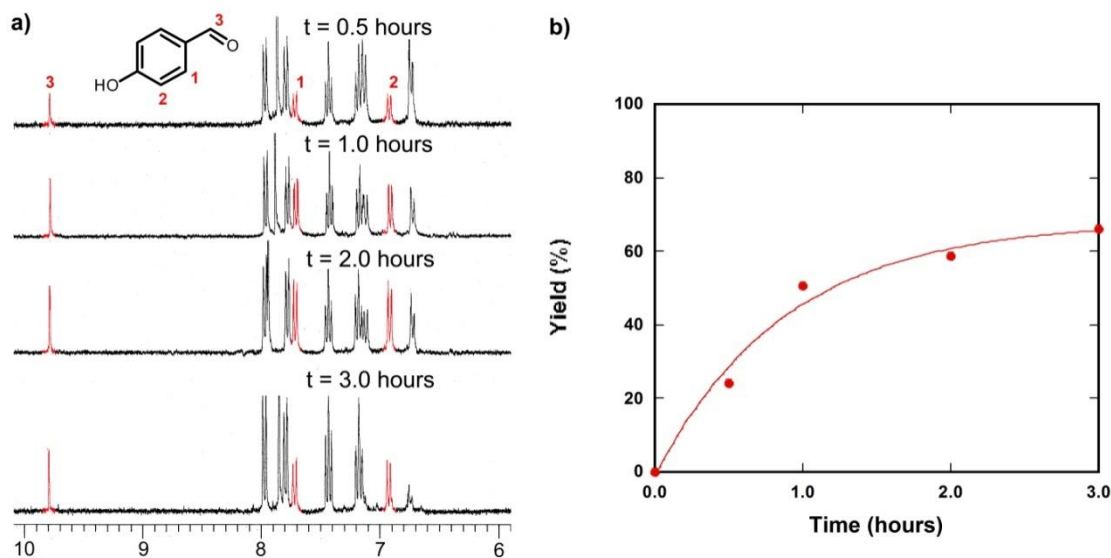


Figure 3-3 a) ¹H NMR spectra of IBX oxidation of 4-hydroxybenzyl alcohol in the presence of HemiQ[6]; b) Kinetic plots of IBX oxidation of 4-hydroxybenzyl alcohol to afford 4-hydroxybenzaldehyde in the presence of HemiQ[6]

The oxidizing activities of the hydroxybenzyl alcohols by IBX in the presence of HemiQ[6] could be comprehended fully from the viewpoints of both thermodynamics and kinetics. 2-Hydroxybenzyl alcohol was the most inert among the bifunctional substrates, with only a 30.5% conversion of 2-hydroxybenzylaldehyde being observed, while the oxidation of 3,4-hydroxybenzyl alcohols provided more products, whose distributions were 56.8% and 66.0%, respectively. It was obvious that the conversion of hydroxybenzyl alcohol depended on the substituent site of the phenolic group on the benzene ring, that is, when the distance between the phenolic hydroxyl group and the alcoholic hydroxyl group was increased, a more effective oxidation at the benzyl alcohol was observed, so the stereo-hindrance effect of HemiQ[6] helped to resist the IBX oxidation of 2-hydroxybenzyl alcohol. However, the oxidation reaction of

4-hydroxybenzyl alcohol had the smallest rate constant of $k = 1.1 \text{ h}^{-1}$, and the rate constant of the IBX oxidation of 3-hydroxybenzyl alcohol was the largest ($k = 4.1 \text{ h}^{-1}$). According to the results obtained in the previous work [19,20], on the electronic effects of substituents on the activity of the IBX oxidation of benzyl alcohols, the meta-substituent with an electron withdrawing group always favored the oxidation due to its strong inductive effect.

2.2 Host-guest interactions between hemicucurbit[6]uril and hydroxybenzyl alcohols

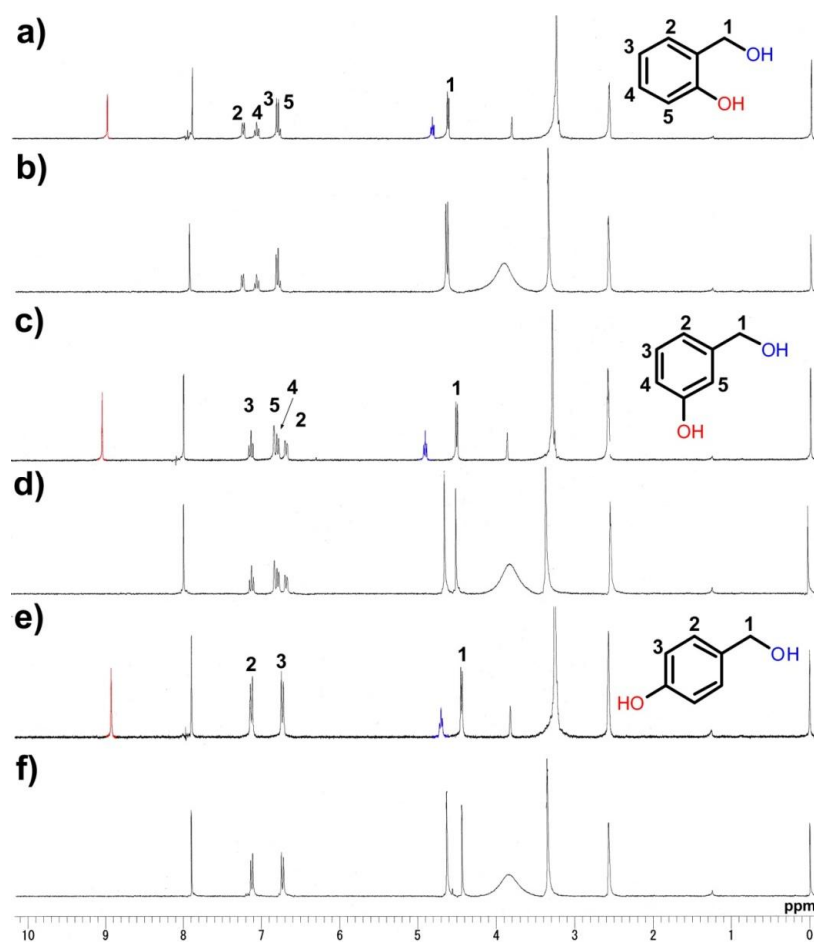


Figure 3-4 ^1H NMR spectra ($\text{CDCl}_3/\text{DMSO}-d_6$, 2:1, v/v) of a) 2-hydroxybenzyl alcohol; b) 2-hydroxybenzyl alcohol in the presence of HemiQ[6] in a ratio of 1 : 1; c) 3-hydroxybenzyl alcohol; d) 3-hydroxybenzyl alcohol in the presence of HemiQ[6] in a ratio of 1 : 1; e) 4-hydroxybenzyl alcohol; f) 4-hydroxybenzyl alcohol in the presence of HemiQ[6] in a ratio of 1 : 1.

To understand the role of HemiQ[6] in this chemo-selective oxidation, the foundations of the host–guest interactions between HemiQ[6] and the hydroxybenzyl alcohols were investigated. ^1H NMR spectroscopy is a common method used to confirm the host–guest interaction models by observation of the changes in the chemical shifts of the guest after addition of the host [3]. In this case, the proton resonances of all of the hydroxybenzyl alcohols did not show any shift in the presence of HemiQ[6] (Figure 3-4), however, all of resonances of the active protons, which appeared at about δ 9.0 ppm, were fading away with the addition of the host and broadened peaks appear from δ 3.6 – δ 4.2 ppm, which revealed the host–guest interaction between hydroxybenzyl alcohols and HemiQ[6] with hydrogen bonds.

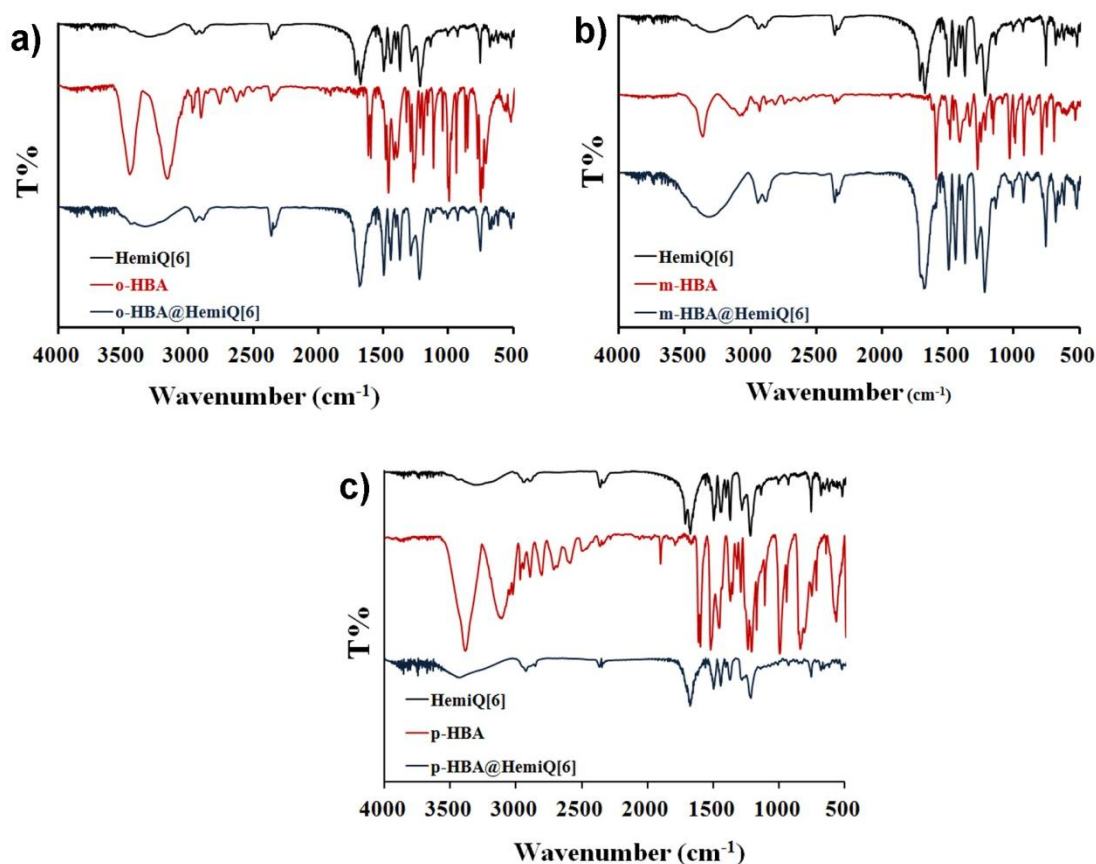


Figure 3-5 IR spectra of HemiQ[6], a) 2-hydroxybenzyl alcohol; b) 3-hydroxybenzyl alcohol; c) 4-hydroxybenzyl alcohol, and the corresponding inclusion complexes.

The formation of supramolecular complexes was also confirmed by the different IR absorptions of the carbonyl groups on binding HemiQ[6] from the those of the free

host (Figure 3-5). Both the bands at 1714 and 1678 cm^{-1} were attributed to the carbonyl stretching vibration in free HemiQ[6], and the IR band at 1710 cm^{-1} in the spectrum of inclusion complex confirmed the host-guest interactions, which were attributed to $\nu_{\text{C=O}}$ of bound HemiQ[6].

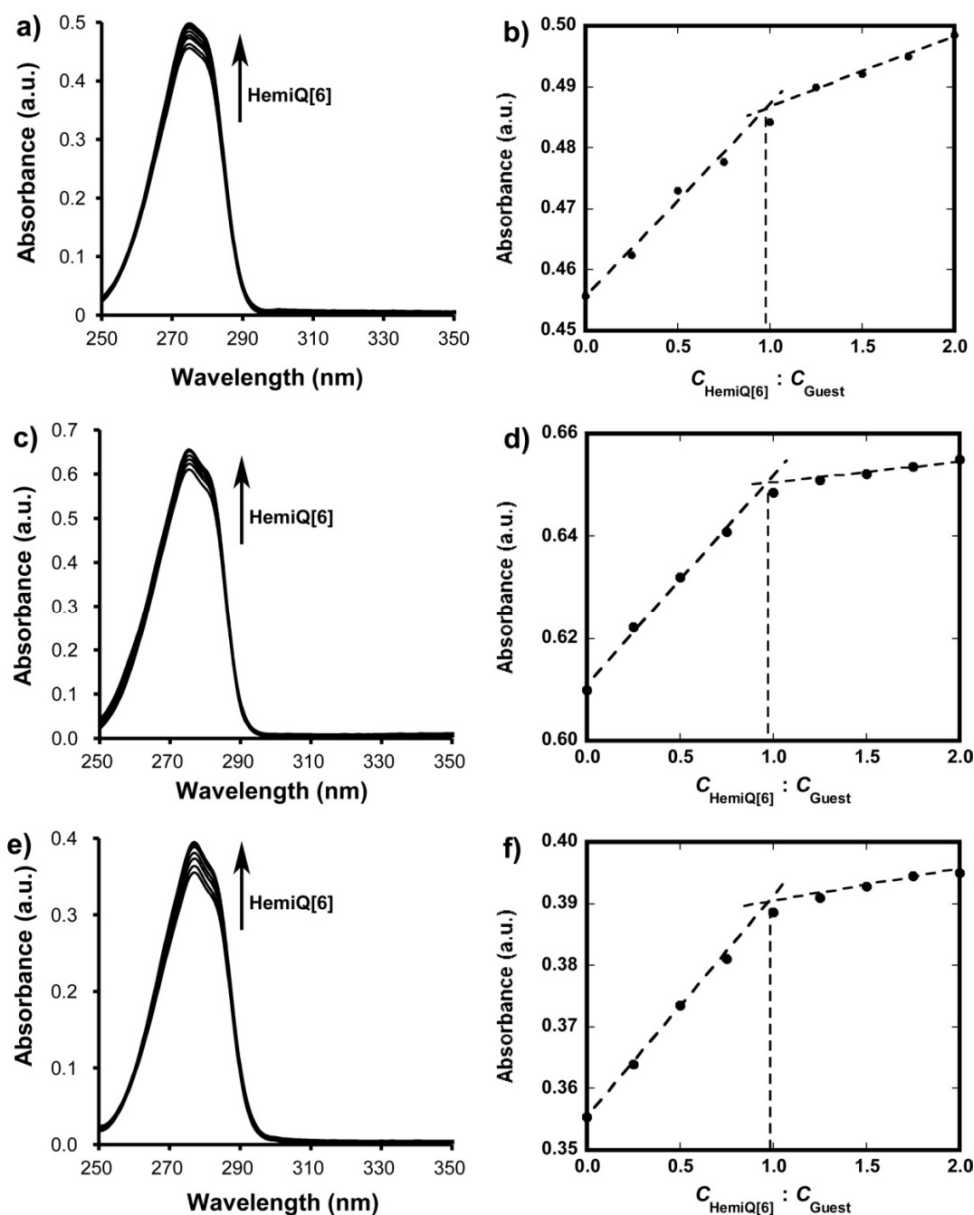


Figure 3-6 UV-vis titration of the host-guest interactions between HemiQ[6] and a) 2-hydroxybenzyl alcohol; c) 3-hydroxybenzyl alcohol; e) 4-hydroxybenzyl alcohol.

The corresponding absorbance versus different ratios of HemiQ[6] to b) 2-hydroxybenzyl alcohol; d) 3-hydroxybenzyl alcohol; f) 4-hydroxybenzyl alcohol.

UV-vis spectroscopic titrations were also employed to monitor the host–guest interactions. To avoid the solvent absorption of DMSO in this wavelength region, a mixed solvent of chloroform and methanol in the ratio of 1 : 1 was applied in the UV-vis titrations. The max electronic absorption of 2-hydroxybenzyl alcohol appeared at 275 nm, which increased with the increasing concentration of HemiQ[6] (Figure 3-6a), and the change in the UV-vis spectra and the variable concentration of the macrocyclic compound could be fitted to give a 1 : 1 interaction model (Figure 3-6b). For 3-hydroxybenzyl alcohol, the UV-vis absorbance at 275 nm was improved by the addition of HemiQ[6] (Figure 3-6c), and the increase in the concentration of HemiQ[6] fitted to a 1 : 1 binding model (Figure 3-6d). A similar change in the UV-vis spectrum was also observed in the host–guest interaction system of 4-hydroxybenzyl alcohol and HemiQ[6] (Figure 3-6e), and the increase in the absorbance band at 277 nm versus the increase in the concentration of HemiQ[6] was fitted to a 1 : 1 binding model (Figure 3-6f). Accordingly, the interaction of 2-hydroxylbenzyl alcohol with HemiQ[6] was weaker than the others, which revealed that a steric hindrance effect is present in the host–guest interaction.

For the host-guest interaction in a ratio of 1 : 1, the equilibrium of H (Host), G (Guest) and H·G (inclusion complex) is expressed by formula (3-2):



The corresponding association constant (K_a) could be obtained by non-linear least square fitting according to formula (3-3):

$$\Delta A = \frac{\Delta \varepsilon ([\text{H}]_0 + [\text{G}]_0 + 1/K_a) \pm \sqrt{\Delta \varepsilon^2 ([\text{H}]_0 + [\text{G}]_0 + 1/K_a)^2 - 4\Delta \varepsilon^2 [\text{H}]_0 [\text{G}]_0}}{2} \quad (3-3)$$

where ΔA was the change in the absorbance of guest on gradual addition of TMeQ[6], whereas $\Delta \varepsilon$ referred to the difference of molar absorptivity between complexed and free G; the total concentration of host and guest was denoted by $[\text{H}]_0$ and $[\text{G}]_0$.

Accordingly, the association constants of the host-guest interactions between HemiQ[6] and *o,m,p*-hydroxybenzyl alcohols were $(4.8 \pm 1.5) \times 10^3 \text{ L} \cdot \text{mol}^{-1}$, $(7.4 \pm 2.2) \times 10^4 \text{ L} \cdot \text{mol}^{-1}$ and $(5.5 \pm 1.6) \times 10^4 \text{ L} \cdot \text{mol}^{-1}$, respectively (Figure 3-7).

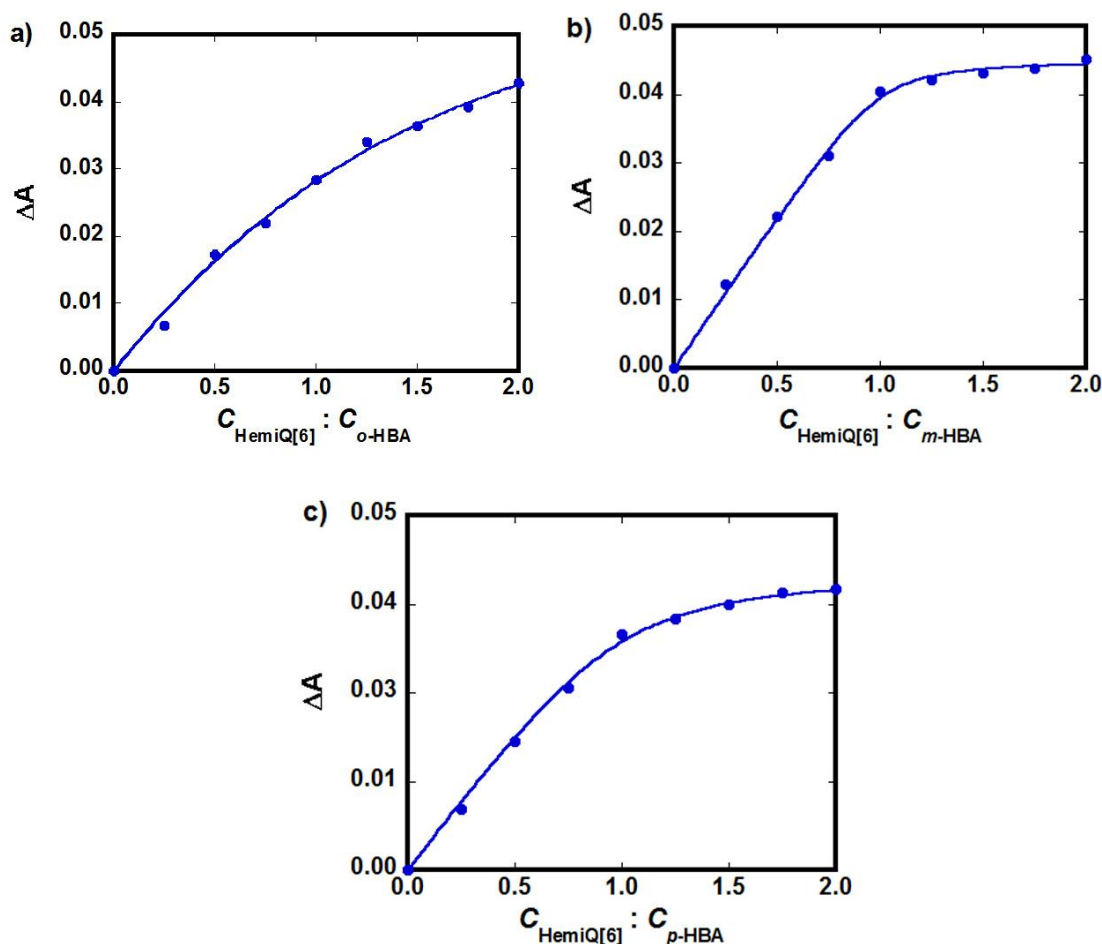


Figure 3-7 Non-linear fitting of UV-vis titrations of a) 2-hydroxybenzyl alcohol; b) 3-hydroxybenzyl alcohol; c) 4-hydroxybenzyl alcohol with HemiQ[6].

Quantum chemistry has developed as an important subject in electronic structure calculations, and density functional theory with dispersion correction (DFT-D) method is now thought to be the most widely applied and is a very well-tested approach for predicting the energy-minimized structure and describing the non-covalent interactions in supramolecular chemistry due to its high accuracy in many different situations [21]. To evaluate the energy-optimized geometries of the above supramolecular structures, quantum chemistry was performed with the DFT-D

method. One can see from the calculation results (Figure 3-8) that the exclusion complexes between hydroxybenzyl alcohols and HemiQ[6] formed with the negative formation energies (ΔE) of -44.4, -59.6, and -58.6 $\text{KJ} \cdot \text{mol}^{-1}$ for 2,3,4-substitution, respectively. The host-guest interactions were stabilized by the formation of hydrogen bindings between the phenolic hydroxybenzyl groups and carbonyl groups on the macocycle, whose distances were found as 1.781, 1.738, and 1.744 Å with the corresponding angles ($\angle \text{O}-\text{H} \cdots \text{O}$) of 156.7°, 162.7°, and 161.7°. Comparatively, the stabilization of the calculated structures were consistent with the activities of IBX oxidation of hydroxybenzyl alcohols in the presence of HemiQ[6].

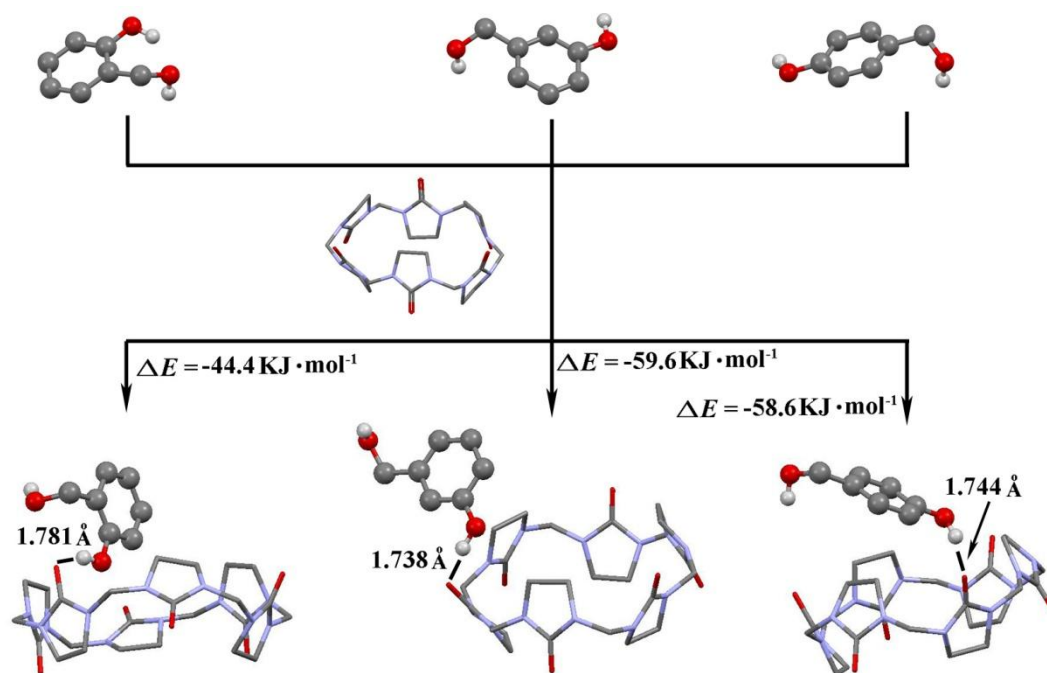


Figure 3-8 Quantum chemistry calculations of the host-guest interactions between hydroxybenzyl alcohols and HemiQ[6]. Color codes: carbon, gray; nitrogen, blue; oxygen, red; hydrogen, white.

3. Conclusions

In summary, we have developed a chemo-selective oxidation reaction for bifunctional substrates, hydroxybenzyl alcohols, with the participation of hemicucurbit[6]uril. The IBX oxidations of hydroxybenzyl alcohols provided a mixture of products, both aldehydes and quinones, due to two hydroxyl groups being present on the benzene ring. However, 50 mol% HemiQ[6] was able to protect the phenolic hydroxyl groups against oxidation by IBX, and produced the corresponding aldehydes as the only product. The oxidations with supramolecular protection were affected by both the steric effects and electronic effects of the substrates. The conversion of 2-hydroxyl alcohol was the lowest, as the two hydroxyl groups were very close to each other. The inductive effect of the phenolic hydroxyl group on 3-hydroxybenzyl alcohol made the reaction faster than the others. The investigation of the host–guest interactions of HemiQ[6] with hydroxybenzyl alcohols with ^1H NMR spectroscopy, IR absorption analysis and UV-vis titration suggested that the hydrogen bonds were formed between HemiQ[6] and the benzyl alcohol guests in a ratio of 1 : 1, through the binding of active hydrogen by the macrocyclic compound. Calculation chemistry was used to investigate the host-guest interactions, and the results indicated the exclusion complexes of HemiQ[6] with 2,3,4-hydroxybenzyl alcohols formed in the ratio of 1 : 1, respectively. The calculated stabilities were consistent with the association constants fitted by UV-vis titrations.

4. Experimental

4.1 Materials and apparatus

HemiQ[6] sample was prepared and purified according to a method in the literature [4] and were characterized by ^1H NMR. HemiQ[6] (CDCl_3 , δ): 3.40 (s, 24H), 4.67 (s, 12H). IBX was prepared with 2-iodobenzoic acid and oxone [22]. ^1H NMR ($\text{DMSO}-d_6$, δ): 7.20 (t, 1H), 7.44 (t, 1H), 7.66 (d, 1H), 7.94 (d, 1H). Mp: 230–233 °C with explosive decomposition. Hydroxybenzyl alcohols and hydroxybenzyl aldehydes were obtained commercially (Tokyo Kasei Kogyo Co., Ltd.) and used without further purification.

^1H NMR spectra were recorded at 25 °C on a JEOL JNM-A100 spectrometer in a mixture of CDCl_3 and $\text{DMSO}-d_6$. UV-vis absorption spectra were recorded on an Perkin-Elmer Lambda 19 UV/Vis/NIR instrument at 25 °C.

4.2 IBX oxidation of hydroxybenzyl alcohols in the absence of HemiQ[6]

In the absence of HemiQ[6], hydroxybenzyl alcohols (0.01 mmol) and IBX (0.01 mmol) were added to a mixture (0.6 mL) of CDCl_3 and $\text{DMSO}-d_6$ (2:1, v/v) in a sealed bottle. The reactions have been carried out at 30 °C for 1 hour, and then the solutions have been detected with ^1H NMR directly.

In the presence of HemiQ[6], hydroxybenzyl alcohols (0.01 mmol), HemiQ[6] (0.005 mmol) and IBX (0.01 mmol) were added to a mixture (0.6 mL) of CDCl_3 and $\text{DMSO}-d_6$ (2:1, v/v) in a sealed bottle. The solution was stirred at 30 °C, and monitored by ^1H NMR over time.

4.3 host-guest interactions

In the UV-vis titration, hydroxybenzyl alcohol solutions were prepared in the mixture of CHCl_3 and CH_3OH (1:1) with a concentration of $2.5 \times 10^{-4} \text{ mol} \cdot \text{L}^{-1}$, this

solution was combined with HemiQ[6] to the guest/HemiQ[6] ratio of 0, 4:1, 2:1, 1:1, and 1:2 and so on.

IR spectra were recorded on a JASCO FT-IR 4200A spectrophotometer using KBr pellets. Each inclusion complex was prepared by stirring the mixture solution of HemiQ[6] with corresponding guest in CHCl_3 in a ratio of 1:1 at 60°C , and then the solvent was removed in vacuum to get the solid inclusion complexes.

All calculations were processed with Gaussian 09 software package [23]. The structures were optimized at the wb97xd/6-311g(*d,p*) level, and single point energies of the optimized geometries and BSSE-corrected (Basis Set Superposition Error corrected) binding energies of the supramolecules were performed at wb97xd/6-311g++(*d,p*) level.

References

1. Cong, H.; Tao, Z.; Xue, S. -F.; Zhu, Q. -J. *Curr. Org. Chem.* **2011**, *15*, 86–95.
2. Raghunathan, R.; Volla, S.; Sivaguru, J. *Chem. Eur. J.* **2012**, *18*, 12178–12190.
3. Masson, E.; Ling, X.; Joseph, R.; Kyeremeh-Mensah, L.; Lu, X.; *RSC Adv.* **2012**, *2*, 1213–1247.
4. Miyahara, Y.; Goto, K.; Oka, M.; Inazu, T. *Angew. Chem. Int. Ed.* **2004**, *43*, 5019–5022.
5. Piancatelli, G.; Scettri, A.; D'Auria, M. *Synthesis* **1982**, 245–258.
6. Delpech, B.; Calvo, D.; Lett, R. *Tetrahedron Lett.* **1996**, *37*, 1019–1022.
7. Dengel, A. C.; El-Hendawy, A. M.; GriYth, W. P.; O'Mahoney, C. A.; Williams, D. J. *J. Chem. Soc., Dalton Trans.* **1990**, 737–742.
8. Green, M. P.; Prodger, J. C.; Hayes, C. J. *Tetrahedron Lett.* **2002**, *43*, 6609–6611.
9. Zimmer, H.; Lankin, D. C.; Horgan, S. W. *Chem. Rev.* **1971**, *71*, 229–246.
10. Kotsovolou, S.; Verger, R.; Kokotos, G. *Org. Lett.* **2002**, *4*, 2625–2628.
11. Dess, D. B.; Martin, J. C. *J. Am. Chem. Soc.* **1991**, *113*, 7277–7287.
12. Duschek, A.; Kirsch, S. F. *Angew. Chem. Int. Ed.* **2011**, *50*, 1524–1552.
13. Frigerio, M.; Santagostino, M. *Tetrahedron Lett.* **1994**, *35*, 8019–8022.
14. More, J. D.; Finney, N. S. *Org. Lett.* **2002**, *4*, 3001–3003.
15. Wu, A.; Duan, Y.; Xu, D.; Penning, T. M.; Harvey, R. G. *Tetrahedron* **2010**, *66*, 2111–2118.
16. Nicolaou, K. C.; Montagnon, T.; Baran, P. S. *Angew. Chem. Int. Ed.* **2002**, *41*, 993–996.
17. Magdziak, D.; Rodriguez, A. A.; Van De Water, R. W.; Pettus, T. R. R. *Org. Lett.* **2002**, *4*, 285–288.
18. Cong, H.; Zhao, F. -F.; Zhang, J. -X.; Zeng, X.; Tao, Z.; Xue, S. -F.; Zhu, Q. -J. *Catal. Commun.* **2009**, *11*, 167–170.
19. Wang, Y. -H.; Cong, H.; Zhao, F. -F.; Xue, S. -F.; Tao, Z.; Wei, G. *Catal. Commun.* **2011**, *12*, 1127–1130.
20. Cong, H.; Li, Z. -J.; Wang, Y. -H.; Tao, Z.; Yamato, T.; Xue, S. -F.; Wei, G. *J.*

Mol. Catal. A: Chem. **2013**, 374–375, 32–38.

21. Grimme, S.; Antony, J.; Schwabe, T.; Mück-Lichtenfeld, C. *Org. Biomol. Chem.* **2007**, 5, 741–758.

22. Frigerio, M.; Santagostino, M.; Sputore, S. *J. Org. Chem.* **1999**, 64, 4537–4538.

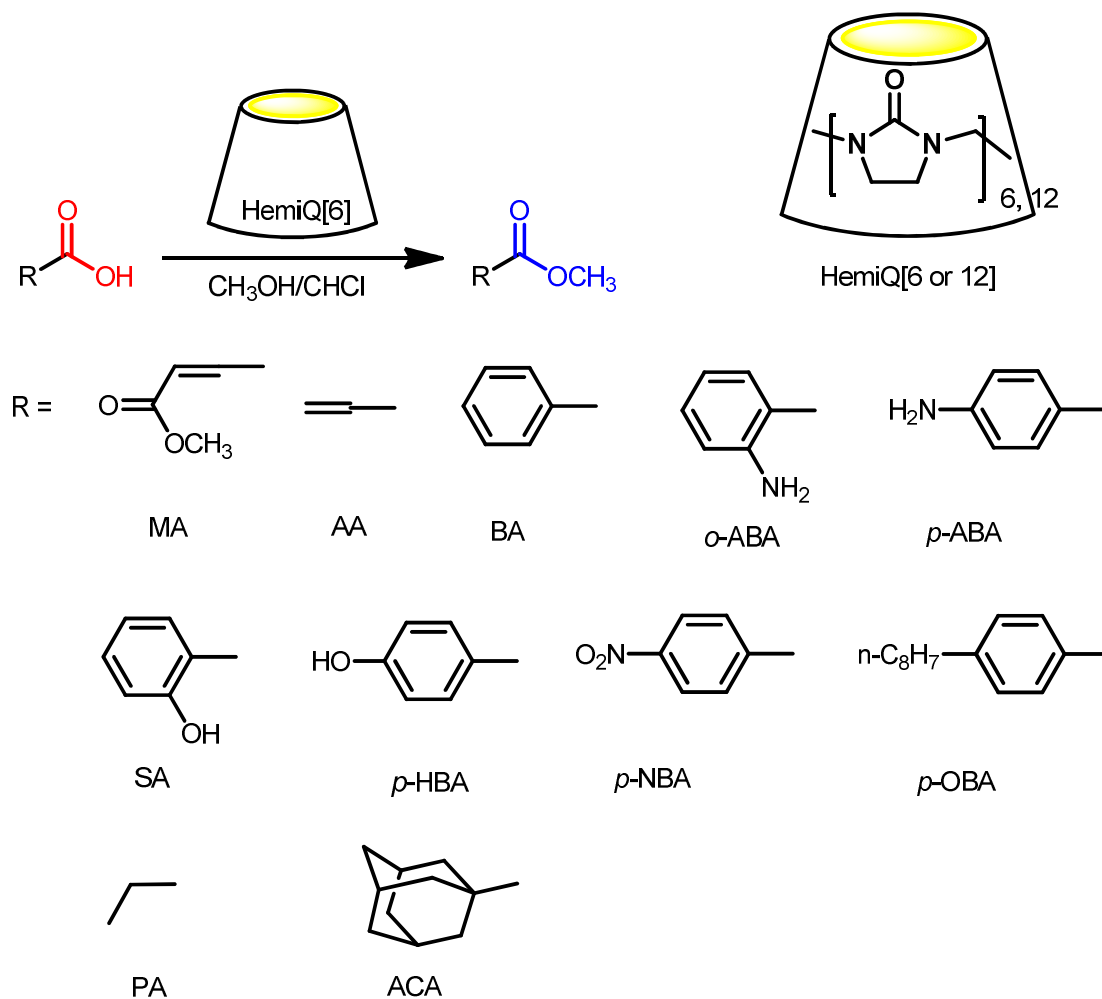
23. Frisch, M. J.; Trucks, G. W.; Schlegel, H. B.; Scuseria, G. E.; Robb, M. A.; Cheeseman, J. R.; Scalmani, G.; Barone, V.; Mennucci, B.; Petersson, G. A.; Nakatsuji, H.; Caricato, M.; Li, X.; Hratchian, H. P.; Izmaylov, A. F.; Bloino, J.; Zheng, G.; Sonnenberg, J. L.; Hada, M.; Ehara, M.; Toyota, K.; Fukuda, R.; Hasegawa, J.; Ishida, M.; Nakajima, T.; Honda, Y.; Kitao, O.; Nakai, H.; Vreven, T.; Montgomery Jr., J. A.; Peralta, J. E.; Ogliaro, F.; Bearpark, M.; Heyd, J. J.; Brothers, E.; Kudin, K. N.; Staroverov, V. N.; Kobayashi, R.; Normand, J.; Raghavachari, K.; Rendell, A.; Burant, J. C.; Iyengar, S. S.; Tomasi, J.; Cossi, M.; Rega, N.; Millam, J. M.; Klene, M.; Knox, J. E.; Cross, J. B.; Bakken, V.; Adamo, C.; Jaramillo, J.; Gomperts, R.; Stratmann, R. E.; Yazyev, O.; Austin, A. J.; Cammi, R.; Pomelli, C.; Ochterski, J. W.; Martin, R. L.; Morokuma, K.; Zakrzewski, V. G.; Voth, G. A.; Salvador, P.; Dannenberg, J. J.; Dapprich, S.; Daniels, A. D.; Farkas, O.; Foresman, J. B.; Ortiz, J. V.; Cioslowski, J.; Fox, D. J. *Gaussian 09, Revision A.02*, **2009**, Gaussian, Inc., Wallingford CT.

Chapter 4

Esterification with Supramolecular Catalysis of Hemicucurbit[6]uril

1. Introduction

The unique property that hemicucurbiturils (Scheme 1, HemiQ[n], $n = 6$ or 12) [1] can be dissolved in CHCl_3 and methanol and binding active proton as mentioned in above case inspired us to develop more supramolecular catalysis of HemiQs. There were a few examples that carbon cation was activated or stabilized by ion-dipole interaction between the carbonyl groups on Q[n] and carbon cation of guests [2-6]. Accordingly, we investigated esterification of organic acids with methanol in the presence of HemiQ[6], which experiences a mechanism including carbon cation intermediate.



Scheme 4-1 Structures of the acids and hemicucurbit[n]uril, $n = 6$ or 12.

Esterification is a classic and fundamental reaction in organic chemistry and biological systems and is catalyzed by acids [7], metal coordination complexes [8] or lipases [9]. Esterification is particularly relevant to biodiesel synthesis in efforts to overcome the scarcity of traditional fossil energy resources and to mitigate greenhouse gas emissions [10]. The reaction is also used in the synthesis of various intermediates and final products for different purposes [11,12]. To gain an understanding of hemicucurbituril-induced esterification, sorts of acids were used as substrates including aryl acids, allyl acids and alkyl acids (Scheme 4-1).

2. Results and discussion

2.1 Esterification of 4-methoxy-4-oxobut-2-enoic acid (MA) in the presence of hemicucurbit[6]uril.

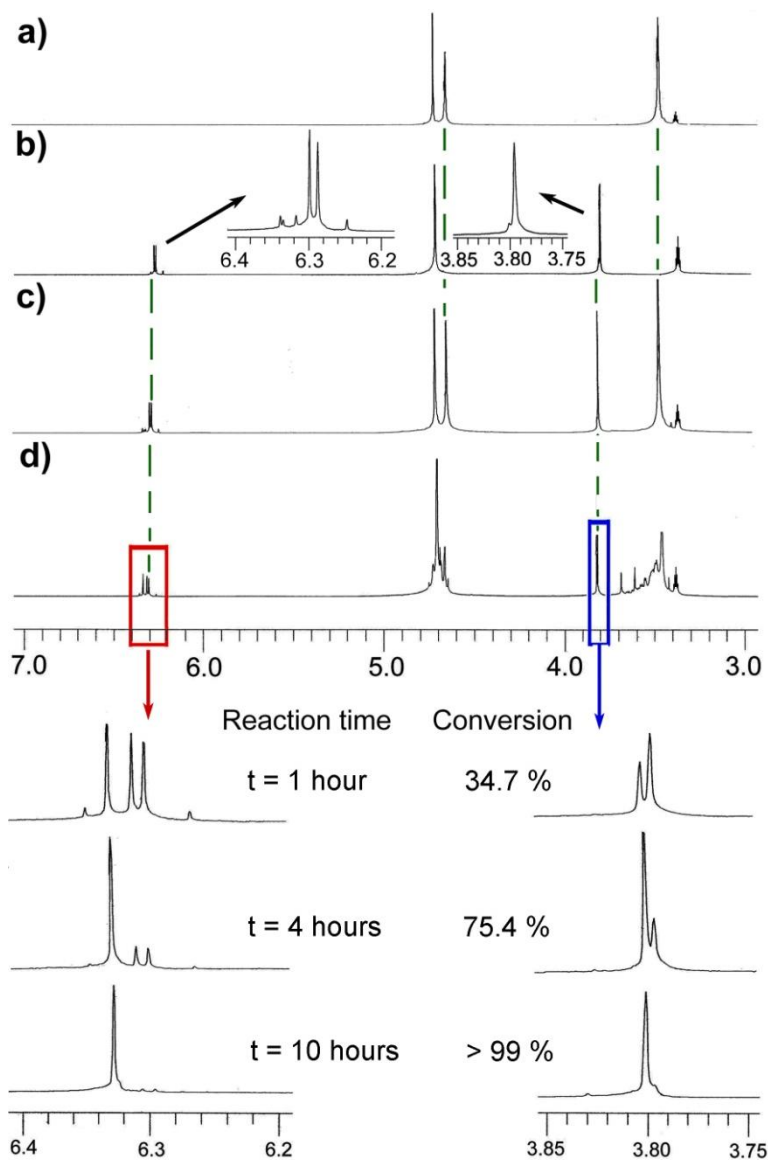


Figure 4-1 ^1H NMR spectra of the esterification of MA in the presence of HemiQ[6].

Spectra of (a) HemiQ[6], (b) MA, (c) a mixture of MA and HemiQ[6] in a ratio of 1 :

1 in $\text{CDCl}_3/\text{CD}_3\text{OD}$ (1 : 1) and (d) after the mixture was heated at 60 °C. The

conversion was confirmed by comparing the integrated proton resonances for the olefin in MA (δ 6.29, 6.30 ppm) with those for the product, dimethyl maleate (δ 6.31 ppm).

MA was the direct product of the alcoholysis reaction of maleic anhydride in methanol, but second-order alcoholysis cannot occur spontaneously and required the attendance of a catalyst such as another organic acid. In the ^1H NMR spectrum of MA (Figure 4-1b), the resonances at δ 6.29 and 6.30 ppm could be attributed to protons on the olefin of MA substrate, which were close to each other as two singlets, and the proton resonance of the $-\text{OCH}_3$ group appeared at δ 3.79 ppm. In general, there are obvious differences in chemical shift patterns between Qs-bound and free guests due to the shielding effect of the macrocyclic cavity and the deshielding effect of the carbonyl groups on the portals. However, compared to spectra of the free guest (Figure 4-1b) and the macrocyclic compound (Figure 4-1a), we observed no change in chemical shift in ^1H NMR spectra of a mixture of MA and HemiQ[6] (Figure 4-1c). Figure 4-1d exhibited broadening of the resonance signals for HemiQ[6] after the mixture was heated, which could be the result from the flexible structure of the host was frozen and included various conformations of the 2-imidazolidinone units and methylene bridges. MA esterification occurred spontaneously, with conversion of 34.7%, and complete conversion was achieved by heating for ~ 10 h. The macrocyclic compound unit was also applied for the screening of the catalysis, but MA cannot be esterified in the presence of 2-Imidazolidinone in a ratio of 1:6. It could be speculated from the result that the cavity of HemiQ[6] is the catalytic residence of the esterification.

The host-guest interaction was also confirmed by the prominent change of IR absorption of the carbonyl groups on binding HemiQ[6] (Figure 4-2). Both the bands at 1714 and 1678 cm^{-1} were attributed to the carbonyl stretching vibration in free HemiQ[6], while the absorption of carbonyl group on free MA guest appeared at 1726 cm^{-1} . Comparing the above absorption, the IR band at 1710 cm^{-1} in the spectrum of inclusion complex confirmed the host-guest interaction, which was attributed to $\nu_{\text{C=O}}$ of bound HemiQ[6].

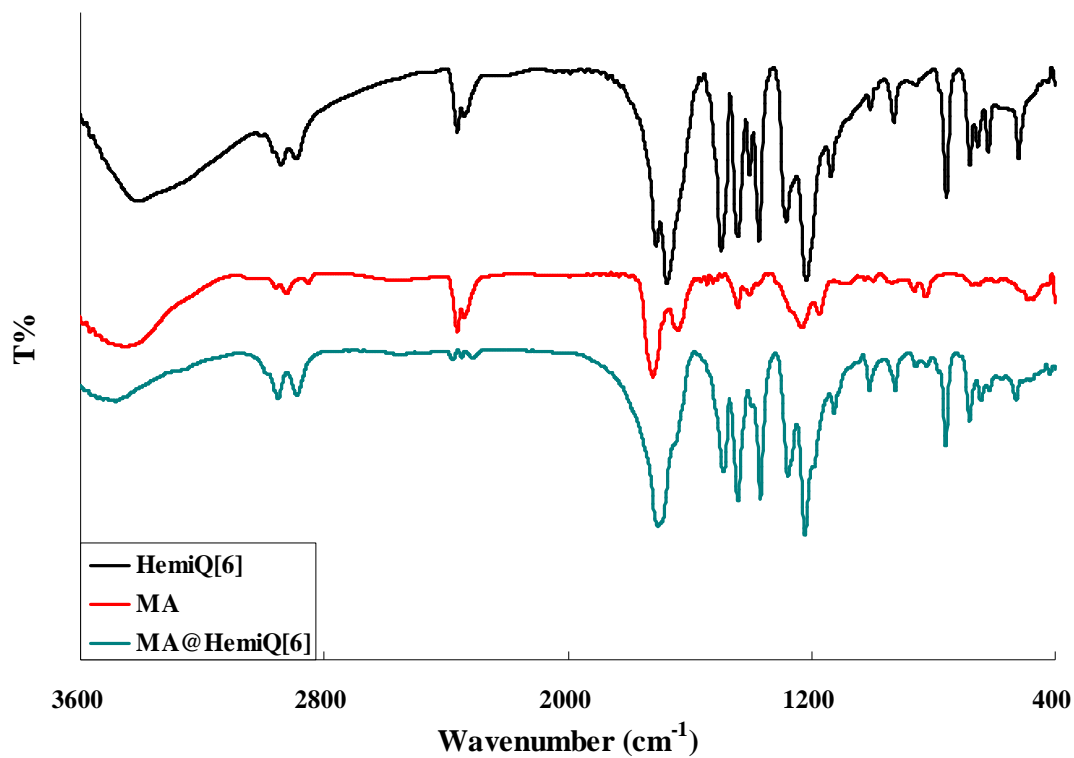


Figure 4-2 IR spectra of HemiQ[6], MA guest and the corresponding inclusion complex.

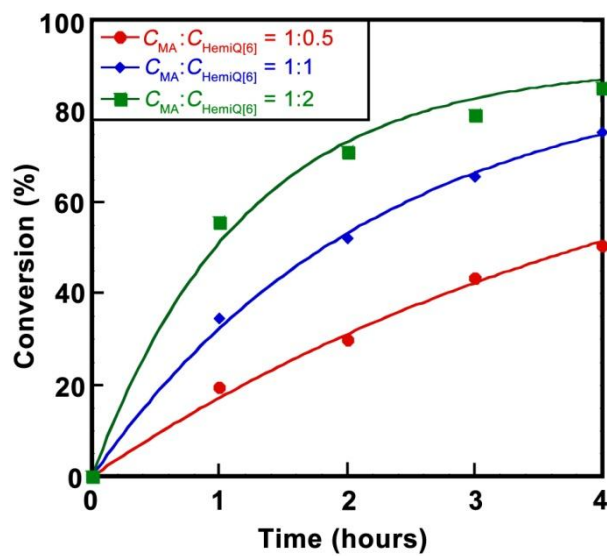


Figure 4-3 Kinetic plots of MA esterification as catalyzed by different ratios of HemiQ[6]

Kinetic plots of the catalytic esterification of MA in the presence of different amounts of HemiQ[6] were shown in Figure 4-3. As expected, the esterification rate increased with the amount of HemiQ[6]. The kinetics of HemiQ[6]-catalyzed esterification can be described by a pseudo-first-order formula [26] :

$$C_t = C_0 \times [1 - \exp(-k_n \times t)], \quad (4-1)$$

where C_0 was the initial concentration of MA substrate and C_t was the concentration of MA substrate at time t , k was the corresponding reaction rate constant, and the subscript n represented the ratio of MA to HemiQ[6].

The calculated kinetic constants suggested that supramolecular catalysis greatly depended on the ratio of MA to HemiQ[6]. Addition of 0.005 mmol of catalyst induced the esterification with a reaction rate constant of 0.18 h^{-1} ($k_{0.5}$). Addition of double this amount to yield a HemiQ[6]/MA ratio of 1 : 1 afforded a constant of $k_{1.0} = 0.36 \text{ h}^{-1}$, which was double the value for $k_{0.5}$. A further increase in the amount of HemiQ[6] in the reaction system improved the percentage conversion of the substrate and a kinetic constant of $k_{2.0} = 0.52 \text{ h}^{-1}$ was obtained, with a curve fitting observed for HemiQ[6]-catalyzed esterification kinetics (Figure 4-3).

2.2 Esterification of acrylic acid (AA) in the presence of hemicucurbit[6]uril.

For the smaller substrate acrylic acid (AA), the HemiQ[6]-catalytic esterification with CD_3OD was also observed. There was no any change of the proton chemical shift of AA in the presence of HemiQ[6] in a 1 : 1 ratio to be observed, and only the broadening resonance peak of HemiQ[6] (Figure 4-4) represented the host-guest interaction as same as that in the case of MA. The conversion of AA at the different time could be non-linear fitted to give a kinetic constant of $k_{\text{AA}} = 1.22 \text{ h}^{-1}$ with the formula 4-1 (Figure 4-4, insert), which was almost 4 folds of the $k_{1.0}$ in the MA system, so the HemiQ[6]-mediated esterification of AA was obviously faster than that

of MA substrate.

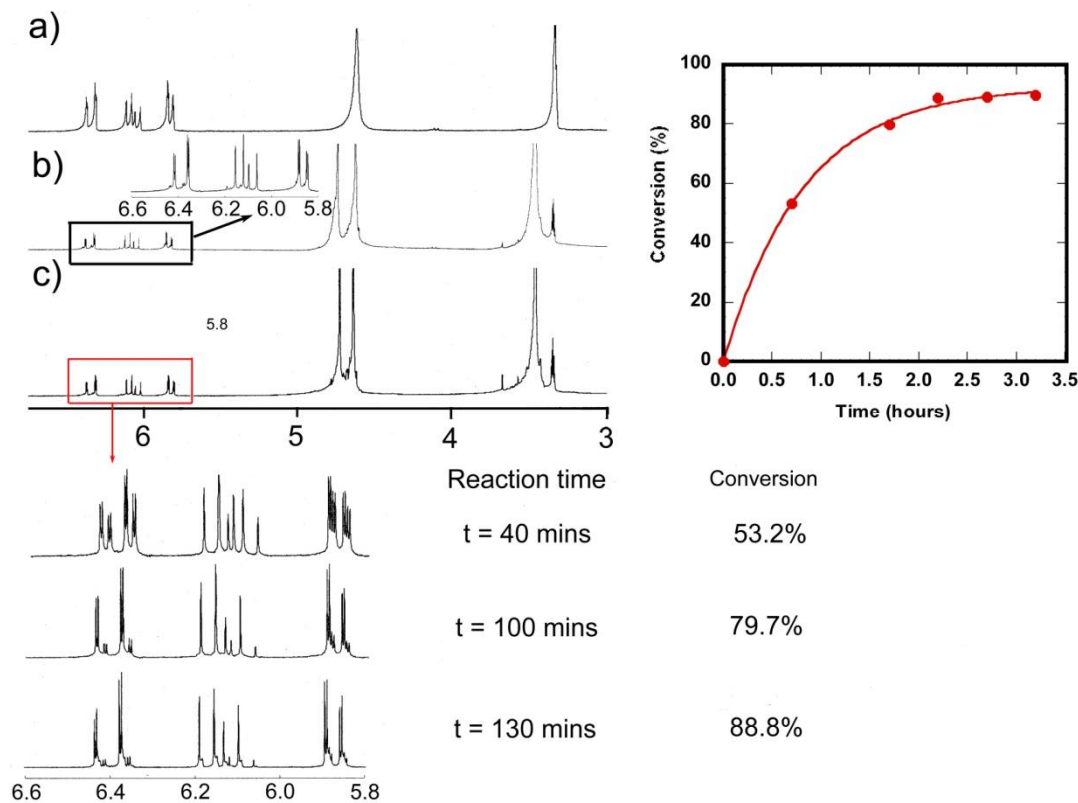


Figure 4-4 ^1H NMR spectra of the esterification of AA in the presence of HemiQ[6]. Spectra of (a) AA, (b) AA and HemiQ[6] in a ratio of 1 : 1 in $\text{CDCl}_3/\text{CD}_3\text{OD}$ (1 : 1) and (c) after the mixture was heated at 60 °C. The conversion was confirmed by comparing the integrated proton resonances for the acrylic group in AA (δ 6.43 ppm) with those for the product, methyl benzoate (δ 6.41 ppm). Insert: Kinetic plots of AA esterification in the presence of HemiQ[6] in the ratio of 1:1.

2.3 Esterification of benzoic acid (BA) in the presence of hemicucurbit[6]uril.

BA was also used to investigate the catalytic activity of HemiQ[6] in the esterification system. ^1H NMR spectra for BA (Figure 4-5a) and a mixture of BA and HemiQ[6] (Figure 4-5b) revealed no obvious changes in resonance signal for protons

on the aryl ring. However, heating of the BA and HemiQ[6] solution induced broadening of the resonance peaks (Figure 4-5c), reflecting interaction between BA and HemiQ[6]. ^1H NMR monitoring of conversion indicated that supramolecular catalysis was still effective for BA esterification at a HemiQ[6]/BA ratio of 1:1, but the reaction was much slower than for HemiQ[6]-catalyzed MA esterification. The conversion of only 45.2% after 5 h was less than two-thirds of that in the MA system. Over the next 5 h, conversion improved by $\sim 13\%$, but the further 4% improvement in conversion at 15 h indicated that esterification was close to the point of chemical equilibrium. The above kinetic plots have been collected in the insert of Figure 4-5 to be curve fitted with the kinetic constant $k_{\text{BA}} = 0.19 \text{ h}^{-1}$, which was almost half of that in the esterification of MA and the one tenth of k_{AA} .

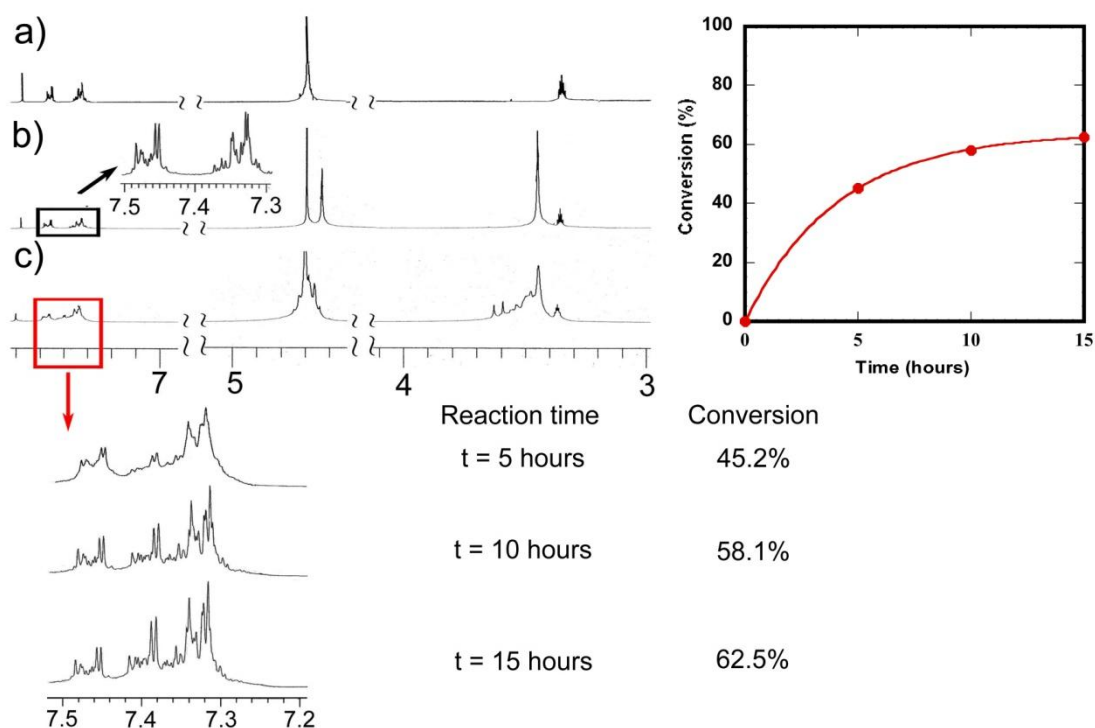


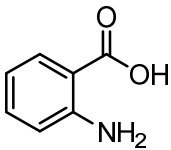
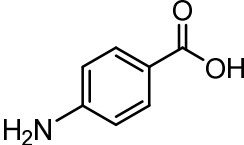
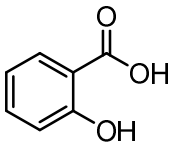
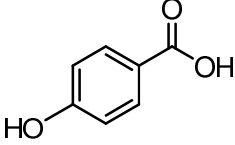
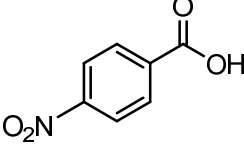
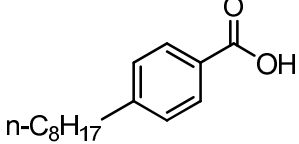
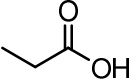
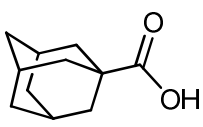
Figure 4-5 ^1H NMR spectra of the esterification of BA in the presence of HemiQ[6]. Spectra of (a) BA, (b) BA and HemiQ[6] in a ratio of 1 : 1 in $\text{CDCl}_3/\text{CD}_3\text{OD}$ (1 : 1) and (c) after the mixture was heated at 60°C . The conversion was confirmed by comparing the integrated proton resonances for the benzyl group in BA (δ 7.45 ppm) with those for the product, methyl benzoate (δ 7.38 ppm). Insert: Kinetic plots of BA esterification in the presence of HemiQ[6] in the ratio of 1 : 1

These results demonstrated that effective esterification largely depended on the substrate structure. The aryl ring of BA was larger than the substituent of MA and AA, and therefore it made against the catalytic esterification by this macrocyclic compound. However, the esterification of the smallest substrate AA could be performed more easily than the others in the presence of HemiQ[6].

2.4 Esterification of other acids in the presence of hemicucurbit[6]uril.

Further studies for the purpose of the universality and selectivity of this supramolecular catalysis was carried out in the presence of equivalent HemiQ[6] in the mixture of CHCl_3 and CH_3OH . As shown in Table 4-1, the results suggested that the catalytic activities should prefer the conjugated structure. Two alkyl acids, PA and ACA, were subjected to the same catalytic esterification, but no reaction occurred. These negative results confirmed that catalysis depended on the substrate structure, and was favored for aryl and allyl substrates. However, there are some different catalytic activities of HemiQ[6] on the esterification of substituted benzoic acid, which tended to prove that the electronic effect and steric effect of the substrates seemed to exist for these aryl acid systems. Almost all of the aryl acids (Entries 1, 2, and 4~6, Table 4-1) can be converted to the corresponding esters with very satisfying conversion in the presence of HemiQ[6], but only 13.1% conversion in the case of SA (Entry 3, Table 4-1) was found. The result indicated that the inductive effect of *o*-OH group should be disadvantage of the esterification, because it was not able to stabilize the carbon cation intermediate in the course of the formation of ester. On the other hand, the conversions of both *o*-ABA (*o*-aminobenzoic acid, Entry 1, Table 4-1) and SA (salicylic acid, Entry 3, Table 4-1) were less than that of the *p*-substituted substrates, *p*-ABA (*p*-aminobenzoic acid, Entry 2, Table 4-1) and *p*-HBA (*p*-hydroxybenzoic acid, Entry 4, Table 4-1), which denoted the existence of the steric effect in this supramolecular catalysis.

Table 4-1 HemiQ[6]-catalytic esterification of acids with methanol

Entries	Substrates	Time (hours)	Conversion ^a (%)
1		12	84.0
2		12	90.7
3		24	13.1
4		24	58.8
5		12	86.9
6		18	70.8
7		24	-
8		24	-

^aThe conversion of entries 1~6 was measured by HPLC, and the esterification of entries 7~8 were traced by ¹H NMR.

2.4 Effect of macrocycle species, amount of methanol on the esterification of acids.

For a random selection, four substrates, MA, BA, ACA and PA, were subjected to esterification with a stoichiometric amount of MeOH in the presence of HemiQ[6] in CDCl_3 , but no ester product was synthesized in more than 24 h. These results indicate that the catalytic activity of HemiQ[6] greatly depends on the substrate concentration and suggest that the mechanism for esterification is a solvolytic reaction between the acids and the CH_3OH solvent.

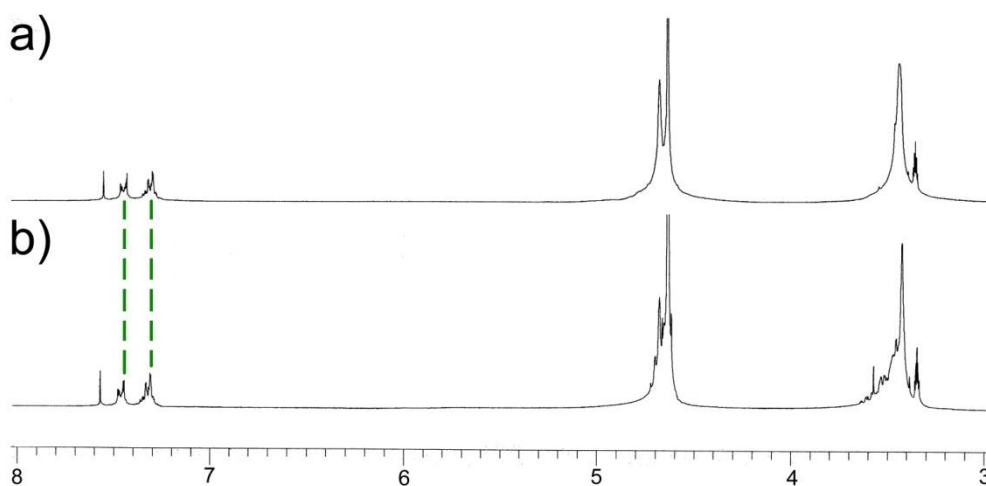
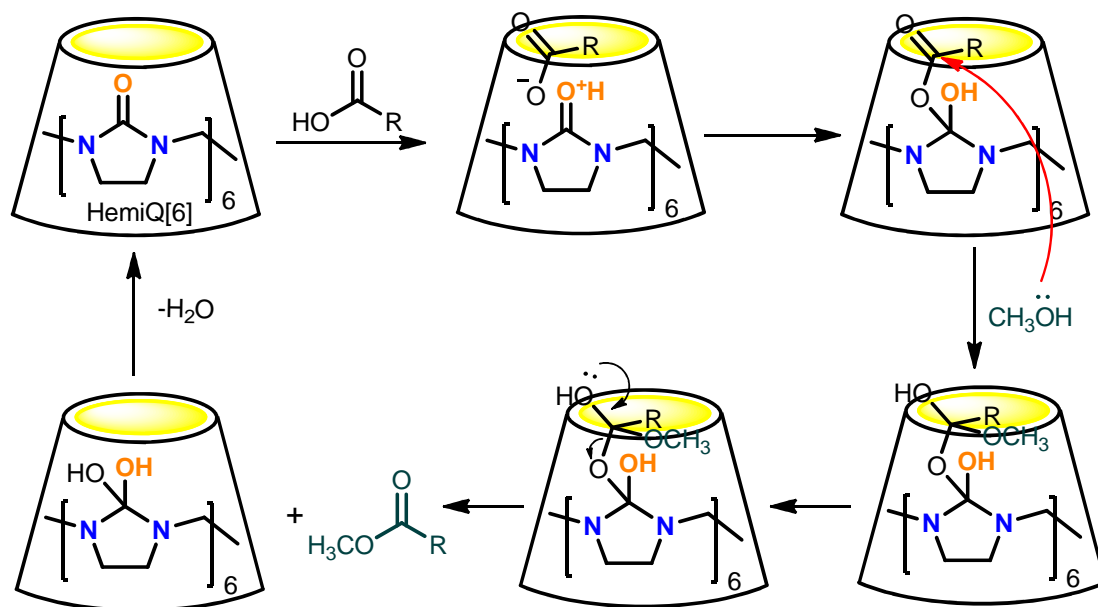


Figure 4-6 ^1H NMR ($\text{CDCl}_3/\text{CD}_3\text{OD}$ 1:1) spectra of (a) a mixture of MA and HemiQ[12] and (b) after the mixture was heated for 12 h.

To understand the dependence of supramolecular catalysis on the structure of the macrocyclic catalyst, HemiQ[12] was used as an alternative to catalyze acid esterification in $\text{CDCl}_3/\text{CD}_3\text{OD}$ (1:1) solution. Only resonance broadening was observed for HemiQ[12] singlets in ^1H NMR spectra of a heated mixture of BA and HemiQ[12] (Figure 4-6), which suggested just formation of host-guest interaction complex, and supramolecular catalysis was ineffective for esterification of the four acids. Thus, a more flexible structure and a larger cavity, as in HemiQ[12], are negative factors in this catalytic esterification.

2.5 Proposed mechanism of the esterification of acids in the presence of hemicucurbit[6]uril.



Scheme 4-2 Proposed mechanism of HemiQ[6]-induced esterification.

According to the above experimental evidence, a possible mechanism of the HemiQ[6]-catalytic esterification was proposed in [Scheme 4-2](#). Firstly, the host-guest interaction occurred with the protonation of HemiQ[6] by the acid guest, and then the carbon cation of carboxyl group on substrate was activated followed by the nucleophilic attack of methanol. The transfer of lone pair electrons afforded the ester product. Finally, the dehydrolysis on the macrocyclic compound completed the catalytic cycle.

3. Conclusion

A method for effective supramolecular hemicucurbit[6]uril catalysis of esterification of carboxylic compounds was developed hereby. HemiQ[6]-induced esterification depended on the amount of macrocyclic compound, that is, application of a greater amount of catalyst was favor to increase the reaction rate. The electronic and steric structures of the substrates affected the supramolecular catalysis; only the conjugated acids could be catalyzed using this method. In the screening of the macrocyclic compound, HemiQ[12] was ineffective in catalyzing the esterification, so the structure of the catalyst should be a crucial factor. The reaction results for the cases of four organic acids selected randomly with a stoichiometric amount of MeOH suggested that the esterification could be alcoholysis of acid substrate in CH₃OH solvent. A possible mechanism was proposed for supramolecular catalytic esterification in the presence of hemicucurbit[6]uril.

4. Experimental

4.1 Materials and apparatus

HemiQ[*n*] (*n* = 6 or 12) samples were prepared and purified according to a method in the literature [12] and were characterized by ¹H NMR. HemiQ[6] (CDCl₃, δ): 3.40 (s, 24H), 4.67 (s, 12H); HemiQ[12] (CDCl₃, δ): 3.36 (s, 24H), 4.67 (s, 12H). The acids were obtained commercially (Tokyo Kasei Kogyo Co., Ltd.) and used without further purification.

¹H NMR spectra were recorded at 25 °C on a JEOL JNM-AI00 spectrometer in a mixture of CDCl₃ and CD₃OD. High Performance Liquid Chromatography (HPLC) was performed using a JASCO with a UV detector. The acids and corresponding esters were successfully separated by a Wakosil 5SIL chromatographic column (250 mm × 4.6 mm).

4.2 Catalytic esterification experiments

In the cases of MA, AA, BA, PA (propanoic acid) and ACA (1-adamantanecarboxylic acid), acids (0.01 mmol) were added to a mixture of CDCl₃ and CD₃OD (1:1, 0.6 ml) and the solution was transferred into an NMR tube. HemiQ[*n*] (*n* = 6 or 12) was added to the acid solution at a corresponding ratio. The NMR tube was directly heated to 60 °C and monitored by ¹H NMR over time. Reactant conversion was directly confirmed by ¹H NMR spectral data. For the other substrates, acids (0.01 mmol) were added to a mixture of CHCl₃ and CH₃OH (1:1, 1.0 ml) and HemiQ[6] was added to the solution in a ratio of 1:1. The solution was heated to 60 °C, and then it was diluted with ethyl acetate to an appropriate concentration for the measure by HPLC.

4.3 IR annlysis of host-guest interactions

IR spectra were recorded on a JASCO FT-IR 4200A spectrophotometer using KBr pellets. Each inclusion complex was prepared by stirring the mixture solution of HemiQ[6] with corresponding guest in CHCl_3 in a ratio of 1 : 1 at 60°C , and then the solvent was removed in vacuum to get the solid inclusion complex.

References

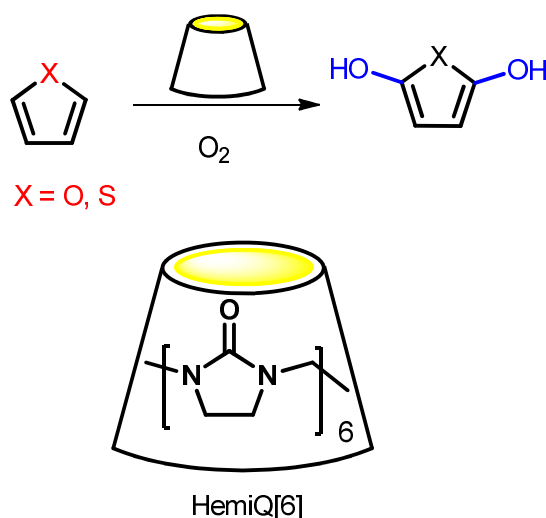
1. Miyahara, Y.; Goto, K.; Oka, M.; Inazu, T. *Angew. Chem. Int. Ed.* **2004**, *43*, 5019–5022.
2. Wang, R.; Macartney, D. H. *Tetrahedron Lett.* **2008**, *49*, 311–314.
3. Bhasikuttan, A. C.; Mohanty, J.; Nau, W. M.; Pal, H. *Angew. Chem. Int. Ed.* **2007**, *46*, 4120–4122.
4. Rawashdeh, A. M. M.; Thangavel, A.; Sotiriou–Leventis, C.; Leventis, N. *Org. Lett.* **2008**, *10*, 1131–1134.
5. Thangavel, A.; Elder, I. A.; Sotiriou–Leventis, C.; Dawes, R.; Leventis, N. *J. Org. Chem.* **2013**, *78*, 8297–8304.
6. Liu, Y.; Shi, J.; Chen, Y.; Ke, C. –F. *Angew. Chem. Int. Ed.* **2008**, *47*, 7293–7296.
7. Reddy, B. M.; Patil, M. K. *Curr. Org. Chem.* **2008**, *12*, 118–140.
8. Zhang, J.; Leitus, G.; Ben-David, Y.; Milstein, D. *J. Am. Chem. Soc.* **2005**, *127*, 10840–10841.
9. Guncheva, M.; Zhiryakova, D. *J. Mol. Catal. B: Enzym.* **2011**, *68*, 1–21.
10. Kouzua, M.; Nakagaito, A.; Hidaka, J. *Appl. Catal. A: Gen.* **2011**, *405*, 36–44.
11. Carmo, A. C.; Souza de, L. K. C.; Costa de, C. E. F.; Longo, E.; Zamian, J. R.; Rocha Filha da, G. N. *Fuel* **2009**, *88*, 461–468.
12. Sejidov, F. T.; Mansoori, Y.; Goodarzi, N. *J. Mol. Catal. A: Chem.* **2005**, *240*, 186–190.

Chapter 5

Aerobic Oxidation of Furans and Thiophene in the Presence of Hemicucurbit[6]uril

1. Introduction

Hemicucurbit[n, n = 6, 12]uril were able to dissolve into both aqueous solvent and organic solvent [1]. The supramolecular catalysis of HemQ[6] in the mixture of either methanol and chloroform or DMSO and chloroform was discovered as mentioned in above cases, which encouraged us to develop novel supramolecular catalysis in aqueous media, with these kinds of macrocyclic compounds. We revealed the catalytic activities of HemiQ[6] for the aerobic oxidation of heterocyclic compounds here, such as furans and thiophene (Scheme 5-1).



Scheme 5-1 Structures of the substrates and HemiQ[n, n = 6 or 12].

Oxidation is a vital chemical process in organic synthesis. It produces oxygen-containing compounds such as alcohols, aldehydes, ketones, carboxylic acids and epoxides from hydrocarbons [2]. For user- and eco-friendly purposes, O₂ (or Air) and H₂O₂ usually serve as the oxygen source. However, the direct application of O₂ is always hindered by a high energy barrier, due to the transition from the triplet state of the oxygen molecule to the singlet state [3]. To overcome this problem, lots of coordination compounds have been developed to capture and activate O₂. Cu²⁺, Mn²⁺, Pd²⁺ and Au⁺ are often used as the central metal cations in coordination compound catalysts [4–7]. An alternative pathway, in which HemiQ[6] was used to allow the aerobic oxidation to be carried out under mild conditions *via* a supramolecular

strategy was developed hereby (Scheme 5-1). The oxidation of furan usually cannot provide the hydroxyfuran product, which was an extremely unstable tautomers of the corresponding oxo derivative [8,9], the enol product, furan-2,5-diol, was able to be stabilized in the presence of HemiQ[6].

2. Results and discussion

2.1 Aerobic oxidation of furan in the presence of hemicucurbit[6]uril

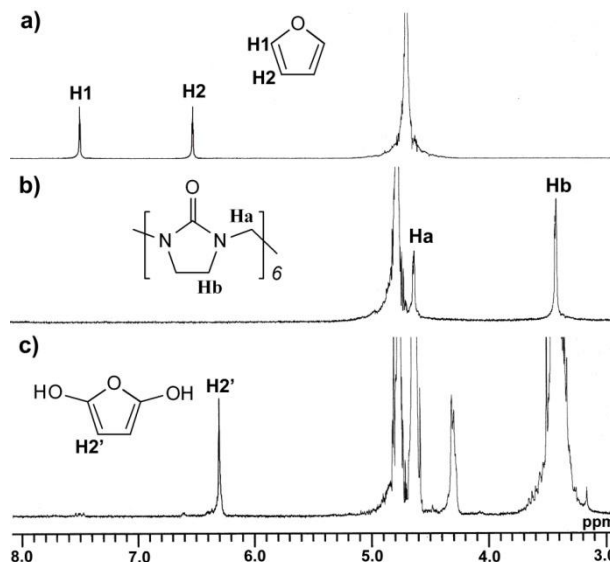


Figure 5-1 ^1H NMR spectra of a) furan; b) HemiQ[6]; c) a D_2O solution of furan after heating for 8 hours in the presence of HemiQ[6].

The oxidation of furan in D_2O was found to take place with addition of HemiQ[6] from the ^1H NMR trace, while no reaction happened in the absence of the macrocyclic compound. As shown in Figure 5-1, the two resonance signals from furan, at δ 6.5 and δ 7.6 ppm (Figure 5-1a), became weaker as its deuterated aqueous solution mixed with HemiQ[6] was heated for 8 hours, and a new singlet appeared at δ 6.3 ppm (Figure 5-1c). Comparing with Figure 5-1b, the proton resonance of Hb on HemiQ[6] did not show any shift, but the proton resonance of Ha became slightly split, which indicated the encapsulation of the product by the HemiQ[6].

The IR absorption of the hydroxyl group shown a slight blue shift, from 3436 to 3446 cm^{-1} , and the carbonyl groups on the binding HemiQ[6] show obvious differences in their IR absorption compared with the free host (Figure 5-2). The proton resonance of -OH group appears at δ 1.07 ppm with the results of hydrogen-deuterium exchange action (Figure 5-3).

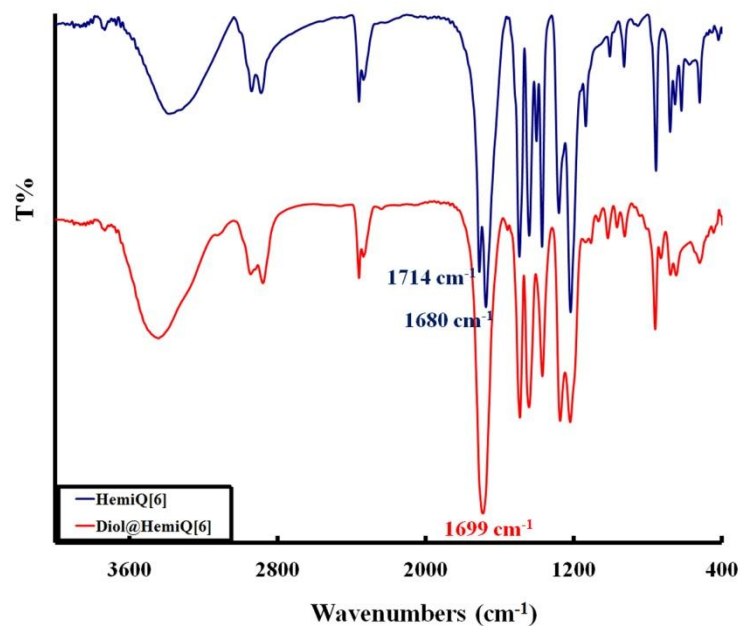


Figure 5-2 IR spectra of free HemiQ[6] and the product of furan-2,5-diol @HemiQ[6].

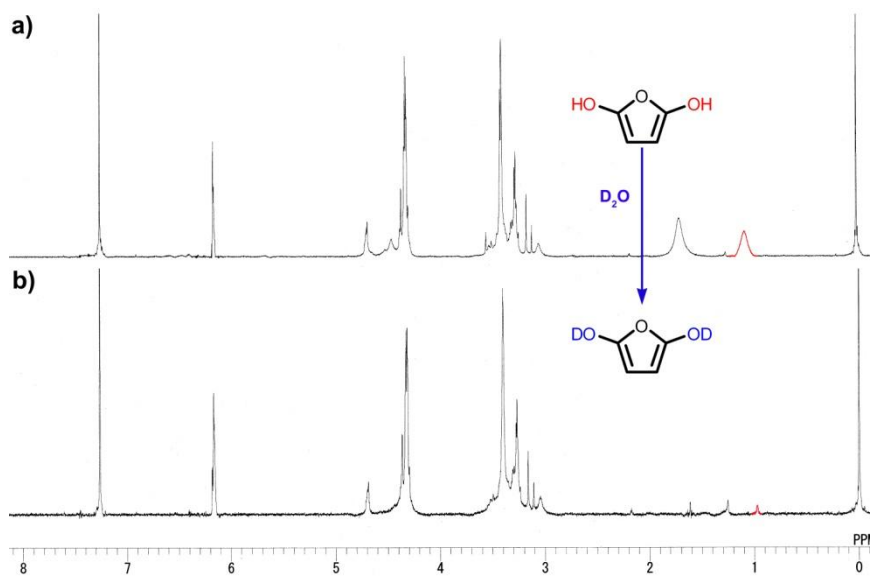


Figure 5-3 ¹H NMR spectra of a) oxidation product of furan in H₂O in the presence of HemiQ[6] followed by extraction with CDCl₃; b) after addition of D₂O. Furan (0.015 mmol) was added into 0.6 mL H₂O with HemiQ[6] in a ratio of 1:1, followed by heating at 65 °C for 10 h and then extraction with CDCl₃. The resonance of an active proton at δ 1.07 ppm faded away with the addition of D₂O.

2.2 Host-guest interaction of furan with of hemicucurbit[6]uril, and protonation of hemicucurbit[6]uril.

The above evidences shown that furan was oxidized to furan-2,5-diol. The heated solution of furan and HemiQ[6] was acidified with DCl and neutralized by addition of solid Na_2CO_3 followed by extraction with CDCl_3 . This presence of the dione, dihydrofuran-2,5-dione was confirmed, with the carbonyl group identified by IR with the absorption at 1683 cm^{-1} . On the other hand, that furan cannot be oxidized in deoxygenated aqueous solution (5% Na_2SO_3 , and Ar atmosphere) even in the presence HemiQ[6] suggested the aerobic process.

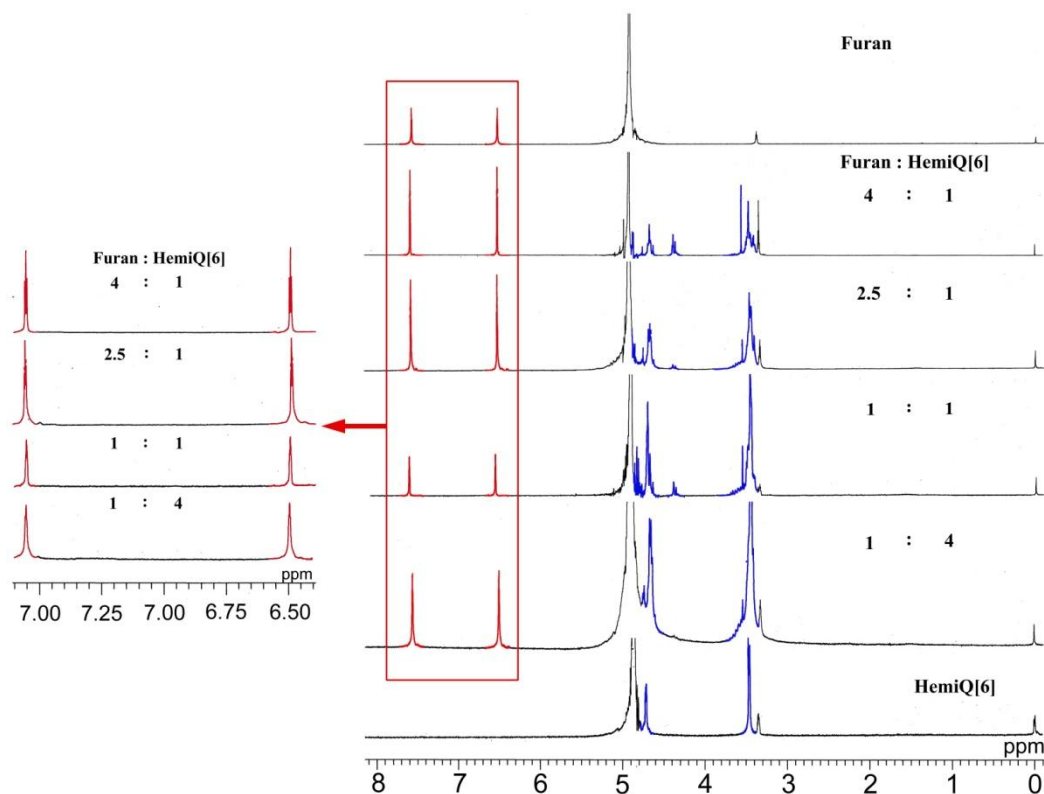


Figure 5-4 ^1H NMR titration of the host-guest interaction between furan and HemiQ[6] at $\text{pD} = 6.3$ (all of attribution refer to TMS) The D_2O solution of 2.5×10^{-3} M furan has been prepared, and the ^1H NMR spectra were recorded with increasing amount of HemiQ[6].

In cucurbituril chemistry, the host-guest interactions are always characterized by changes of chemical shifts of the encapsulated guest in ^1H NMR, that is, the shielding effect leads to an upward shift of the resonance signals of guest when it is inserted into the core of the macrocyclic cavity, while the deshielding effect from the carbonyl groups on the portals makes the ^1H NMR response of the guest remaining at the portal to shift down [10,11]. However, no chemical shift was observed here for furan in the presence of HemiQ[6], as reported previously [12], simply broadening of the furan peaks with addition of the macrocyclic compound, while the appearance of a complicated resonance of HemiQ[6] in the presence of furan guest in the ratio of above 1 : 1 (Figure 5-4).

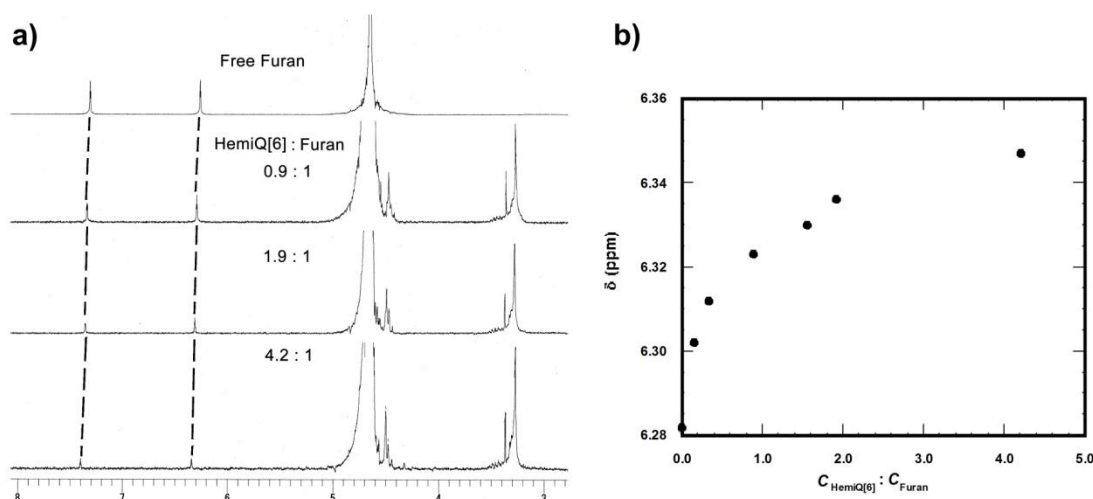


Figure 5-5 a) ^1H NMR titration of the host-guest interaction between furan and HemiQ[6] at $\text{pD} = 2.0$ (all attributions with reference to TMS); b) changes of the chemical shift of proton H2 on furan ring in the presence of different ratio of HemiQ[6].

Fortunately, the improvement of acidity allowed the host-guest interaction model between furan and HemiQ[6] to be detected with ^1H NMR analysis (Figure 5-5). In the presence of HemiQ[6] at $\text{pD} 2.0$, the resonance signals of all protons on the furan ring underwent a very slight downfield shift, which suggested that the guest remained in the deshielding area around the carbonyl groups on HemiQ[6] (Figure 5-5a). The trace plots of these chemical shift changed from δ 6.28 to δ 6.35 ppm when the ratio

of $C_{\text{HemiQ}[6]}/C_{\text{furan}}$ is up to 4.2:1 indicated a 1 : 1 binding model with a weak association constant $K_a = (5.2 \pm 2.4) \times 10^2 \text{ L}\cdot\text{mol}^{-1}$ (Figure 5-5b). Accordingly, the host-guest interaction between furan and HemiQ[6] was possibly improved by the participation of proton.

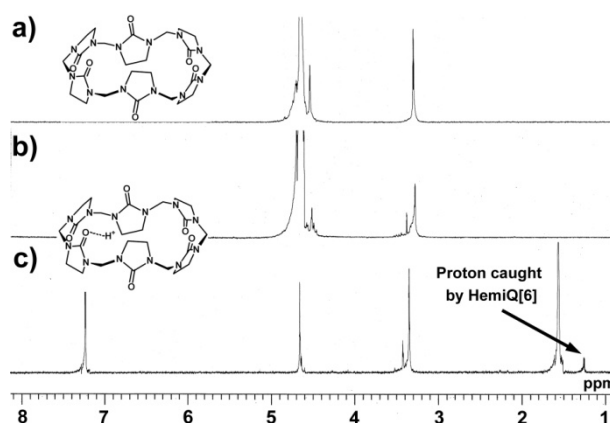


Figure 5-6 ¹H NMR spectra of HemiQ[6] in a) D₂O; b) DCl/D₂O, pD = 2.0; c) CDCl₃ extracted from DCl/D₂O at pH = 2.0.

The proposal in Miyahara's pioneering work [1], that HemiQ[6] bond to protons in the crystallographic structure, prompted us to investigate the protonation of this macrocyclic compound in solution. Comparing the ¹H NMR spectrum of HemiQ[6] in neutral and acidic D₂O (Figure 5-6a), the proton resonance appeared broadened in acidified solution (Figure 5-6b). To provide clear evidence that a proton can be captured by this host, HemiQ[6] was dissolved in acidic aqueous solution (pH = 2.0) followed by extraction with CDCl₃. Subsequently, the spectrum of the organic layer exhibited the resonance signal of an active proton at δ 1.23 ppm (Figure 5-6c). We proposed that the presence of the proton, with its positive charge, decreased the repulsion between the electron-rich furan ring and the carbonyl groups on the HemiQ[6] and therefore stabilizes the host-guest interaction complex.

2.3 Kinetics of aerobic oxidation of furan in the presence of hemicucurbit[6]uril.

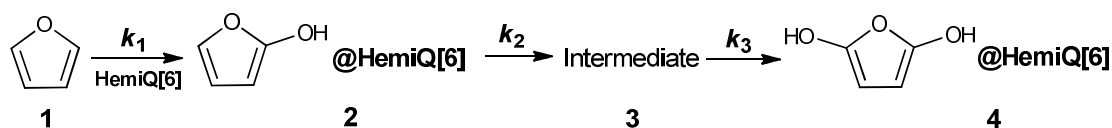
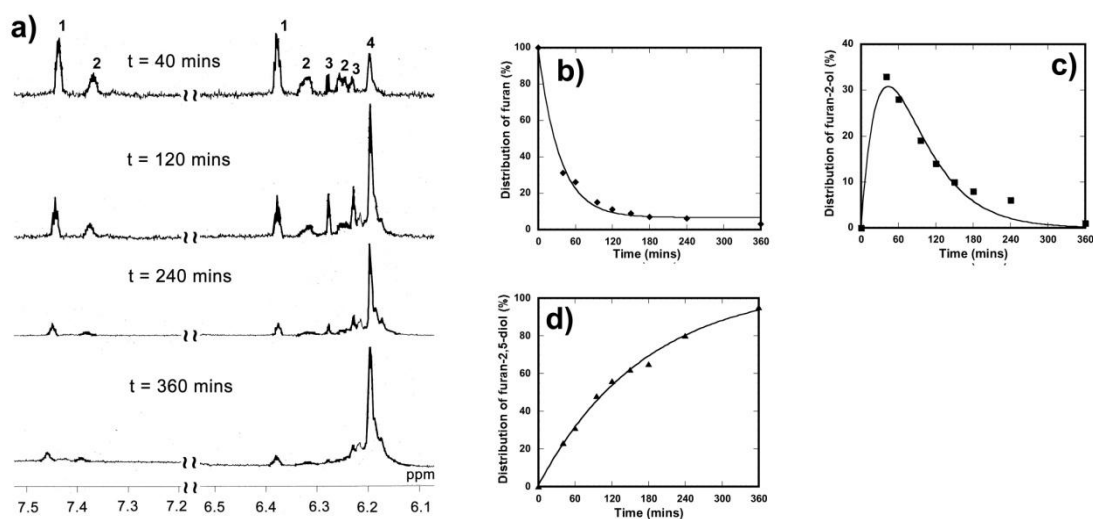
**Scheme 5-2** Oxidation of furan in the presence of HemiQ[6].

Figure 5-7 a) ¹H NMR traces showing the progress of the aerobic oxidation of furan in the presence of 1 equiv HemiQ[6] in neutral conditions (pD = 6.3) (1: furan, 2: furan-2-ol, 3: intermediate, 4: furan-2,5-diol), and the distribution plots of b) furan, c) furan-2-ol, and d) furan-2,5-diol.

To understand the role of protons in this example of supramolecular catalysis, the kinetics of the aerobic oxidation with 1 equiv HemiQ[6] was investigated at different pH values (Scheme 5-2). The ¹H NMR trace of the oxidation at pD = 6.3 shown that it was a typical consecutive reaction, with 3 steps (Figure 5-7a). Firstly, furan was oxidized to furan-2-ol, which was the main product, accounting for more than 30% in this first stage. Subsequently, further oxidation weakened the proton resonance at δ 7.39 ppm and both resonance signals, at δ 6.32 and 6.25 ppm, shown a positive shift. We concluded that there was an intermediate based on the furan-2-ol structure but

without oxidation of the β -H. However, the secondary hydroxyl was not yet fully bound. Finally, the oxidation produced a singlet at δ 6.20 ppm, which indicated that furan-2,5-diol was produced, with about 90% conversion.

The above reaction sequence could be described by the following kinetic formulas:

$$\frac{dC_{\text{furan}}}{dt} = -k_1 \cdot C_{\text{furan}} \quad (5-1)$$

$$\frac{dC_{\text{furan-2-ol}}}{dt} = k_1 \cdot C_{\text{furan}} - k_2 \cdot C_{\text{furan-2-ol}} \quad (5-2)$$

$$\frac{dC_{\text{furan-2,5-diol}}}{dt} = k_3 \cdot C_{\text{furan-2,5-diol}} \quad (5-3)$$

where k_1 , k_2 , and k_3 referred to the rate constants for the HemiQ[6]-induced aerobic oxidation reaction in the first, second, and third elementary reactions, respectively. These formulas could be integrated to give:

$$(C_{\text{furan}})_t = e^{-k_1 t} \quad (5-4)$$

$$(C_{\text{furan-2-ol}})_t = \frac{k_1}{k_2 - k_1} \cdot (e^{-k_1 t} - e^{-k_2 t}) \quad (5-5)$$

$$(C_{\text{furan-2,5-diol}})_t = 1 - e^{-k_3 t} \quad (5-6)$$

The distribution plots for furan, furan-2-ol and furan-2,5-diol at different times were able to be non-linearly fitted to formulas (5-4)~(5-6) (Figure 5-7b-d) to give the corresponding kinetic constants $k_1 = 2.9 \times 10^{-2} \text{ min}^{-1}$, $k_2 = 2.7 \times 10^{-2} \text{ min}^{-1}$, and $k_3 = 5.7 \times 10^{-3} \text{ min}^{-1}$. Clearly, the secondary oxidation in the third step was more difficult than the previous steps (k_3 is the smallest rate constant), so this should be the rate-determining step in the overall reaction.

The oxidation of furan was slow down with the decreased amount of supramolecular catalyst, in the presence of 0.5 equiv. HemiQ[6], the rate constants were $k_1 = 5.5 \times 10^{-3} \text{ min}^{-1}$, $k_2 = 5.1 \times 10^{-3} \text{ min}^{-1}$, and $k_3 = 2.0 \times 10^{-3} \text{ min}^{-1}$ (Figure 5-8), respectively, while they are increased to $k_1 = 5.2 \times 10^{-2} \text{ min}^{-1}$, $k_2 = 6.4 \times 10^{-2} \text{ min}^{-1}$, and $k_3 = 1.3 \times 10^{-2} \text{ min}^{-1}$ with addition of 2.0 equiv. HemiQ[6] (Figure 5-9).

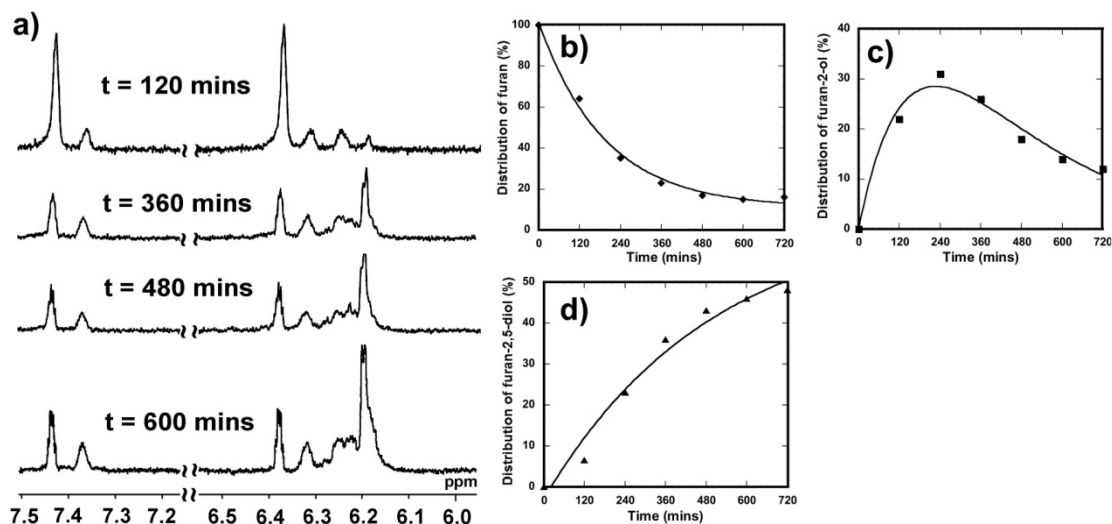


Figure 5-8 a) ^1H NMR traces showing the progress of the aerobic oxidation of furan in the presence of 0.5 equiv HemiQ[6] in neutral conditions ($\text{pD} = 6.3$), and the distribution plots for b) furan, c) furan-2-ol, and d) furan-2,5-diol.

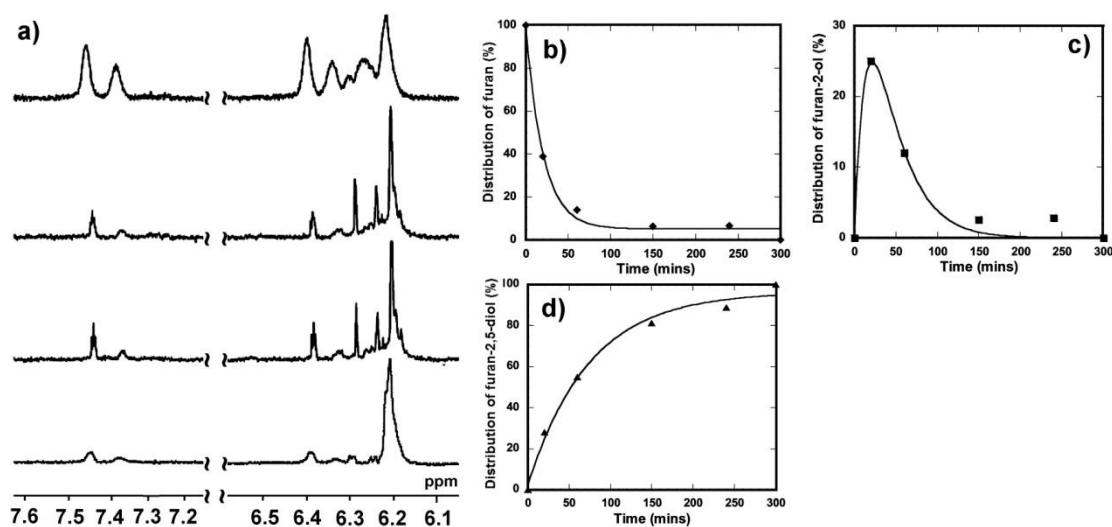


Figure 5-9 a) ^1H NMR traces showing the progress of the aerobic oxidation of furan in the presence of 2.0 equiv HemiQ[6] in neutral conditions ($\text{pD} = 6.3$), and the distribution plots for b) furan, c) furan-2-ol, and d) furan-2,5-diol.

The oxidation of furan in the presence of HemiQ[6] at $\text{pD} = 2.0$ was also tracked using ^1H NMR spectra (Figure 5-10a) and a similar process, involving three elementary steps, was found. However, the reaction rates for all stages were clearly faster than those in neutral condition, as found from fitting the kinetic plots using

formulas (5-4)~(5-6) (Figure 5-10b-d). The improvement of the kinetic constants ($k_1 = 7.2 \times 10^{-2} \text{ min}^{-1}$, $k_2 = 5.2 \times 10^{-2} \text{ min}^{-1}$, and $k_3 = 1.4 \times 10^{-2} \text{ min}^{-1}$) demonstrated that the oxidation could be accelerated in acidic conditions, that is, the proton affected not only the host-guest interaction between HemiQ[6] and furan, but also the process of aerobic oxidation.

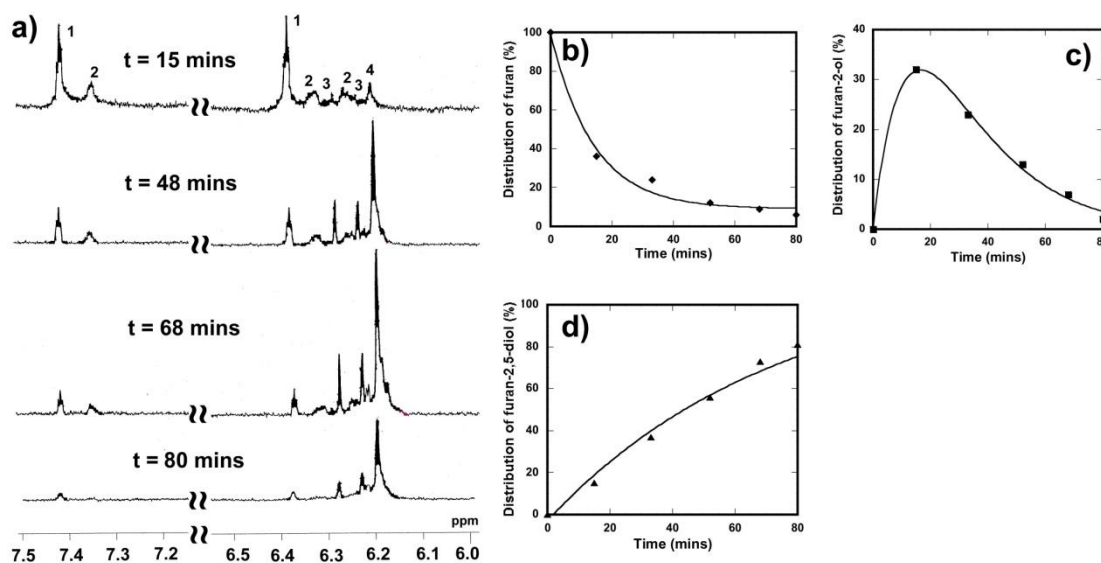


Figure 5-10 a) ¹H NMR traces showing the progress of the aerobic oxidation of furan in the presence of 1 equiv HemiQ[6] in acid conditions (pD = 2) 1: furan, 2: furan-2-ol, 3: intermediate, 4: furan-2,5-diol), and the distribution plots for b) furan, c) furan-2-ol, and d) furan-2,5-diol.

2.4 Mechanism of aerobic oxidation of furan in the presence of hemicucurbit[6]uril.

Moreover, the crucial role of the proton was proved by independent experiments which shown that when the HemiQ[6]-catalytic oxidation of furan was carried out in different organic solvents and alkaline aqueous solution, the same product, furan-2,5-diol, was observed in methanol after heating for 15 h, but there was no reaction in either the aprotic solvent chloroform or an aqueous solution of Na₂CO₃ (pD = 10). The other members of the cucurbituril family, HemiQ[12], Q[6] and Q[7], were also tested in this system, but no oxidation was observed, only the host-guest

interaction between furan and Q[7], in which the up-shift of proton resonances of furan indicated guest was encapsulated within the cavity of Q[7] (Figure 5-11). It was concluded that this supramolecular catalysis was dependent on the structure of the macrocyclic compound. To confirm the functionalization of HemiQ[6]'s cavity, imidazolidin-2-one was also subjected to the oxidation of furan but no observation of any reactivity.

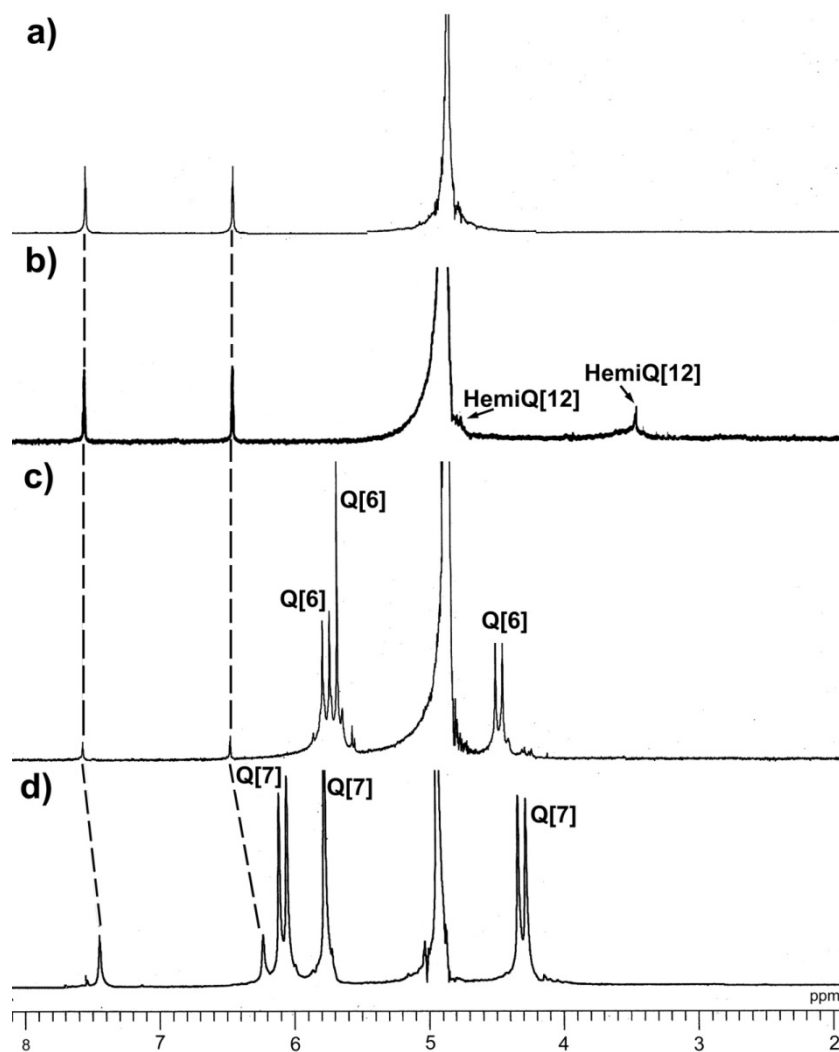
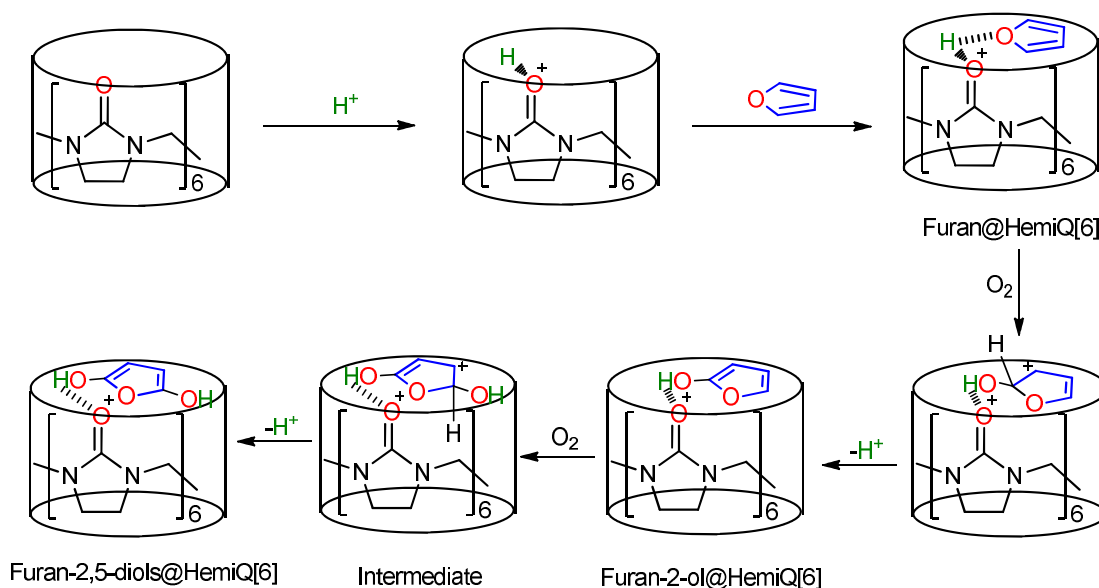


Figure 5-11 ¹H NMR spectra of furan a) in the absence of Qs; b) in the presence of HemiQ[12] (the solubility of HemiQ[12] in water is very poor); c) in the presence of Q[6]; d) in the presence of Q[7]. The D₂O solution of 2.5×10^{-3} M furan has been prepared, and the ¹H NMR spectra were recorded with corresponding macrocyclic compounds in a ratio of 1 : 1, respectively.



Scheme 5-3 Possible pathway for the aerobic oxidation of furan in the presence of HemiQ[6].

From the experimental evidence for the host-guest interaction, as presented above, and the kinetic analysis of the aerobic oxidation of furan in the presence of HemiQ[6], a speculative mechanism was established (Scheme 5-3). The capture of a proton by HemiQ[6], which induced the formation of an inclusion complex between furan and HemiQ[6] with the protonation. Subsequently, an oxygen attacked to the α -carbon on furan, and the higher electronegativity of oxygen led to an electron transfer from furan, to provide the hydroxyl group and produce furan-2-ol in the presence of HemiQ[6]. The intermediate included closing of the second hydroxyl group and losing of proton. Finally, the proton leaving from the α -carbon provided the corresponding product, inclusion complex of furan-2,5-diol with HemiQ[6].

Quantum chemical calculations were performed to evaluate the above hypothesis. The results of the calculations confirmed that there was no energy barrier in the proposed pathway for the proton-induced interaction of furan with HemiQ[6] (Figure 5-12). The protonation of HemiQ[6] released a high binding energy of $707.4 \text{ kJ} \cdot \text{mol}^{-1}$, and in the energy-minimized structure of the inclusion complex, furan stayed at

the portal of HemiQ[6], which explained the the ^1H NMR titration results. A proton rich medium lead to the associations between the furan and HemiQ[6], with a short ($\text{O}\cdots\text{H}\cdots\text{O}$) distance of 1.72 Å and a bond angle $\angle\text{OHO} = 153.0^\circ$. The negative energy changes declared that the presence of proton should be in favor of the host-guest interaction.

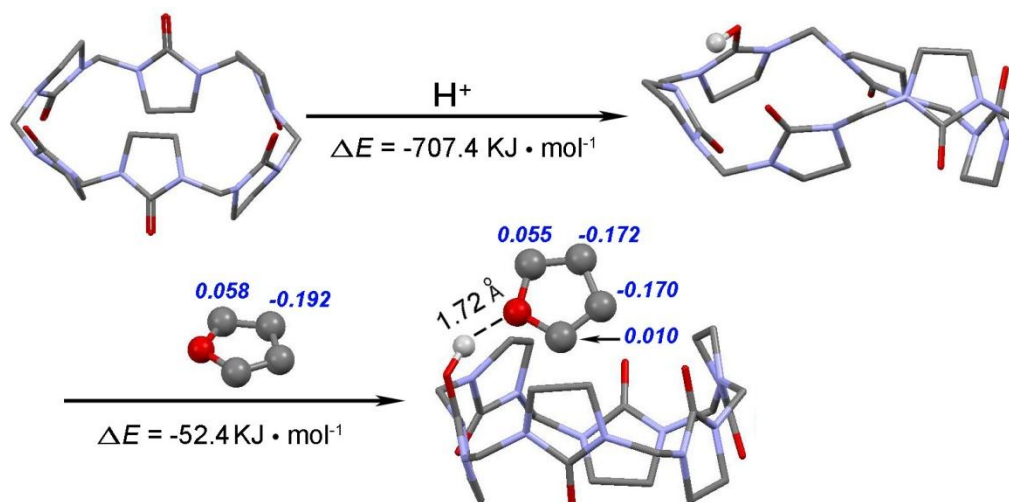


Figure 5-12 Results of calculations for host-guest interaction of furan with HemiQ[6].

Color codes: carbon, gray; nitrogen, blue; oxygen, red; hydrogen, green. Mulliken charges were marked in blue and italic.

The role of the proton in this supramolecular catalysis was to induce the redistribution of electron density in the furan ring and analysis of the Mulliken charges shown that there was richer electron density on the binding furan with HemiQ[6] (Figure 5-12). Mulliken charge of the α -carbon on furan ring at the portal of HemiQ[6] decreased from 0.058 to 0.010, which improved the reaction activity, that is, the more negative was the active site, the more easily it was to combine with oxygen and so be oxidized. Comparing with the free guest, the Mulliken charge on the β -carbon of the encapsulated furan was more positive, so it should have less reducing power. Accordingly, with the proton-mediated host-guest interaction, the redistribution of electrons on the furan ring held with HemiQ[6] brought on a regio-selective oxidation at the α -carbon.

2.5 Aerobic oxidation of 2-methylfuran in the presence of hemicucurbit[6]uril.

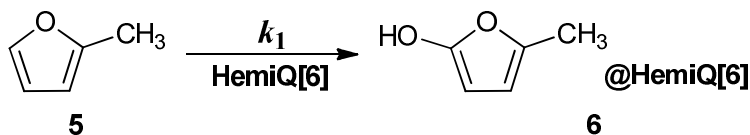
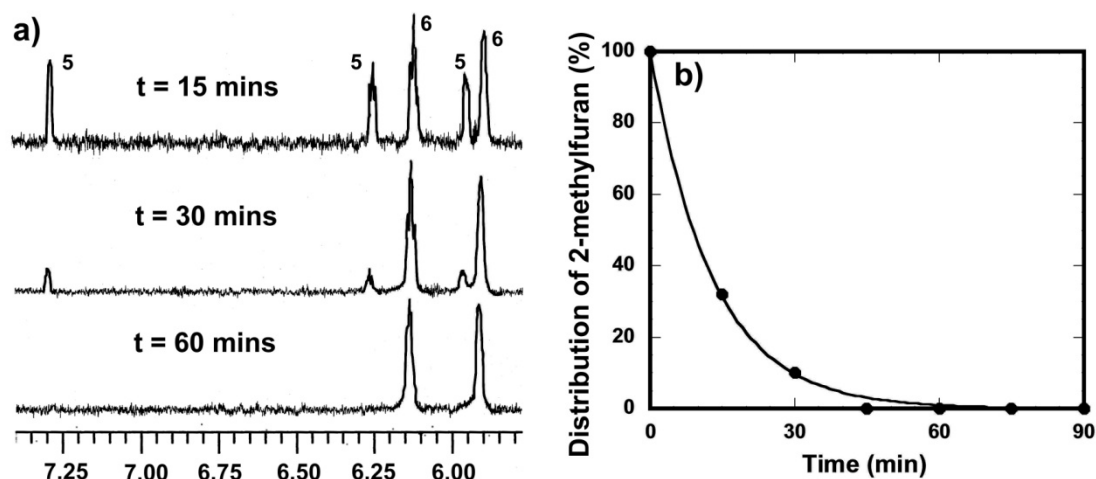
**Scheme 5-4** Oxidation of 2-methyl-furan in the presence of HemiQ[6].

Figure 5-13 a) ^1H NMR traces showing progress of the aerobic oxidation of 2-methylfuran in the presence of 1 equiv HemiQ[6] in neutral conditions (pD = 6.3) (5: 2-methylfuran, 6: furan-2-methyl-5-ol); b) the distribution plot for 2-methylfuran.

The substituted furan, 2-methylfuran, was also used in this HemiQ[6]-catalytic aerobic oxidation (Scheme 5-4). This was recorded with ^1H NMR, as shown in Figure 5-13a, whilst the proton resonances of the product 2-methylfuran-5-ol appear at δ 5.92 and δ 6.18 ppm. The conversion of the 2-methylfuran substrate was non-linearly fitted to formula (5-4) and revealed that the kinetics follow first-order behavior, with $k_1 = 7.7 \times 10^{-2} \text{ min}^{-1}$ (Figure 5-13b). This was about 3 times greater than for the oxidation of furan. The improved rate can be considered as a result of the relationship between the structure of 2-methyl-furan and the electron distribution, namely, that there was higher electron density on the unsubstituted α -carbon of the substrate due to the presence of the electron donating methyl group. The oxidation of 2-methylfuran was too rapid in acid solution (pD = 2) to be traced and provide an exact kinetic

constant, but it was confirmed that the oxidation was accelerated by the addition of the proton. The HemiQ[6]-catalytic aerobic oxidation product of 2-methylfuran was treated with DCl and neutralized with Na_2CO_3 followed by extraction with CDCl_3 same as that of furan. This result strongly supports the aerobic oxidation of 2-methylfuran does occur in the presence of HemiQ[6] under the conditions used.

2.6 Aerobic oxidation of thiophene in the presence of hemicucurbit[6]uril.

The oxidation of another five-member heterocyclic compound, thiophene, in the presence of HemiQ[6] (Scheme 5-5), proceeded very slowly in neutral conditions (Figure 14a), and less than 5 % of the product thiophene-2,5-diol was found after heating for 720 minutes. For this reason, the complete oxidation in this case may take a couple of days which made it very difficult to describe the full kinetics. The initial rates of conversion of thiophene and the yield of thiophene-2,5-diol were employed to estimate the kinetic properties, and the kinetic data have been linearly fitted to give the corresponding $k_1 = 4.1 \times 10^{-2} \text{ min}^{-1}$ and $k_2 = 6.6 \times 10^{-3} \text{ min}^{-1}$ (Figure 7b,c). As in the case of the oxidation of furan, the secondary oxidation was slower than the initial step, and it was taken for granted that this was the rate-determining step in this procedure. On the other hand, the different activities between furan and thiophene could be considered to arise because the association of the sulfur on thiophene with the proton captured by HemiQ[6] was weaker than in the case of furan.



Scheme 5-5 Oxidation of thiophene in the presence of HemiQ[6].

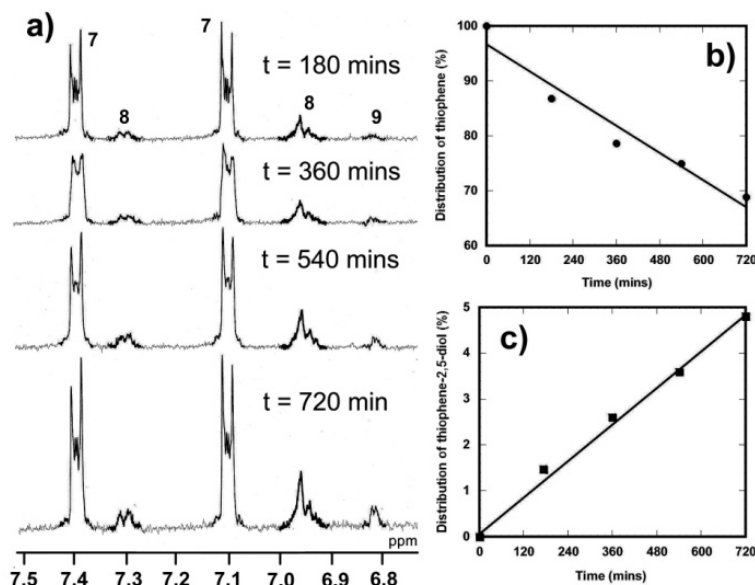


Figure 14 a) ¹H NMR traces showing progress of the aerobic oxidation of thiophene in the presence of 1 equiv HemiQ[6] in neutral conditions (pD = 6.3) (**7**: thiophene, **8**: thiophene-2-ol, **9**: thiophene-2,5-diol), and the distribution plots for b) thiophene, c) thiophene-2,5-diol.

The acceleration of the HemiQ[6]-induced oxidation of thiophene with the addition of a proton was also observed. In acidic conditions (pD = 2.0), the ¹H NMR trace indicated that the conversion was faster than that in neutral solution (Figure 15a); the kinetic data were fitted with initial rates of $k_1 = 8.9 \times 10^{-2} \text{ min}^{-1}$ and $k_2 = 2.1 \times 10^{-2} \text{ min}^{-1}$ (Figure 15b,c). These were clearly improved by 2 or 3 times upon acidification. Interestingly, the last two plots of thiophene conversion departed from the line of fit (Figure 15b) due to the fact that the first oxidation of the substrate was resisted by the rate determining step, secondary oxidation, so it seemed that the oxidation preferred thiophene-2-ol as product over thiophene-2,5-diol.

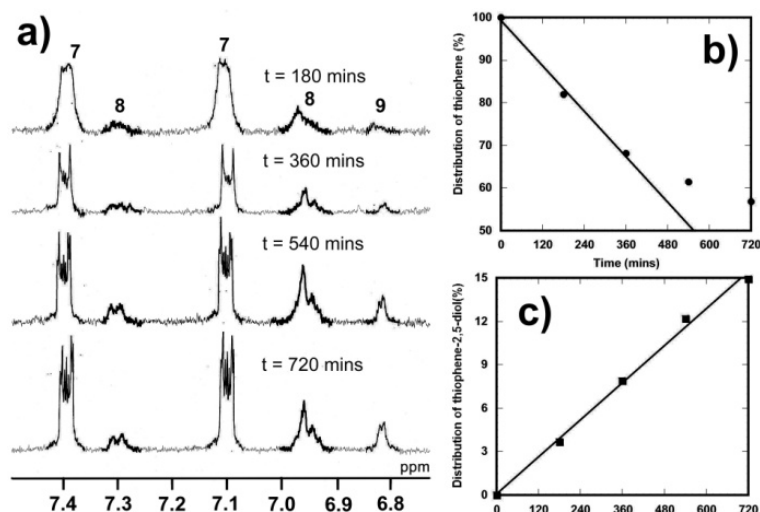


Figure 5-15 a) ¹H NMR traces showing progress of the aerobic oxidation of thiophene in the presence of 1 equiv HemiQ[6] in acid conditions (pD = 2.0) (**7**: thiophene, **8**: thiophene-2-ol, **9**: thiophene-2,5-diol), and the distribution plots for b) thiophene, c) thiophene-2,5-diol.

3. Conclusion

In summary, we developed a novel aerobic oxidation system catalyzed by HemiQ[6] in water. As a model substrate, furan encapsulated within HemiQ[6], was oxidized to form furan-2,5-diol regio-selectively. The supramolecular catalytic oxidation could be improved by acidification, due to the protonation of HemiQ[6]. According to analysis of the oxidation kinetics using a ^1H NMR trace, a plausible mechanism was proposed, including the host-guest interaction between furan and the protonated HemiQ[6], the attack of oxygen molecule to α -carbon of binding furan, and the proton transfer to introduce the hydroxyl groups on to the furan ring. The HemiQ[6]-induced aerobic oxidation was also effective on the substrates of 2-methylfuran and thiophene.

The HemiQ[6]-catalytic oxidation of heterocyclic compounds in aqueous solution *via* a supramolecular strategy offered an alternative to aerobic oxidation with no participation by any metal cation. Furthermore, the unique ability of HemiQ[6] to capture protons could be applied to other acid-assisted chemical systems, giving the prospect of further revelations in cucurbituril chemistry.

4. Experimental

4.1 Materials and apparatus

HemiQ[*n*] (*n* = 6 or 12) samples were prepared and purified according to the method reported elsewhere [1] and were characterized by ¹H NMR, giving resonances for HemiQ[6] (CDCl₃, δ) at 3.40 ppm (s, 24H) and 4.67 ppm (s, 12H) and for HemiQ[12] (CDCl₃, δ) at 3.36 ppm (s, 24H) and 4.67 ppm (s, 12H). Q[*n*] were prepared and purified according to the methods reported in literature [13]. Furan, 2-methylfuran and thiophene were obtained commercially (Tokyo Kasei Kogyo Co., Ltd.) and used without further purification.

¹H NMR spectra were recorded at 25 °C on a JEOL JNM-A100 spectrometer (300 MHz) in D₂O, with TMS is used as an internal reference.

4.2 Catalytic Oxidation experiments

The heterocyclic compounds (0.015 mmol) were added to 0.6 mL D₂O and then HemiQ[6] was added to the solution in a 1:1 ratio. The solution was heated to 65 °C and monitored by ¹H NMR over time. The reactant conversion was directly confirmed by ¹H NMR spectral data.

4.3 Computational method

All calculations were processed with Gaussian 09 software package [15]. The structures were optimized at the wb97xd/6-311g(*d,p*) level, and single point energies of the optimized geometries and BSSE-corrected (Basis Set Superposition Error corrected) binding energies of the supramolecules were performed at wb97xd/6-311g++(*d,p*) level.

References

1. Miyahara, Y.; Goto, K.; Oka, M.; Inazu, T. *Angew. Chem. Int. Ed.* **2004**, *43*, 5019–5022.
2. Parmeggiani, C.; Cardona, F. *Green Chem.* **2012**, *14*, 547–564.
3. Endo, Y.; Bäckvall, J. –E. *Chem. Eur. J.* **2011**, *17*, 12596–12601.
4. Markó, I. E.; Gautier, A.; Dumeunier, R.; Doda, K.; Philippart, F.; Brown, S. M.; Urch, C. J. *Angew. Chem. Int. Ed.* **2004**, *43*, 1588–1591.
5. Melikyan, G. G. *Synthesis* **1993**, 833–850.
6. Stahl, S. S. *Science* **2005**, *309*, 1824–1826.
7. Guan, B.; Xing, D.; Cai, G.; Wan, X.; Yu, N.; Fang, Z.; Yang, L.; Shi, Z. *J. Am. Chem. Soc.* **2005**, *127*, 18004–18005.
8. Spellmeyer, D. C.; Houk, K. N.; Rondan, N. G.; Miller, R. D.; Franz, L.; Fickes, G. N. *J. Am. Chem. Soc.* **1989**, *111*, 5356–5367.
9. Fall, O. A.; Sène, M.; Tojo, E.; Gómez, G.; Fall, Y. *Synthesis* **2010**, *20*, 3415–3417.
10. Masson, E.; Ling, X.; Joseph, R.; Kyeremeh–Mensah, L.; Lu, X. *RSC Adv.* **2012**, *2*, 1213–1247.
11. Cong, H.; Li, C. –R.; Xue, S. –F.; Tao, Z.; Zhu, Q. –J.; Wei, G. *Org. Biomol. Chem.* **2011**, *9*, 1041–1046.
12. Cong, H.; Yamato, T.; Feng, X.; Tao, Z. *J. Mol. Catal. A: Chem.* **2012**, *365*, 181–185.
14. Zhang, G. –L.; Xu, Z. –Q.; Xue, S. –F.; Zhu, Q. –J.; Tao, Z. *Chin. J. Inorg. Chem.* **2003**, *19*, 655–659.
15. Frisch, M. J.; Trucks, G. W.; Schlegel, H. B.; Scuseria, G. E.; Robb, M. A.; Cheeseman, J. R.; Scalmani, G.; Barone, V.; Mennucci, B.; Petersson, G. A.; Nakatsuji, H.; Caricato, M.; Li, X.; Hratchian, H. P.; Izmaylov, A. F.; Bloino, J.; Zheng, G.; Sonnenberg, J. L.; Hada, M.; Ehara, M.; Toyota, K.; Fukuda, R.; Hasegawa, J.; Ishida, M.; Nakajima, T.; Honda, Y.; Kitao, O.; Nakai, H.; Vreven, T.; Montgomery Jr., J. A.; Peralta, J. E.; Ogliaro, F.; Bearpark, M.; Heyd, J. J.; Brothers, E.; Kudin, K. N.; Staroverov, V. N.; Kobayashi, R.; Normand, J.; Raghavachari, K.;

Rendell, A.; Burant, J. C.; Iyengar, S. S.; Tomasi, J.; Cossi, M.; Rega, N.; Millam, J. M.; Klene, M.; Knox, J. E.; Cross, J. B.; Bakken, V.; Adamo, C.; Jaramillo, J.; Gomperts, R.; Stratmann, R. E.; Yazyev, O.; Austin, A. J.; Cammi, R.; Pomelli, C.; Ochterski, J. W.; Martin, R. L.; Morokuma, K.; Zakrzewski, V. G.; Voth, G. A.; Salvador, P.; Dannenberg, J. J.; Dapprich, S.; Daniels, A. D.; Farkas, O.; Foresman, J. B.; Ortiz, J. V.; Cioslowski, J.; Fox, D. J. *Gaussian 09, Revision A.02*, **2009**, Gaussian, Inc., Wallingford CT.

Summary

Cucurbit[n]uril (Q[n], $n=5\sim 8$ or 10) is a family of cage-like host molecules oligomerized between glycoluril and formaldehyde, and the enclosed hydrophobic cavity, with two identical portal regions lined by carbonyl oxygen, is always able to bond non-covalently to organic and inorganic guests with weak ion-dipole, hydrogen binding, hydrophobic or hydrophilic properties. Depending on the host-guest chemistry, cucurbituril-induced supramolecular catalysis has made a significant contribution to organic synthesis including photodimerization, hydrolysis, and oxidation so on.

The cucurbit[8]uril-catalytic oxidation of alcohols by IBX (*o*-iodoxybenzoic acid) has been explored in pioneering work, but the mechanism was unclear. To get the foundation information of this supramolecular catalysis, veratryl alcohol was employed as a model substrate, which was the first case subjected to this catalytic oxidation, to investigate the host-guest interaction with Q[8]. The evidences of both fluorescence spectrometry and electrochemical analysis suggested a ternary complex formed between IBX, veratryl alcohol and Q[8] in a molar ratio of 1 : 1 : 1. Quantum chemistry was carried out according to above experimental results, and revealed the presence of Q[8] was in favor of the formation of the iodoester intermediate in the process of IBX oxidizing veratryl alcohol due to the encapsulation in the cavity of Q[8]. Two series of aromatic alcohol substrates, 2,3,4-methoxybenzyl alcohol and 2,3,4-pyridinemethanol hydrochlorides, were subjected to this Q[8]-catalytic oxidation, and the results of kinetic and thermodynamic analysis revealed that the electronic property of the substituent affected significantly the supramolecular catalysis, that is, the conversion of aromatic alcohol was seriously dependent on substituent structure of substrate, which indicated that electron distribution on the α -carbon was mechanistically connected to the IBX oxidation procedure. In the absence of Q[8], the α -carbon could be stabilized by with conjugated electron-rich substituent and easily oxidized, while the presence of Q[8] improved the oxidation of

alcohols with negative inductive effect substituent.

The applications of cucurbituril family have been limited in aqueous solution due to their insolubility in any organic solvent. The appearance of hemicucurbit[n, n = 6 or 12]uril (HemiQ[n]) and their unique solubility in chloroform or alcohol afforded a new opportunity to develop the platform of the supramolecular chemistry of cucurbiturils, sequently, a few applications of HemiQ[n] for supramolecular catalysis have been developed.

2,3,4-Hydroxybenzyl alcohols are a kind of bifunctional substrates embracing synchronously phenolic and alcoholic hydroxyl groups, both which could be carried out the IBX oxidation to provide a mixture of both aldehyde and quinone products. With the participation of 50 mol% hemicucurbit[6]uril, phenolic hydroxyl groups were able to be protected against oxidation by IBX to realize the chemo-selective oxidation reaction, and the corresponding aldehydes were observed as the only product species. The kinetics in the presence of HemiQ[6] revealed that the oxidation depended on both the steric effects and electronic effects of the substrates, namely, the reactivity of 2-hydroxyl alcohol was thermodynamically the lowest, as the two hydroxyl groups were very close to each other. The oxidation of 3-hydroxybenzyl alcohol was faster than the others as the result of inductive effect of its phenolic hydroxyl group. ¹H NMR spectroscopy, IR absorption analysis and UV-vis titrations indicated the host-guest interactions of HemiQ[6] with hydroxybenzyl alcohols in a ratio of 1 : 1 with the formation of hydrogen bonds between HemiQ[6] and the benzyl alcohol guests through the binding of active hydrogen by the macrocyclic compound. And the host-guest interactions were also evaluated by calculation chemistry, and the results afforded the inclusion complexes of HemiQ[6] with 2,3,4-hydroxybenzyl alcohols in the ratio of 1 : 1, respectively. The calculated binding energies were sequentially consistent with the association constants fitted by UV-vis titrations.

The esterification of carboxylic compounds in the presence of hemicucurbit[6]uril *via* a supramolecular strategy was discovered. The kinetics of esterification with addition of 0.5, 1.0, and 2.0 equiv. HemiQ[6] revealed the reactivity was related to the amount of macrocyclic compound, that is, the reaction

rate could be improved by application of a greater amount of catalyst, and the supramolecular catalytic activity was also affected by the electronic and steric structures of the substrates; only the conjugated acids could be esterified with the catalysis of HemiQ[6]. Another member of hemicucurbiturils, HemiQ[12], was not to catalyze this esterification possibly the cavity was too large to stabilize the intermediate, so the structure of the catalyst played an important role in this catalysis. The failure of esterification of acid substrates with a stoichiometric amount of CH_3OH suggested that the esterification could be alcoholysis. A possible mechanism was proposed involving HemiQ[6]-stabilized carbon cation, which could be attacked by CH_3OH to form the ester product.

A novel aerobic oxidation system catalyzed by HemiQ[6] in water was explored. Furan was employed as a model substrate, which was encapsulated by HemiQ[6], to carry out an aerobic oxidation to produce furan-2,5-diol regio-selectively. Kinetics of the supramolecular catalytic oxidation suggested the activity of macrocycle could be improved in acidic solution as a result of the protonation of HemiQ[6]. A plausible mechanism was proposed, including the host-guest interaction between furan and the protonated HemiQ[6], the attack of oxygen molecule to α -carbon of binding furan, and the proton transfer to introduce the hydroxyl groups on to the furan ring. 2-Methylfuran and thiophene were also subjected to the standard conditions and underwent the aerobic oxidation in the presence of HemiQ[6].

In summary, a few supramolecular catalysis systems of cucurbiturils were developed, and afforded new applications in cucurbituril chemistry. The investigations on host-guest interaction between IBX, Iveratryl alcohol and Q[8], as well as IBX oxidation of aromatic alcohols in the presence of cucurbit[8]uril, provided fundamental evidences to establish the mechanism of Q[8]-improved oxidation. The application of hemicucurbit[6]uril for IBX oxidation of hydroxylbenzyl alcohols realized a chemo-selective reaction. HemiQ[6]-induced esterification offered an alternative manner to produce ester without participation by any acid. The protonation of HemiQ[6] can catalyze the aerobic oxidation of heterocyclic compounds.

Acknowledgements

I would like to express my gratitude to all those who helped me during my doctoral course in last three years.

My deepest gratitude goes first and foremost to Professor Dr. Takehiko Yamato, for his instructive advice and useful suggestions on design and performance of my thesis. He has walked me through all the stages of my doctoral course, involving experimental, data analysis, and mechanism establishment so on, and I am deeply grateful of his help in the completion of this thesis.

High tribute shall be paid to Professor Zhu Tao Ph.D. and Professor Xi Zeng, Guizhou University, P. R. China, for their profound knowledge triggering my exploration in the research filed of supramolecular chemistry.

I am also deeply indebted to all the other teachers and tutors in Saga University for their direct and indirect help to me.

Special thanks should go to all the members in Prof. Yamato's laboratory, for their kind help and companies in these three years.

I also appreciate the technical support of the high performance computing platform of Guizhou University.

Finally, my gratitude also extends to my beloved family for their continuous support and encouragement.

Publications

1. Host-guest interaction of hemicucurbiturils with phenazine hydrochloride salt
D.-D. Xiang, Q.-X. Geng, **H. Cong**, Z. Tao and T. Yamato,
Supramolecular Chemistry in press.
2. Chemo-selective oxidation of hydroxybenzyl alcohols with IBX in the presence
of hemicucurbit[6]uril
H. Cong, T. Yamato and Z. Tao,
New J. Chem., **2013**, 37, 3778–3783.
3. Hemicucurbit[6]uril-induced aerobic oxidation of heterocyclic compounds
H. Cong, T. Yamato and Z. Tao,
J. Mol. Catal. A: Chem., **2013**, 379, 287–293.
4. Substituent effect of substrates on cucurbit[8]uril- catalytic oxidation of aryl
alcohols
H. Cong, Z.-J. Li, Y.-H. Wang, Z. Tao, T. Yamato, S.-F. Xue and G. Wei,
J. Mol. Catal. A: Chem., **2013**, 374–375, 32–38.
5. Supramolecular catalysis of esterification by hemicucurbiturils under mild
conditions
H. Cong, T. Yamato, X. Feng and Z. Tao,
J. Mol. Catal. A: Chem., **2012**, 365, 181–185.